Recycling the tail-gas during the Low Temperature Fischer-Tropsch Process

Thesis submitted for the Taught Masters in Catalysis degree in the Department of Chemical Engineering at the University of Cape Town.

by

NILENINDRAN SUNDRA GOVENDER

Hons. B.Sc. (CHEM) (University of South Africa)

B.Sc. (CHEM) (University of Natal)

Supervisor: Prof. Eric van Steen, UCT

Co-Supervisor: Dr Matthys Janse van Vuuren, Sasol

Cape Town

2005

ACKNOWLEDGEMENTS

I would like to thank the following people and organisations for their help and support throughout this study:

Dr Matthys Janse van Vuuren for his contribution as co-supervisor.

Prof. Eric van Steen for his assistance and guidance as supervisor.

Sasol Technology, Research and Development Division for funding this research project and the Catalysis Research Unit, Chemical Engineering Department, UCT for valuable information learned during the course work and for feedback during the presentations. Prof. Mark Dry, Dr. Michael Claeys and Walter Böhringer for insightful discussions during my short stay at UCT.

My dear wife for all her encouragement, interest and support, especially during the 6 months whilst I was away from home.

I would also like to thank my colleagues at Sasol Technology for all their support and motivation, especially Thobeka Pete, Don Hauman, Ryno Kotze, Tumelo Sekhoto and Gerry Masters.

ABSTRACT

For the economically viable operation of an iron-based Fischer-Tropsch technology, two options are available: (i) use a diluted feed, such as nitrogen-rich synthesis gas, thereby saving on synthesis gas costs [Jess *et al.*, 1999] or (ii) recycle of the unconverted synthesis gas that leaves the reactor, after condensation of the liquid products (or use a number of reactors in series with intermediate condensation of the products). The tail-gas from the Fischer-Tropsch reactor contains un-reacted synthesis gas, CO_2, water vapour and lower hydrocarbons (olefins, paraffins and oxygenates). This stream can in principle be recycled back to the Fischer-Tropsch reactor, and thereby reducing the load on the reformers. However, it is necessary to understand what effects the constituents in the tail gas will have on the Fischer-Tropsch process when this stream is recycled back directly to the Fischer-Tropsch reactors.

The effect of recycling the tail-gas back to the reactor, during the low temperature Fischer-Tropsch process, was investigated for different H_2/CO ratios in the fresh feed on a precipitated iron catalyst using a micro-slurry reactor. The H_2/CO ratio in the fresh feed was varied from 1.0 to 2.0 and the recycle ratio from 0 to 2.0. The temperature and pressure were kept constant at 240°C and 20bar respectively.

It was shown that the H_2/CO-ratio in the gas fed to the reactor depends on both the H_2/CO ratio in the fresh feed and the usage ratio of the catalyst. For an H_2/CO in the fresh higher than the usage ratio, the H_2/CO ratio in the reactor increases with the recycle ratio whereas the converse is true for lower H_2/CO ratios. For negligible change in the Fischer-Tropsch selectivity during external recycle, the H_2/CO ratio in the fresh feed should match the usage ratio of the catalyst. Upon reducing the recycle ratio back to zero, the performance of the

system was identical to that before the introduction of the recycle which indicates that permanent deactivation did not occur.

Recycling the tail gas back to the reactor increases the overall conversion of carbon monoxide significantly. The overall conversion of CO increases further upon increasing the recycle ratio. The benefit of recycling the tail gas is more pronounced for a synthesis gas with a higher H_2/CO-ratio than for a synthesis gas with a low H_2/CO ratio.

Recycling the cold tail gas back to the Fischer-Tropsch reactor alters the partial pressures in the reactor and hence the rate of the Fischer-Tropsch synthesis. Recycled CO_2 does not seem to affect the Fischer-Tropsch synthesis and can be considered as an inert. Re-adsorption of reactive, primarily formed 1-olefins can be accounted for by the model developed by Schulz and Claeys [1999]. Re-adsorption of olefins and in particular ethene is shown to be important.

TABLE OF CONTENTS

ACKNOWLEDGEMENTS I

SYNOPSIS II

CHAPTER 1: INTRODUCTION 1

1.1. BACKGROUND 1

1.2. THESIS AIMS AND SCOPE 4

CHAPTER 2: LITERATURE REVIEW 6

2.1. USAGE RATIO IN THE FISCHER-TROPSCH SYNTHESIS 8

2.2. SYNTHESIS GAS PREPARATION 9

2.2.1. Natural Gas Reforming 10

2.2.2. Coal Gasification 12

2.2.3. Co-Gasifying Coal and Natural Gas 13

2.2.4. Biomass Gasification 13

2.3. CURRENT AND FUTURE FISCHER-TROPSCH COMPLEXES 14

2.3.1. Lay-out of the Low Temperature Fischer-Tropsch Plant at Sasol (Sasolburg, South Africa) 16

2.3.2. Lay-out of the High Temperature Fischer-Tropsch Plant at Sasol (Secunda, South Africa) 17

2.3.3. Lay-out of the High Temperature Fischer-Tropsch Plant at PetroSA (Mossel Bay, South Africa) 18

2.3.4. Lay-out of the low temperature Fischer-Tropsch Plant at Shell (Bintulu, Malaysia) 19

2.3.5. Lay-out of the Exxon AGC-21 Process 20

2.3.6. Lay-out of the Syntroleum Process 21

2.4. RECYCLING DURING THE FISCHER-TROPSCH PROCESS 22
2.4.1. Influence of Recycling on Activity 22
2.4.1.1. Effect of changing H_2/CO ratio 22
2.4.1.2. Effect of CO_2 24
2.4.1.3. Effect of Water 26
2.4.2. Secondary Reactions during the Fischer-Tropsch Synthesis 26
2.4.2.1. Effect of changing H_2/CO ratio 27
2.4.2.2. Effect of recycling olefins 28
2.4.2.2.1. Modeling Olefin re-adsorption 30
2.4.2.3. Effect of recycling alcohols 30
2.5. REACTION KINETICS 32
2.5.1. Rate of the Fischer-Tropsch Reaction 32
2.5.2. Rate of CO_2-Formation under Fischer-Tropsch conditions 33
2.6. CHAPTER SUMMARY AND RELATION TO PRESENT STUDY 35

CHAPTER 3: EXPERIMENTAL APPARATUS AND PROCEDURES 37
3.1. REACTOR SET-UP 37
3.1.1. Catalyst Loading 39
3.1.2. Reduction and Start-up of the Fischer-Tropsch synthesis 39
3.1.3. Start-up of Recycle 39
3.2. PRODUCT ANALYSIS 40
3.3. DATA EVALUATION 43
3.3.1. Calculation of flow rates of various compounds from gas chromatographic analysis 43
3.3.2. Calculation of partial pressures in the reactor 45
3.3.3. Calculation of conversion and rate of reaction 45
3.3.4. Calculation of selectivity 46
3.4. EXPERIMENTS 46

CHAPTER 4: RESULTS 48
4.1. FEED TO THE REACTOR 48
4.1.1. Molar H_2/CO ratios 48
4.1.2. Organic product compounds fed to the reactor 51
4.2. INFLUENCE OF RECYCLE ON CONVERSION 53
4.2.1. Conversion of Carbon Monoxide 53
4.2.2. CO-conversion for the formation of organic product compounds 56
4.2.3. Selectivity for the formation of carbon dioxide 56
4.2.4. Usage Ratio 61
4.3. PARTIAL PRESSURES IN THE REACTOR 63
4.4. INFLUENCE OF RECYCLE ON PRODUCT SELECTIVITY 66
4.4.1. Methane Selectivity 67
4.4.2. Chain growth probability 68
4.4.3. Secondary reaction of primarily formed olefins 69
4.4.3.1. Double bond isomerisation 72
4.4.4. Formation of Oxygenates 74

CHAPTER 5: DISCUSSION 78
5.1. MODELING THE FORMATION OF ORGANIC PRODUCT COMPOUNDS 78
5.2. MODELING THE FORMATION OF CARBON DIOXIDE 82
5.3. MODELING USAGE RATIO 85
5.4. MODELING ORGANIC PRODUCT SELECTIVITY 86
5.4.1. Effect of recycle ratio on 1-olefin content 86

CHAPTER 6: CONCLUSIONS **95**

REFERENCES 97

APPENDICES 107

APPENDIX A: Data used for testing the FT and WGS rate expressions 107

APPENDIX B: Experimental data and catalytic performance results (from TCD analyses) for the different H_2/CO ratios in the fresh feed with and without recycle 108

APPENDIX C: Results of the selectivity calculations for the different H_2/CO ratios in the fresh feed with and without recycle 115

APPENDIX D: Data for the olefin readsorption model 130

LIST OF TABLES

CHAPTER 2: LITERATURE REVIEW

Table 2.1. Comparison of synthesis gas production technologies from methane 11

Table 2.2. Methodologies for adjusting H_2/CO ratios in synthesis gas 12

Table 2.3. Existing and planned Fischer-Tropsch plants in the world 15

Table 2.4. Comparison of a single pass reactor with a recycle reactor 23

Table 2.5. Control measures and results for optimum control scheme 24

Table 2.6. Summary of published research on co-feeding olefins during Fischer-Tropsch Synthesis (on Fe catalysts) 29

Table 2.7. Summary of published research on co-feeding alcohol during Fischer-Tropsch Synthesis (on Fe catalysts) 31

CHAPTER 3: EXPERIMENTAL APPARATUS AND PROCEDURES

Table 3.1. Summary of the details for the GC's utilised 40

Table 3.2. Experimental conditions for the varying H_2/CO ratio in the fresh feed and varying recycle ratios in a micro-slurry reactor 47

CHAPTER 4: RESULTS

Table 4.1. Average partial pressures in the reactor as a function of the fresh feed composition and the recycle ratio 66

CHAPTER 5: DISCUSSION

Table 5.1. Obtained kinetic parameters for the rate of the Fischer-Tropsch synthesis and goodness of fit 80

Table 5.2. Comparison of the kinetic coefficients obtained from fitting experimental data to the rate expression proposed by Schulz and van Steen [1999] 81

Table 5.3. Obtained kinetic parameters for the rate of formation of CO_2 in the Fischer-Tropsch synthesis and goodness of fit 83

LIST OF FIGURES

CHAPTER 2: LITERATURE REVIEW

Figure 2.1. The change in the exit H_2/CO ratio of a FT reactor for a cobalt based catalyst for different conversions when the inlet H_2/CO ratio is different from the usage ratio 9

Figure 2.2. Flow sheet for the synthesis gas production from coal and natural gas co-gasifying 13

Figure 2.3. Flow sheet for the Sasol LTFT plant in Sasolburg, South Africa 16

Figure 2.4. Flow sheet for the Sasol HTFT plant in Secunda, South Africa 17

Figure 2.5. Flow sheet for the high temperature Fischer-Tropsch plant (PetraSA, Mossel Bay, South Africa) 18

Figure 2.6. Flow sheet for the Shell FT plant in Bintulu, Malaysia 19

Figure 2.7. Flow sheet for the proposed Exxon AGC-21 process 20

Figure 2.8. Flow sheet for the proposed Syntroleum process 21

Figure 2.9. The selectivity of hard wax (bpt. > 500°C) as a function of the H_2/CO ratio 27

Figure 2.10. Kinetic scheme of the secondary olefin reactions taking into account the solubility of olefins in liquid FT product 30

CHAPTER 3: EXPERIMENTAL APPARATUS AND PROCEDURES

Figure 3.1. Flow Scheme of Micro-Slurry Reactor with recycle 38

Figure 3.2. TCD-analysis of calibration gas on Gow-Mac 600 showing analysis of H_2, Ar, N_2, CO, CH_4 and CO_2 41

Figure 3.3. FID-analysis of organic product compounds in tail-gas 41

Figure 3.4. FID-analysis of organic product compounds in the oil-phase 42

Figure 3.5. FID-analysis of organic product compounds in the water-phase 42

Figure 3.6. FID-analysis of liquid organic product compounds in the hot trap 43

CHAPTER 4: RESULTS

Figure 4.1. Molar H_2/CO ratio in the fresh feed, the gas fed to the reactor, and the tail gas as a function of time-on-stream 49

Figure 4.2. Concentration of organic product compounds as a function of carbon number in the cold tail gas and in the feed to the reactor for a fresh feed with H_2/CO=1.50 and a recycle ratio of 0.84 52

Figure 4.3. Distribution of organic product compounds as a function of carbon number in the feed to the reactor for a fresh feed with H_2/CO=1.50 and a recycle ratio of 0.84 52

Figure 4.4. Olefin content in the fraction of linear olefins and paraffins as a function of carbon number in the cold tail gas and in the feed to the reactor for a fresh feed with H_2/CO=1.50 and a recycle ratio of 0.84 53

Figure 4.5. Overall conversion of carbon monoxide and the conversion of carbon monoxide per pass as a function of time-on-stream 54

Figure 4.6. Overall conversion of carbon monoxide and the conversion of carbon monoxide per pass as a function of time-on-stream 57

Figure 4.7. Selectivity for the formation of CO_2 as a function of time-on-stream 59

Figure 4.8. Fraction of water being converted in the water-gas shift reaction as a function of the recycle ratio 60

Figure 4.9. Water-gas shift reaction product ratio as a function of the recycle ratio 61

Figure 4.10. Usage ratio, defined as the amount of hydrogen consumed relative to the amount of carbon monoxide consumed, as a function of the recycle ratio 62

Figure 4.11. Usage ratio, defined as the amount of hydrogen consumed relative to the amount of carbon monoxide consumed, relative to the hydrogen to carbon monoxide ratio in the fresh feed as a function of the recycle ratio 63

Figure 4.12. Partial pressure of hydrogen, carbon monoxide, water and carbon dioxide in the reactor as calculated from the tail gas composition as a function of time-on-stream 64

Figure 4.13. Anderson-Schulz-Flory distribution of C_1-C_{20} compounds calculated

together from the analysis of the tail gas and the oil phase for the experiment with $H_2/CO)_{fresh\ feed}$ = 1.50 with and without recycle (recycle ratio equals 0.84) 67
Figure 4.14. Methane selectivity in C-% as a function of recycle ratio for the various fresh feed ratios recycle 68
Figure 4.15. Chain growth probability in the range C_{15}-C_{20} as a function of recycle ratio for the various fresh feed ratios recycle 69
Figure 4.16. Olefin content defined as the amount of n-olefins in the fraction of linear hydrocarbons as a function of carbon number calculated together from the analysis of the tail gas and the oil phase for the experiment with $H_2/CO)_{fresh\ feed}$ = 2.01 with and without recycle (recycle ratios of 0.82 and 1.78) 70
Figure 4.17. Olefin content defined as the amount of n-olefins in the fraction of linear hydrocarbons as a function of the recycle ratio 71
Figure 4.18. 1-Olefin content defined as the amount of 1-olefins in the fraction of linear olefins as a function of carbon number calculated together from the analysis of the tail gas and the oil phase for the experiment with $H_2/CO)_{fresh\ feed}$ = 1.50 with and without recycle (recycle ratios of 0.84) 72
Figure 4.19. -1Olefin content defined as the amount of 1-olefins in the fraction of linear olefins as a function of the recycle ratio 73
Figure 4.20. Oxygenate content in the fraction of linear product compounds content defined as the amount of oxygenates (alcohols, aldehydes plus ketones) in the fraction of linear product compounds ((oxygenates, olefins and paraffins) as a function of carbon number calculated together from the analysis of the tail gas, the water phase and the oil phase for the experiment with $H_2/CO)_{fresh\ feed}$ = 1.50 with and without recycle (recycle ratios of 0.84) 74
Figure 4.21. Alcohol content defined as the amount of n-alcohol in the fraction of linear C_{10}-product compounds 75
Figure 4.22. Alcohol Selectivity in C-% as a function of recycle ratio for the various fresh feed ratios 76

CHAPTER 5: DISCUSSION

Figure 5.1. Fit of the experimental data to the linearised forms of the proposed rate expressions in literature to describe the rate of the Fischer-Tropsch synthesis, i.e. the rate of carbon incorporation in organic product compounds) 79

Figure 5.2. Parity plot of the calculated rate of the Fischer-Tropsch synthesis using the optimized kinetic constants 80

Figure 5.3. Parity plot of the proposed rate expressions in literature to describe the rate of formation of CO_2 in the Fischer-Tropsch synthesis 84

Figure 5.4. Parity plot for the usage ratio 85

Figure 5.5. 1-Olefin content in the fraction of linear hydrocarbons as a function of carbon number for the experiment with $(H_2/CO)_{fresh\ feed}$ = 2.01 and a recycle ratio of 0.8 88

Figure 5.6. Ratio of rate of desorption as an olefin to the rate of desorption as a n-paraffin from a surface species Sp_N, which participates in chain growth, as a function of recycle ratio and the hydrogen to carbon monoxide ratio in the fresh feed 89

Figure 5.7. Ratio of rate of desorption as a n-paraffin to the rate of desorption as an 1-olefin from a surface species Sp_N, which participates in chain growth, as a function of the square root of the hydrogen partial pressure 90

Figure 5.8. Lumped parameter describing the ratio of the rate of desorption as an 1-olefin from species Sp'_N and the rate of desorption from species Sp_N and the parameter describing the ratio of the rate of desorption as an end-product from species Sp'_N and the rate of desorption as an end-product from species Sp_N as a function of the recycle ratio 91

Figure 5.9. The rate of re-adsorption yielding surface species Sp_N relative to the rate of transport out of the reactor through the gas phase as a function of the recycle ratio 92

Figure 5.10. The rate of re-adsorption yielding surface species Sp'_N relative to the rate of transport out of the reactor through the gas phase as a

function of the recycle ratio 93
Figure 5.11. Ratio of the volumetric flow rate of the liquid leaving the reactor relative to the volumetric flow rate of the gas phase leaving the reactor as a function of time-on-stream 94
Figure 5.12. Reactivity of ethene relative to the reactivity of other 1-olefins as a function of recycle ratio 94

LIST OF SYMBOLS

K_p = water gas shift equilibrium constant

$m_{catalyst}$ = mass of the unreduced catalyst

N_c = Carbon number

p_i = the partial pressure of component i

$p_{reactor}$ = total reactor pressure

RR = Recycle Ratio

r_{FT} = the rate of formation of organic Fischer-Tropsch products

r_{WGS}, r_{CO2} = rate of the water gas shift reaction

S_i = the selectivity of component *i*

TOS = Time on Stream

U = usage ratio

$X_{i,per\ pass}$ = Per Pass conversion of component i

$X_{i,overall}$ = Overall conversion of component i

1

INTRODUCTION

1.1. BACKGROUND

The increasing demand for energy, especially from rapidly developing countries such as China and India [Asian Tribune, 2003], coupled with the uncertainty and expense of crude oil imports has led to a renewed interest in alternative sources of liquid fuels. For countries with cheap natural gas in remote areas, a low cost technology for the conversion of this natural gas to liquid organic products, through the Fischer-Tropsch synthesis can be economically viable. Countries with huge coal reserves, which lack petroleum and natural gas reserves, may also consider the production of liquid fuels via coal gasification and the Fischer-Tropsch (FT) technology.

The production of liquid organic products from either natural gas or coal via the Fischer-Tropsch process proceeds step-wise. In the first step natural gas or coal is being converted into synthesis gas, a mixture of hydrogen and carbon monoxide. Synthesis gas produced by coal gasification is typically lean in hydrogen, often having a H_2/CO ratio of about 0.6 to 0.7 [Clark and Walker, 2002], whereas production of synthesis gas from natural gas tends to be richer in hydrogen with a H_2/CO ratio of 2.0 or larger.

The Fischer-Tropsch process refers to the synthetic production of hydrocarbons by catalytically reacting carbon monoxide (CO) and hydrogen (H_2). The reaction

for converting CO and H_2 (commonly referred to as syngas) is characterized by the following reaction:

$$CO + 2\ H_2 \rightarrow -CH_2- + H_2O \qquad \Delta H^R(250°C) = -142\ kJ/mol\ CO\ converted$$

The water produced in the Fischer-Tropsch reaction can be consumed in the water gas shift reaction yielding CO_2 and H_2.

$$CO + H_2O \rightarrow CO_2 + H_2 \qquad \Delta H^R(250°C) = -41\ kJ/mol\ CO_2\ formed$$

The Fischer-Tropsch synthesis is thus a highly exothermic reaction, and the combination of the Fischer-Tropsch synthesis with the water gas shift reaction increases the overall heat generated even more. Thus, the heat removal in this process is one of the technological challenges to make the process viable.

The Fischer-Tropsch synthesis produces one mole of water for every mole of CO converted to carbon in an organic product compound. The usage ratio of hydrogen to carbon monoxide, i.e. the rate at which hydrogen is consumed relative to the rate at which carbon monoxide is being consumed, equals 2, if the water gas shift reaction does not occur. If all the water formed in the Fischer-Tropsch reaction is consumed in the water gas shift reaction, then the overall H_2/CO usage ratio would be 0.5. Knowledge on the actual usage ratio is important, since the hydrogen content in the effluent depends on the hydrogen content in the feed gas and the usage ratio. Furthermore, the water gas shift reaction results in a significant loss of carbon to CO_2.

The water gas shift reaction is suppressed, if cobalt is used as the catalyst for the Fischer-Tropsch synthesis, as proposed for gas-to-liquid Fischer-Tropsch based processes (GTL). In the absence of the water gas shift reaction, the H_2/CO usage ratio is around 2 matching the hydrogen to carbon monoxide ratio of the synthesis gas [Clark and Walker, 2002]. Iron based catalysts, which catalyze the water gas shift reaction, are preferred for coal-to-liquids Fischer-Tropsch processes (CTL) since synthesis gas produced from coal have a significant lower H_2/CO-ratio [Clark and Walker, 2002].

The Fischer-Tropsch process is very capital intensive [Jess *et al.*, 1999]. For a typical Fischer-Tropsch plant, purified syngas production normally accounts for 60-70% of costs of the end products [Dry, 2002]. Therefore efficient use of the synthesis gas, and matching the synthesis gas composition to the H_2/CO usage ratio in the Fischer-Tropsch reaction is imperative for the overall economics of a Fischer-Tropsch plant.

Raje *et al.* [1997a] argues that the CO conversion per pass of a low temperature Fischer-Tropsch reactor must be limited, since at high CO conversion the methane selectivity increases. However, a low CO conversion results in a lower rate of hydrocarbon production, and typically a higher selectivity for the water gas shift reaction, i.e. a higher CO_2-selectivity. This will thus result in a lower H_2/CO-usage ratio.

For the economically viable operation of an iron-based Fischer-Tropsch technology, two options are available: (i) use a diluted feed, such as nitrogen-rich synthesis gas, thereby saving on synthesis gas costs [Jess *et al.*, 1999] or (ii) recycle of the unconverted synthesis gas that leaves the reactor, after condensation of the liquid products (or use a number of reactors in series with intermediate condensation of the products).

Syntroleum has developed the concept on utilization of a diluted feed further by the production of synthesis gas by gasification using air in the reformers, which yields a nitrogen rich synthesis gas [Arcuri *et al.*, 2001; Kennedy, 2001]. It was claimed that this is more economical than the traditional Fischer-Tropsch process. The tail-gas from the Fischer-Tropsch processes using a nitrogen-rich synthesis gas cannot be recycled because of the high inert (nitrogen) content. A combined power plant uses this tail-gas to generate electricity making the process more attractive. However, this process concept still needs to be proven on a larger scale.

Recycling of the unconverted tail-gas into the Fischer-Tropsch reactor will result in higher overall conversions and hence more efficient use of the synthesis gas. The tail-gas from the Fischer-Tropsch reactor contains un-reacted synthesis gas, CO_2, water vapour and lower hydrocarbons (olefins, paraffins and oxygenates).

Most low temperature Fischer-Tropsch process flow diagrams do not consider recycling the tail-gas directly back into the Fischer-Tropsch reactor because of varying H_2/CO ratio and the high CO_2 content. In most process flow diagrams the tail-gas is recycled back to the synthesis gas preparation section. In the recycle loop the condensable material (organic product compounds and water) are removed. In principal carbon dioxide can be removed as well [Benham *et al.*, 1997; Clark and Walker, 2000; Bohn and Benham, 2001] or can be fed back to the synthesis gas preparation section [Arcuri *et al.*,2001; Schanke *et al.*, 2003].

1.2. THESIS AIMS AND SCOPE

The major aim of this thesis is to understand the effect of recycling the tail gas directly back into the Fischer-Tropsch process utilizing an iron-based catalyst. Recycling the tail gas will lead to a variation in the hydrogen to carbon monoxide ratio of the feed. Thus, the effect of H_2/CO ratio in the fresh feed will be investigated as well. More specifically, the following key questions will be investigated:

i) How does the recycle ratio, with varying H_2/CO ratios in the feed, affect the conversion?
ii) Do any of the constituents in the tail-gas participate in secondary reactions and to what degree?
iii) Does recycling CO_2 in the tail-gas change the water gas shift activity, and the product selectivity?

2

LITERATURE REVIEW

Fischer-Tropsch synthesis is a heterogeneously catalysed process whereby synthesis gas (a mixture of carbon monoxide and hydrogen) is converted to a range of alkenes, alkanes and oxygenated compounds. Synthesis gas can be produced from carbon-based materials such as coal, biomass, refinery bottoms and natural gas. Hence, the Fischer-Tropsch synthesis can be considered as an alternate to crude oil for the production of liquid fuels (gasoline and diesel) and chemicals [Dry, 1999].

There are a number of metals, which have sufficient activity in the Fischer-Tropsch synthesis for industrial application, such as iron, cobalt, nickel and ruthenium [Schulz, 1999; Dry, 2003]. Nickel is, however, too hydrogenating, resulting in high CH_4 yields whereas ruthenium is rare and too expensive for use in large scales. Therefore, only iron and cobalt-based catalysts are being used in commercial Fischer-Tropsch plants.

Vosloo *et al.* [2004] presented a realistic comparison of cobalt and iron based catalysts for the FT process from Sasol's perspective. They showed that cobalt based catalyst are more suitable for natural gas processes whilst iron based catalysts can be used for both natural gas and coal derived synthesis gas processes. Furthermore, they showed that iron based catalysts are preferred at higher temperatures for the production of gasoline and chemicals.

There are currently two modes of operation for the Fischer-Tropsch synthesis, each with its specific selectivity targets. The high temperature (300–350°C) Fischer-Tropsch process (HTFT) aims at the production of gasoline and linear low molecular mass olefins whereas the low temperature (200–240°C) Fischer-Tropsch process (LTFT) is used for the production of diesel and high molecular mass linear waxes [Dry, 2002].

The Fischer-Tropsch reaction yields a wide spectrum of hydrocarbons and oxygenated compounds [Wender, 1996]. These reactions producing water as a co-product can stoichiometrically be written as:

Methanation	$3H_2 + CO$	→	$CH_4 + H_2O$
Paraffins	$(2n + 1)H_2 + nCO$	→	$C_nH_{2n+2} + nH_2O$
Olefins	$2nH_2 + nCO$	→	$C_nH_{2n} + nH_2O$
Methanol	$2H_2 + CO$	→	CH_3OH
Higher Alcohols	$2nH_2 + nCO$	→	$C_nH_{2n+1}OH + (n\text{-}1)H_2O$

The formation of methane is a limiting case in the Fischer-Tropsch synthesis, in which the formation of the C-C bond does not occur. Olefins and paraffins are the major products of the Fischer-Tropsch synthesis. The formation of oxygenated compounds, such as alcohols, is observed to some extent during the Fischer-Tropsch synthesis [Wender, 1996].

Water can react further in the water gas shift reaction yielding carbon dioxide.

Water Gas Shift	$H_2O + CO$	→	$CO_2 + H_2$

Other reactions that may occur under the conditions of the Fischer-Tropsch synthesis are:

Carbon deposition	$H_2 + CO$	→	$C + H_2O$
Boudouard reaction	$2CO$	→	$C + CO_2$
Carbide formation	$xM + C$	→	M_xC

The valuable products of the Fischer-Tropsch synthesis can be condensed out. What remains is the tail-gas, which comprises of water vapour, CO_2, N_2, unreacted synthesis gas and gaseous hydrocarbons (C_1-C_5). The FT tail-gas can be recycled back to the synthesis gas preparation units or back to the FT reactor inlet or burned as fuel or sent to a power generation plant [Shah *et al.*, 2003].

2.1. USAGE RATIO IN THE FISCHER-TROPSCH SYNTHESIS

The usage ratio is the amount of hydrogen consumed relative to the amount of carbon monoxide consumed in the Fischer-Tropsch process. In order to obtain a high overall conversion of the synthesis gas fed to the Fischer-Tropsch reactor, the composition of the feed gas should match the usage ratio of the Fischer-Tropsch synthesis. According to the stoichiometric equations a usage ratio of 2.0 is obtained, if only alcohols and alkenes are formed. The usage ratio for the formation of paraffins is higher than 2.0 and decreases with increasing carbon chain length to approach the limiting case of a usage ratio of 2.0 for paraffins with an infinite long chain length. Dry [2002] states that the usage ratio for a cobalt based catalyst under typical low temperature Fischer-Tropsch (LTFT) conditions to be about 2.15. This is higher than 2.0 due to the formation of paraffins. For iron-based catalysts, the usage ratio is typically lower due to the simultaneous WGS reaction. The usage ratio for an iron-based catalyst in a fixed bed reactor at 225°C is *ca.* 1.65 [Dry, 2003].

The exit H_2/CO ratio in the Fischer-Tropsch synthesis can be lower or higher than the initial H_2/CO ratio at the inlet of the reactor, depending on whether the initial H_2/CO ratio is lower or higher than the usage ratio. Espinoza *et al.* [2004] illustrated the change in the exit H_2/CO ratio of a FT reactor with a cobalt-based catalyst for different conversions when the initial H_2/CO ratio is below, at and above the usage ratio of 2.15 (see Figure 2.1).

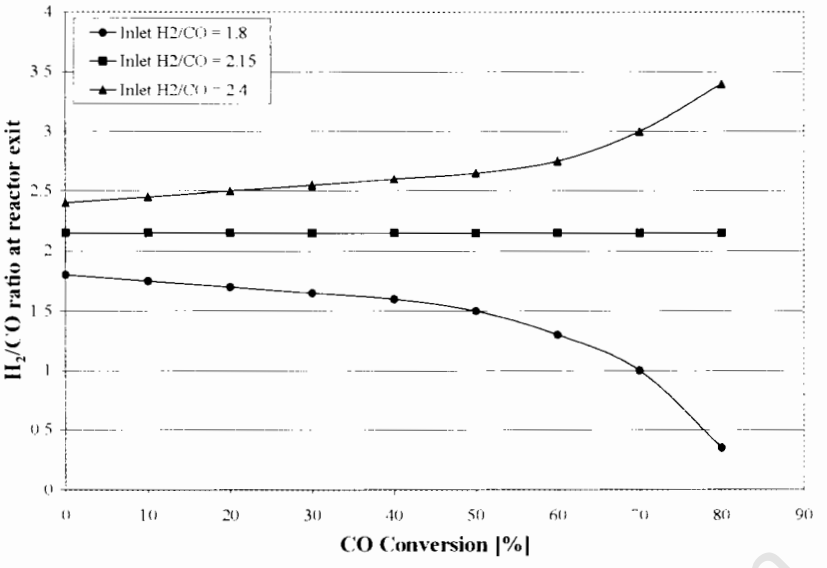

Figure 2.1 The change in the exit H_2/CO ratio of a FT reactor for a cobalt based catalyst for different conversions when the inlet H_2/CO ratio is different from the usage ratio (adapted from Espinoza *et al.* [2004]).

Hence, when the initial H_2/CO ratio is lower than the usage ratio, then the H_2/CO will be even lower at the exit of the reactor, and with recycle or using multistage reactor systems, the H_2/CO with decrease with each successive pass through the reactor. On the other hand, when the initial H_2/CO is higher than the usage ratio, the H_2/CO will increase with each successive pass through the reactor. Boelee *et al.* [1989] reported similar trends for an iron based catalyst.

2.2. SYNTHESIS GAS PREPARATION

The composition of synthesis gas must match the usage ratio in the Fischer-Tropsch synthesis in order to minimize wastage of carbon monoxide or hydrogen. This is of great importance to the economics of the Fischer-Tropsch process, since synthesis gas production accounts for more than half the capital cost investment and a disproportionate share of the operating costs for a GTL

complex [Wilhelm *et al.*, 2001]. The normal production route of synthesis gas is by partial oxidation of carbonaceous materials such as methane, coal, biomass, naphtha, residual oil and petroleum coke.

2.2.1. Natural Gas Reforming

The principal technologies for producing synthesis gas from natural gas feed are summarized and compared in Table 2.1 [Wilhelm *et al.*, 2001].

Steam methane reforming (SMR), in which methane and steam are catalytically converted to synthesis gas is the predominant commercial technology. An alternative is partial oxidation, which is the non-catalytic reaction of methane and oxygen to produce synthesis gas. The partial oxidation process of methane is an exothermic process whereas steam reforming of methane is an endothermic process. The other major difference is the resulting composition of the synthesis gas. The synthesis gas produced by steam reforming of methane has a higher H_2/CO ratio than the synthesis gas produced by partial oxidation of methane. The synthesis gas composition from either process can be manipulated by altering various process conditions and/or by means of additional process steps as shown in Table 2.2. Nonetheless, neither process is ideally suited for GTL applications since FT synthesis with a cobalt based catalyst requires a H_2/CO ratio of about 2.

An alternative to this is autothermal reforming (ATR), which combines partial oxidation with catalytic steam reforming in one reactor. ATR is basically a stand alone, single step process for feedstock conversion to synthesis gas. However, the same idea can be applied to reactors fed by partial reformed gases from a primary reformer. This is commonly referred to secondary reforming.

Table 2.1 Comparison of synthesis gas production technologies from methane [Wilhelm *et al.*, 2001].

Technology	Advantages	Disadvantages
Steam Methane Reforming (SMR)	Commercial experience	H_2/CO ratio higher than required for FT
	Oxygen is not required	Highest air emissions
	Lowest process temperature	
Partial Oxidation (POX)	Feedstock desulphurization is not needed	H_2/CO ratio lower than required for FT, especially for cobalt based catalysts.
	Expensive catalyst not needed	
	Lower CO_2 content in synthesis gas	Higher process temperature
	Low methane slip	Requires oxygen
		Soot formation adds complexity
Autothermal Reforming (ATR)	H_2/CO ratio favourable for FT	Limited commercial experience
	Low methane slip	Requires oxygen
	Lower process temperature than POX	
Heat exchange reforming	Compact size	Limited commercial experience
	Flexibility to increase capacity	In most cases, must be used in tandem with another method
Two-step reforming (SMR followed by oxygen-blown secondary reformer)	Size of SMR is reduced	Higher process temperature than SMR
	Low methane slip	Requires Oxygen

Table 2.2 Methodologies for adjusting H_2/CO ratios in synthesis gas.

Technique	Decreases H_2/CO ratio	Increases H_2/CO ratio
Recycle CO_2	X	
Import CO_2	X	
Remove H_2 via membrane	X	
Remove CO_2		X
Increase steam		X
Add shift converter		X

In the case of an iron based FT process the tail-gas contains CO_2, which can be recycled to the reformers and can thus aid in the reduction of the resulting H_2/CO-ratio, since it participates directly in the reforming reaction as reported by Dry [2003].

$$CH_4 + CO_2 \rightarrow 2CO + 2H_2$$

2.2.2. Coal Gasification

Coal gasification is the only important method for synthesis gas production from coal. Some processes have achieved commercial success on an industrial scale over the past several decades such as the Lurgi pressure gasification process and the Kopper-Totzek atmospheric gasification process [Song and Gou, 2004].

Coal gasification is influenced by a number of parameters such as operating temperature and pressure, but also by the characteristics of the coal used such as coal rank, pore structure and mineral matter content. The low hydrogen content of coal results in a H_2/CO ratio far below 1 after gasification. Steam is usually added to increase the H_2/CO ratio. The synthesis gas is purified to remove CO_2 and H_2S before being sent to the Fischer-Tropsch reactors. The H_2/CO ratio of the Sasol/Lurgi gas after purification is about 1.8, which is well suited for the low temperate FT process using an iron based catalyst [Dry, 2002].

2.2.3. Co-Gasifying Coal and Natural Gas

Song and Gou [2004] presented a new process for synthesis gas production based on co-gasifying coal and natural gas. This process (see Figure 2.2) can theoretically produce a synthesis gas with the desirable H_2/CO ratio by varying the feedstock. The ratio of oxygen to methane in the feed is the key factor in determining the final H_2/CO ratio and the concentration of H_2 and CO. When the O_2/CH_4 ratio is below 1, the H_2/CO ratio is greater than 1 and the concentration of H_2 and CO in the raw synthesis gas is greater than 90%.

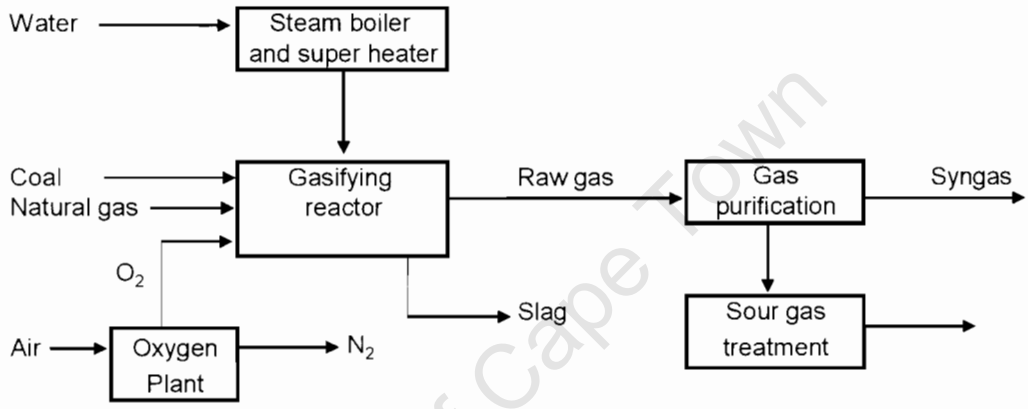

Figure 2.2 Flow sheet for the synthesis gas production from coal and natural gas co-gasifying [Song and Gou, 2004].

2.2.4. Biomass Gasification

The Fischer-Tropsch synthesis utilizing synthesis gas derived from biomass has received some interest recently [Jun *et al.*, 2004]. The biomass-derived synthesis gas consists of H_2, CO, CO_2 and CH_4. Although the composition is not suitable for direct use in FT, its composition can be adjusted by methane reforming, water-gas shift reaction and CO_2 removal.

Biomass growth by photosynthesis from CO_2 and H_2O is an attractive alternative to fossil fuels because it is a useful source for recycle and for fixation of CO_2. An almost infinite number of different feeds, process and product

combinations exist but not all are feasible. For instance, direct combustion of high moisture content algae is technically possible but energetically unfavourable [Slaghuis, 1995].

2.3. CURRENT AND FUTURE FISCHER-TROPSCH COMPLEXES

The Fischer-Tropsch synthesis is currently commercially applied at four different locations in the world, i.e. Sasolburg, Secunda, and Mossel Bay (all in South Africa) and Bintulu (Malaysia). The increasing demand for energy, especially from rapidly developing countries such as China, coupled with the uncertainty and expense of crude oil imports has led to a renewed interest in Fischer-Tropsch technology. Table 2.3 lists the announcements of new Fischer-Tropsch projects worldwide, and confirms the interest by the major petrochemical companies in the Fischer-Tropsch technology. ExxonMobil, Syntroleum and Rentech are the major new companies involved in Fischer-Tropsch; Gas-to-Liquids (GTL) conversion projects. Sasol and Shell are considered as the forerunners since they both have commercial operations (the PetroSA/Mossgas plant in South Africa is operated using Sasol's proprietary knowledge).

Vosloo [2001] attributed to this renewed interest to the improved cost-effectiveness of the Fischer-Tropsch technology, in conjunction with the need to monetize remote or stranded natural gas fields and the environmental pressure to minimize flaring gas associated with oil drilling. Others have stated that the Fischer-Tropsch technology is still above its break-even-point, due to the high capital costs associated with the Fischer-Tropsch process [Jess *et al.*, 1999]. For a typical FT plant, Dry, [2002] reports that purified synthesis gas production normally accounts for 60-70% of costs of the end products. However, the alternatives to the Fischer-Tropsch process, such as liquefaction of natural gas and its transportation are also uneconomical over these distances. This requires a capital-intensive cryogenic chain: a liquefaction plant, cryogenic tankers, and a re-gasification plant at the receiving terminal. The chemical liquefaction of the

natural gas via the Fischer Tropsch process at the source will dramatically reduce these costs.

Table 2.3 Existing and planned Fischer-Tropsch plants in the world

Name of company	Scale of production [bpd]	Location
	Existing plants	
Sasol	105 000	Secunda, South Africa
	20 000	Sasolburg, South Africa
PetroSA (Mossgas)	30 200	Mossel Bay, South Africa
Shell	12 500 – 15 000	Bintulu, Malaysia
	Plants under construction	
Sasol-Chevron	30 000	Nigeria
Qatar Shell GTL Ltd	140 000 *)	Qatar
Sasol and QP	30 000	Qatar
	Feasibility studies under way	
Shell	70 000	Trinidad
Shell	70 000	Argentina
Shell	70 000	Sabah, Malaysia
Shell	70 000	Indonesia
Shell	70 000	Egypt
Shell	70 000	Iran
Syntroleum	10 000	Australia
	Business plans	
ExxonMobil	50 000	Angola
ExxonMobil	50 000	North Slope, Alaska
QP and ExxonMobil	100 000	Qatar
Rentech	15 000	Indonesia
Rentech	2 000	Commerce City, USA
Reema International	10 000	Trinidad

(Sources: www.vs.ag.ida.gtl_marketibilty and *) www.shell.com)

Various Fischer-Tropsch plant layouts have been proposed. Of particular interest is the inclusion of recycle streams in the various plant lay-outs. Dry [2003] gives more detailed description of these plant layouts.

2.3.1 Lay-out of the Low Temperature Fischer-Tropsch Plant at Sasol (Sasolburg, South Africa)

The low temperature Fischer-Tropsch (LTFT) process (see Figure 2.3) is operated at the Sasolburg plant using an iron-based catalyst in both multi-tubular and slurry reactors [Dry, 2003]. The process is optimized to produce linear alkanes and waxes, which are hydro-treated and fractionated into various products. The plant was initially designed to operate with synthesis gas produced from coal gasification but has recently changed to synthesis gas derived from natural gas via methane reforming [Dry, 2003].

The tail-gas from the Fischer-Tropsch reactors, which contains methane, ethylene, ethane and unconverted synthesis gas, is treated in a cryogenic unit to extract the hydrogen for ammonia synthesis [Dry, 2003]. Town gas, which is used for heating purposes, is obtained by blending a part of the tail-gas with methane and Rectisol gas (a purified synthesis gas stream). The remaining gas is recycled to the reactors after being catalytically reformed and scrubbed to lower the carbon dioxide content.

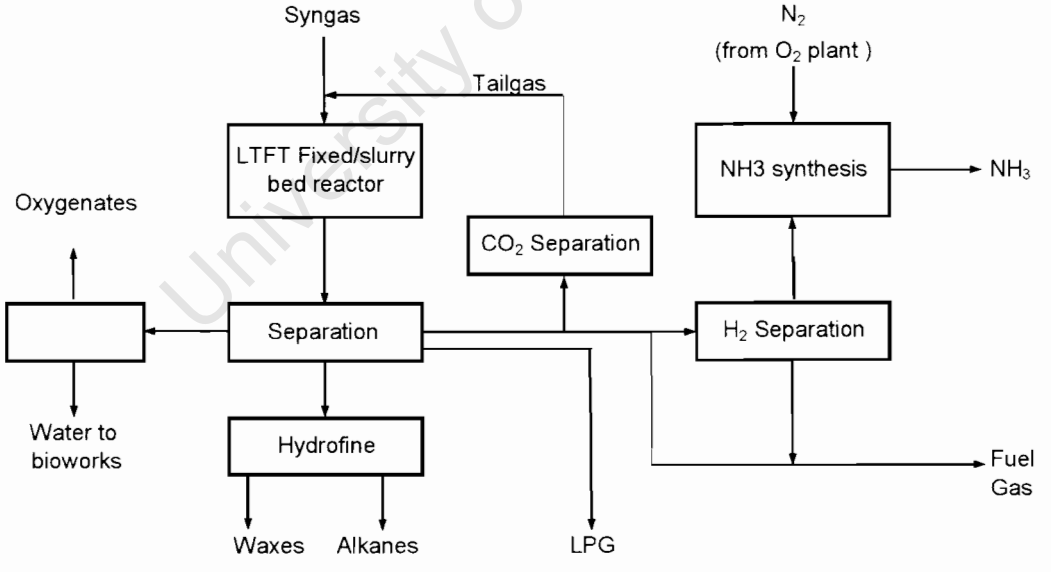

Figure 2.3 Flow sheet for the Sasol LTFT plant in Sasolburg, South Africa. [Dry, 2003].

2.3.2 Lay-out of the High Temperature Fischer-Tropsch Plant at Sasol (Secunda, South Africa)

The high temperature Fischer-Tropsch (HTFT) operated at Secunda utilizes fluidized-bed reactors to maximize the yield of alkenes and gasoline [Dry, 2003]. Figure 2.4 shows a simplified block diagram of the overall process. The synthesis gas production and associated ammonia plants are similar to the Sasolburg plant, when coal gasification was utilized at that site.

The tail-gas is, just like in the case of the Low Temperature Fischer-Tropsch Synthesis (see chapter 2.3.1), cryogenically converted into hydrogen rich, methane rich and three light hydrocarbon streams. The latter is further fractionated and purified to produce pure 1-alkenes. The bulk of the methane rich gas is catalytically reformed auto-thermally [Dry, 2003] and the synthesis gas is recycled to the FT reactors with the balance sold as fuel gas.

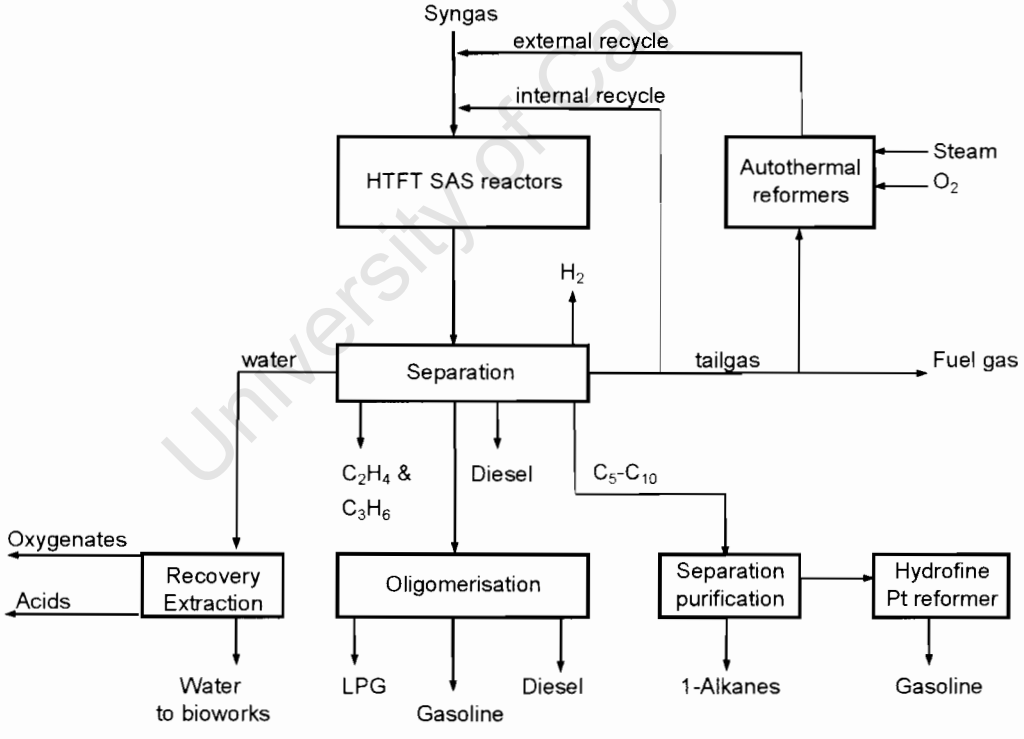

Figure 2.4 Flow sheet for the Sasol HTFT plant in Secunda, South Africa [Dry, 2003].

2.3.3 Lay-out of the High Temperature Fischer-Tropsch Plant at PetroSA (Mossel Bay, South Africa)

The high temperature Fischer-Tropsch (HTFT) operated in Mossel Bay by PetroSA utilizes circulating fluidized bed reactors [Dry, 2003]. Figure 2.5 shows a simplified block diagram of the overall process. The plant, which came on stream in 1992, produces gasoline and diesel from a synthesis gas derived from off-shore natural gas. The synthesis gas is fed to circulating-fluidised-bed (CFB) reactors over an iron-based catalyst.

The hydrocarbons in the tail-gas are recovered in a cryogenic unit. Butane from the natural gas is isomerized with the C_3 and C_4 alkenes produced in the Fischer-Tropsch synthesis to produce high-octane gasoline [Dry, 2003]. The tail-gas containing unconverted synthesis gas, carbon dioxide, methane, ethylene and ethane is recycled to the secondary reformers before being fed back into the FT reactors [Dry, 2003].

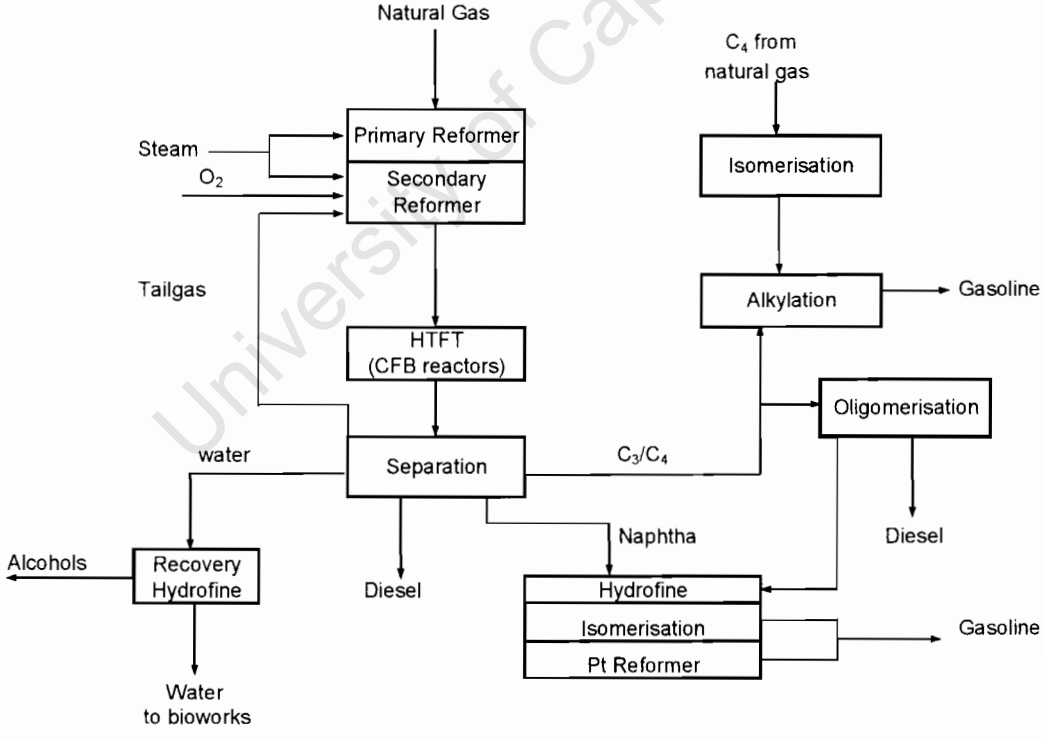

Figure 2.5 Flow sheet for the high temperature Fischer-Tropsch plant (PetroSA, Mossel Bay, South Africa) [Dry, 2003].

2.3.4 Lay-out of the Low Temperature Fischer-Tropsch Plant at Shell (Bintulu, Malaysia)

The Shell Middle Distillate Synthesis (SMDS) plant, which came on-stream in 1993, produces wax through the Fischer-Tropsch process from synthesis gas [Dry, 2003]. Figure 2.6 shows a simplified block diagram of this process. The synthesis gas is produced from off-shore natural gas using Shell gasification. The H_2/CO ratio of the synthesis gas is approximately 1.7 and since this is below the usage ratio of about 2.15 required for the cobalt-based catalyst, additional hydrogen-rich gas is required. This is provided by catalytically reforming of the tail gas produced in the Fischer-Tropsch process. After condensing the FT products the tail-gas is fed to the catalytic reformer to generate synthesis gas with a high hydrogen content, which is recycled to the FT reactors.

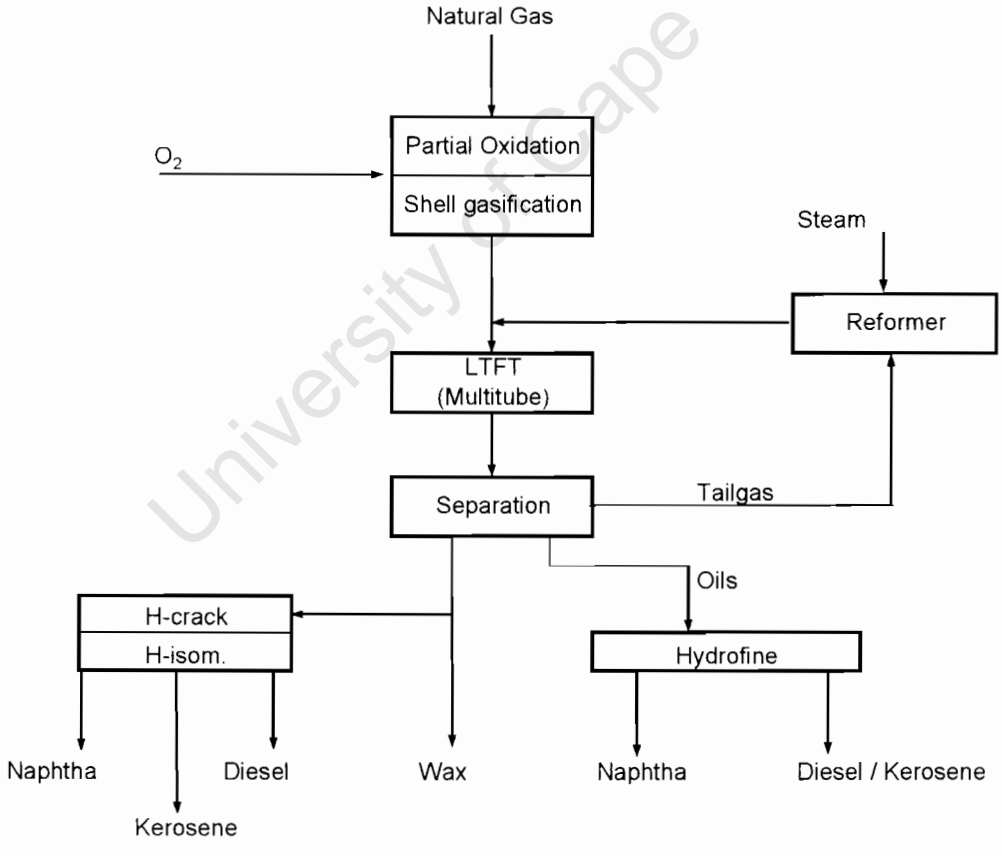

Figure 2.6 Flow sheet for the Shell FT plant in Bintulu, Malaysia [Dry, 2003].

2.3.5 Lay-out of the Exxon AGC-21 Process

Exxon developed the Advanced Gas Conversion for the twenty-first century (AGC-21) process (see Figure 2.7) with the aim of exploiting natural gas in remote areas. The proposed process is a three-staged operation:

(i) synthesis gas production

(ii) slurry FT synthesis

(iii) hydro-isomerisation/hydro-cracking of the heavy FT products to transportable liquids.

The AGC-21 process has been demonstrated by Exxon in a 8000ton/year unit at Baton Rouge (Louisiana, USA) using a cobalt-based catalyst [Dry, 2003]. The proposed process shows a part of the tail-gas, containing C_1-C_4 hydrocarbons, is recycled with the remainder being used as fuel gas.

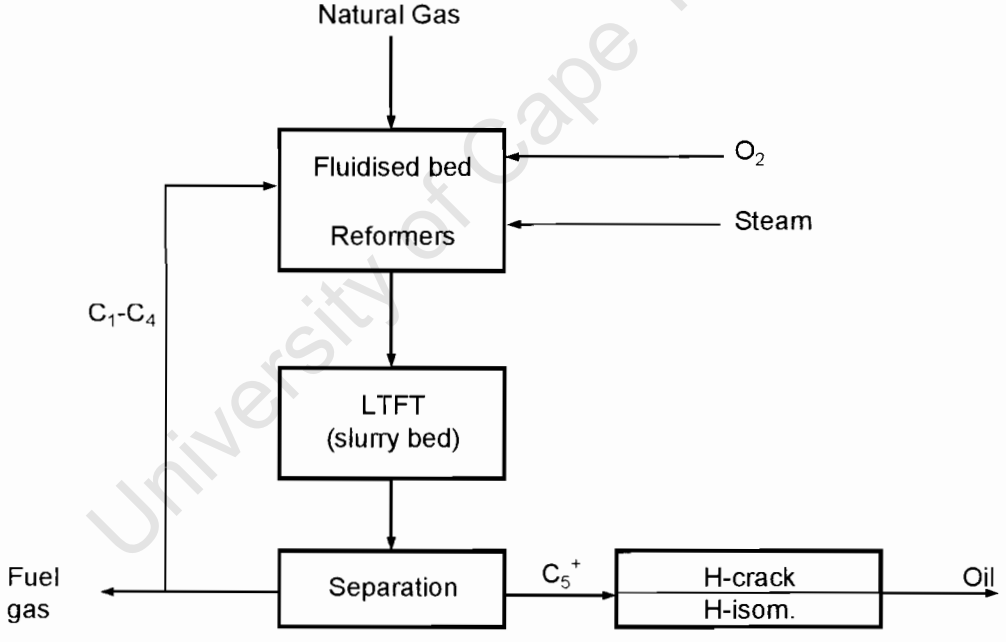

Figure 2.7 Flow sheet for the proposed Exxon AGC-21 process [Dry, 2003].

2.3.5 Lay-out of the Syntroleum Process

Syntroleum developed a process based on the gasification using air instead of oxygen (see Figure 2.8). A low-pressure air blown autothermal reformer is followed by low pressure FT synthesis [Dry, 2003]. This results in a lower cost of synthesis gas production since the oxygen plant and recycle compressor are not needed. Adjusting the water and carbon dioxide fed to the reformer controls the H_2/CO ratio of the synthesis gas. However, the synthesis gas contains approximately 50% nitrogen, since air is being used for the production of synthesis gas.

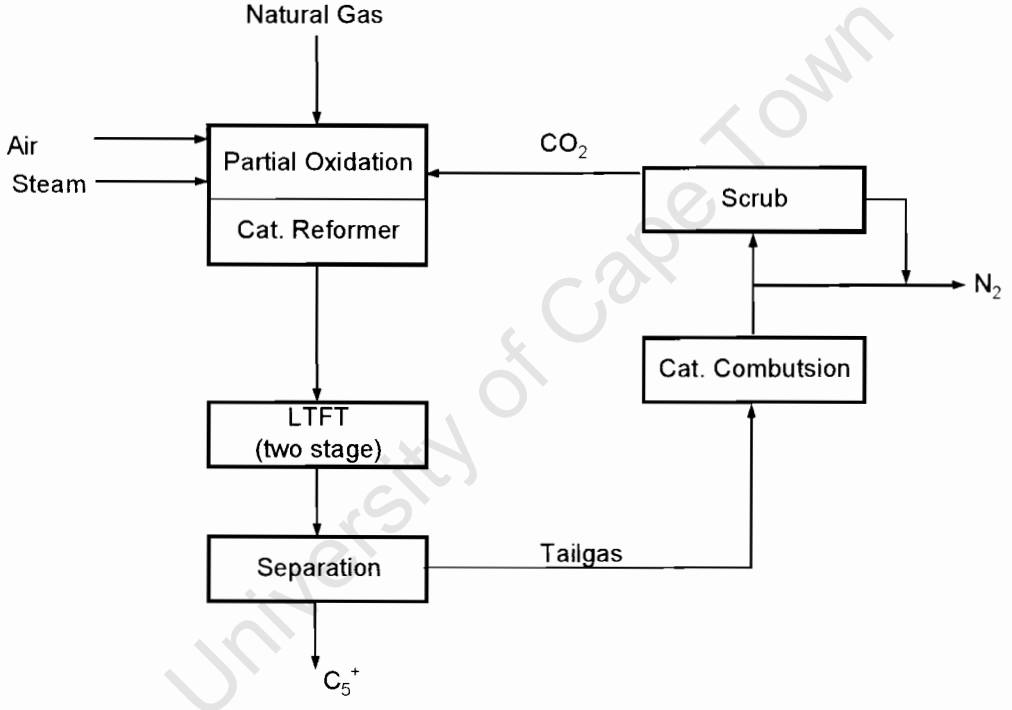

Figure 2.8 Flow sheet for the proposed Syntroleum process [Dry, 2003].

The tail-gas, which contains all the C_1-C_5 hydrocarbons, is catalytically combusted. A portion of the CO_2 produced is recovered and recycled to the reformer. The disadvantage of this process is that the Fischer-Tropsch tail-gas cannot be recycled to the reformer because of the high N_2 content and the wax

selectivity is low due to the low pressure used in the Fischer-Tropsch synthesis [Dry, 2003]. However, Syntroleum has proposed using a combined electricity plant, which uses the tail-gas from the FT unit to drive the turbines. This has made the Syntroleum process an interesting concept but there's a need for a demonstration plant on a larger scale. Furthermore, increasing the wax selectivity will also make the process more feasible.

2.4. RECYCLING DURING THE FISCHER-TROPSCH PROCESS

The most common FT plant schemes recycle the tail-gas back to the synthesis gas preparation section with CO_2-removal [Benham *et al.* 1997; Clark and Walker, 2000; Bohn and Benham, 2001] or without CO_2 removal [Arcuri *et al.*, 2001; Schanke *et al.*, 2003].

The tail-gas from the Fischer-Tropsch reactor contains un-reacted synthesis gas, CO_2, water vapour and lower hydrocarbons (olefins, paraffins and oxygenates). This stream can in principal be recycled back to the Fischer-Tropsch reactor, and thereby reducing the load on the reformers. However, it is necessary to understand what effects of the constituents in the tail gas will have on the Fischer-Tropsch process when this stream is recycled back directly to the Fischer-Tropsch reactors.

2.4.1 Influence of Recycling on Activity

2.4.1.1 Effect of changing H_2/CO ratio

Raje and Davis [1997b] illustrated the benefits of low single-pass synthesis gas conversion with recycle (see Table 2.4). The H_2/CO ratio of the unconverted recycle synthesis gas and the fresh feed is the same for this case and hence need not be adjusted. The recycle reactor can process more than double the volume of synthesis gas per weight of iron and produces twice as much hydrocarbons as the single pass reactor. The yield of the light alkenes was also increased. This is expected since the space velocity through the recycle reactor

was higher. Furthermore, the removal of CO_2 from the recycle stream was considered, which is, however, a costly step.

Table 2.4. Comparison of a single pass reactor with a recycle reactor [Raje and Davis, 1997b]

	Single pass reactor	Recycle reactor
Single pass CO conversion, %	90 %	67 %
Fresh feed : recycle ratio	-	2 : 1
Space velocity through reactor, Nl/h-gFe	3.1	10
Synthesis gas throughput, Nl/h-gFe	3.1	6.7
Total hydrocarbon yield, g/h-gFe	0.55	1.1
C_2 and C_3 alkene yield, g/h-gFe	0.06	0.15
Linear C_6 1-alkene yield, g/h-gFe	0.006	0.018
Linear C_{10} 1-alkene yield, g/h-gFe	0.0015	0.007
Linear C_{14} 1-alkene yield, g/h-gFe	0.0005	0.002

Sorensen *et al.* [2003] claim a control scheme for optimum liquid fuel production in a slurry reactor using a variable syngas composition. This is accomplished by adjusting the recycle ratio, water addition and bypass glow. Table 2.5 summarises these results. Case 1 is the base case with the H_2/CO ratio equal to 1 and the recycle ratio equal to 0.5. Cases 2 and 3 represent a swing to CO-rich and H_2-rich syngas respectively.

Over the range of cases illustrated, the methanol production rate and purge gas rate are controlled within 5% of the base case. For the CO-rich syngas, water was added to shift the water gas shift equilibrium and thereby increasing the H_2/CO ratio within the reactor. In contrast, for the H_2-rich syngas, the recycle ratio is reduced to zero and there is no water addition. In this thesis, a similar optimum control scheme for wax production will be developed by varying the recycle ratio and fresh feed syngas composition.

Table 2.5 Control measures and results for optimum control scheme [Sorenson et al., 2003]

	Case 1	Case 2	Case 3	Case3A
Control measures:				
Recycle ratio	0.5	2.0	0.0	0.5
Water addition, lb moles/hr	0	200	0	0
Bypass flow, lb moles/hr	0	0	0	300
Results:				
Space velocity, l/hr-kg	4500	9000	3000	3150
% conversion	40.0	41.4	39.3	55.9
Methanol production rate, lb moles/hr.	122	123	118	116
Fuel Gas purge rate, MMBtu/hr LHV	61.0	61.0	60.0	60.1

2.4.1.2 Effect of CO_2

Recently a variety of countermeasures have been undertaken to mitigate the accumulation of CO_2 in the atmosphere. Among the methods of chemical fixation, the catalytic hydrogenation of CO_2 into liquid fuels via the FT process has received much interest.

Riedel *et al.* [1999] showed that iron and cobalt catalysts behaved differently in CO_2 hydrogenation. With the iron catalyst, the same hydrocarbon product distribution was obtained with a H_2/CO and H_2/CO_2 syngas, whereas with a cobalt catalyst, the product composition shifted towards CH_4 at lower CO content in the syngas. A similar conclusion was obtained by Zhang *et al.* [2002] for a cobalt based catalyst.

Hong *et al.* [2001] studied the deactivation on precipitated Fe-Cu-K-Al catalysts in CO_2 hydrogenation. Significant decreases in activity and selectivity were observed after 1500h at 300°C and 10atm. In this work, lower temperatures are employed which will result in less reverse water gas shift activity and hence lower water partial pressures in the reactor. Furthermore, based on the work by

Riedel *et al.* [1999], the recycling of CO_2 should not show a major deviation in the product distribution.

Chemicals, mainly olefins and alcohols, via the FT process have also received attention due to demand of these high value products. Fiato *et al.* [1992] claims a process for producing C_2-C_{20} olefins from a feed stream consisting of H_2 and CO_2 using an iron-carbide catalyst at LTFT conditions. Both oxygenates and hydrocarbons were produced when CO_2 was added to the syngas feed, as reported by Xu *et al.* [1997]. In that study it was also shown that when CO_2 is present at low concentrations (0.2 mol % of CO), it can initiate chain growth but does not contribute to a measurable amount of chain propagation. However, when CO_2 is present in a larger amount relative to CO (CO_2/CO = 3), the water gas shift reaction was rapid relative to that of the FT reaction.

For high temperature Fischer-Tropsch synthesis the water gas shift reaction is sufficiently rapid so that it is nearly at equilibrium [Dry, 2003], whereas at low temperature Fischer-Tropsch conditions, the reaction is far from equilibrium. The removal of water causes in the case of high temperature Fischer-Tropsch synthesis the water gas shift equilibrium to shift so that it favours the production of CO. The CO formed, as a result undergoes hydrogenation yielding hydrocarbons.

Unlike the above studies in which CO_2 was hydrogenated directly, Kölbel [1954] used a multistage recycle reactor system where substantial amounts of water were removed between the stages. Various hydrocarbons were produced using an iron oxide based catalyst at temperatures between 280 and 340ºC. Kölbel's work is different from the prior art where neither recycle nor water removal are employed and different from this thesis where lower temperatures are used. Moreover, Kölbel's process required several passes to efficiently convert the recycled CO_2.

2.4.1.3 Effect of water

Iron-based catalysts have a high activity for the water gas shift reaction. For the high temperature Fischer-Tropsch synthesis the water gas shift reaction is at equilibrium and this determines the partial pressure of water. At low temperature Fischer-Tropsch conditions, the reaction is far from equilibrium. Davis [2003] studied the effect of water partial pressure on a Fe-based catalyst at 270°C, H_2/CO = 0.7 and 11.6bar. Davis reported that above 50% CO conversion, the water gas shift reaction becomes rate controlling, i.e. the FTS rate becomes dependent upon the production of H_2 by the water gas shift reaction. They also reported little impact of water in the fresh feed upon the Fischer-Tropsch synthesis at low concentration of water. However, when H_2O/CO levels in the feed reached a high level (significantly greater than 1), the catalyst oxidizes, which results in loss of all FTS activity. A similar result was recently observed by Biel [2004] as well.

2.4.2 Secondary Reactions during the Fischer-Tropsch Synthesis

The tail gas contains besides unreacted syngas, CO_2, water vapour and some inerts, also olefins and alcohols. These compounds may undergo secondary reactions [Schulz and Claeys, 1999]. Secondary reactions are defined as reactions following re-adsorption of primarily formed products on the surface sites. Primarily formed 1-olefins may undergo following secondary reactions:

- Double bond isomerisation yielding internal olefins;
- Hydrogenation yielding a paraffin;
- Chain initiation;
- Insertion into a growing hydrocarbon chain;
- Cracking/hydrogenolysis.

Co-feeding alkenes and small oxygenates (methanol, ethanol, DME, etc) to the synthesis feed gas during Fischer-Tropsch (FT) synthesis has been the subject of many studies [Boelee *et al.*, 1989; Hanlon and Satterfield, 1998; Schulz and Claeys, 1999; Snel and Espinoza, 1987, 1989a, 1989b, 1989c; Tau et al., 1987,

1990, 1991, 1992] concerned with the determination of reaction intermediates, the role of secondary reactions and the possibility of changes to the usual Anderson-Schulz-Flory distribution.

2.4.2.1 *Effect of changing H_2/CO ratio*

Recycling the tail gas back to the reactor will alter the hydrogen to carbon monoxide ratio in the reactor. This is the most important parameter [Dry, 1981], which controls the selectivity for the precipitated iron catalyst at low temperatures, whereas the CO_2 partial pressure appeared to dictate the product selectivity for the fused catalysts at higher temperatures. An increase in the H_2 partial pressure results in termination of the surface species to paraffins whilst an increase in the CO partial pressure results in higher probability of the chain growth. Thus one could expect that the higher the H_2 partial pressure and the lower the CO partial pressure or the higher the H_2/CO ratio, the higher will be the production of CH_4 and lighter hydrocarbons and the lower the production of heavier hydrocarbons such as wax. This relationship is shown in Figure 2.9 for the selectivity for hardwax.

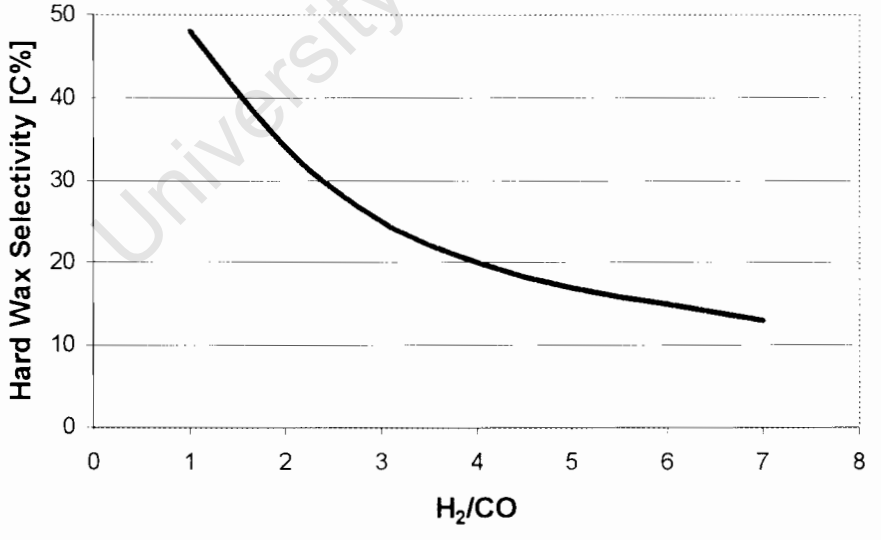

Figure 2.9: The selectivity of hard wax (bpt. > 500°C) as a function of the H_2/CO ratio. *Adapted from Dry [2002].*

2.4.2.2 Effect of recycling olefins

The tail gas contains olefins, since linear α-olefins are the main primary organic products of FT synthesis. Once formed they can readsorb at the catalyst surface and undergo secondary reactions: hydrogenation, isomerisation (double-bond shift), re-insertion, hydrogenolysis and hydroformylation. These secondary reactions strongly depend on reaction conditions (temperature, partial pressure of H_2, CO and H_2O and residence time), the catalyst used and olefin chain length. Table 2.6 summarizes the findings reported in literature. These studies were done at different reaction conditions than used during low temperature Fischer-Tropsch synthesis (240°C and 20bar with H_2/CO = 1.8). Furthermore it must be noted that most of the experiments were performed in fixed micro-bed reactors.

A few researchers have reported a decrease in the CH_4 formation during their co-feeding studies. Snel and Espinoza [1987, 1989a, 1989b, 1989c] co-fed different olefins with varying concentrations mixed with syngas over an iron catalyst at 270ºC and 20bar. They reported a 50% decrease in CH_4 selectivity when co-feeding 10% ethene with the synthesis gas and suggested that fast ethene readsorption followed by incorporation and hydrogenation reactions with C_1 and H-surface species were the reasons for this decline in CH_4 formation. Furthermore they reported that CH_4 formation was suppressed when the ethene concentration was 5 mol% and higher. This concentration-dependent decrease in CH_4 was also reported with butene and propene.

Schulz and Claeys [1999] reacted 1-olefins of different chain lengths over a cobalt catalyst. They confirmed a chain length dependency of secondary olefin reactions. This is a relevant result since the tail-gas contains olefins of different chain lengths. It is expected that these olefins will react differently and also exhibit competitive adsorption with the other species such as the alcohols in the tail-gas.

Table 2.6 Summary of published research on co-feeding olefins during Fischer-Tropsch Synthesis (on Fe catalysts)

INVESTIGATION	EXPERIMENTAL CONDITIONS	CONCLUSIONS	REFERENCE
Co-feeding 1-olefins	Slurry reactor with fused magnetite catalyst at 248°C and 7.8-15 bar.	Olefin was hydrogenated to the corresponding paraffin or isomerised to the 2-olefin. CH_4 formation decreased and olefin/paraffin ratio increased when ethylene was added. No effect on chain growth probability..	Hanlon and Satterfield, 1998
Co-feeding ethene	Fixed bed micro-reactor with Fe catalyst at 270°C and 20 bar.	Initiates Fischer-Tropsch synthesis without altering chain growth probability. CH_4 formation was suppressed (for ethene concentration > 5 mol%).	Snel and Espinoza, 1987
Co-feeding propene	Fixed bed micro-reactor with Fe catalyst at 270°C and 20 bar.	Propene acts as a scavenger of surface hydrogen, thereby causing a propene concentration-dependent increase in olefin selectivity and a decrease in CH_4 selectivity.	Snel and Espinoza, 1989b
Co-feeding butane	Fixed bed micro-reactor with Fe catalyst at 270°C and 20 bar.	Both branched and linear butenes can initiate chain growth but not propagation. Activity and CH_4 formation dependent on butene concentration.	Snel and Espinoza, 1989c
Addition of alkenes	CSTR with promoted fused iron catalyst at 260°C and 7 bar.	Pentenes, both 1-pentene and a mixture of *cis*-2- plus *trans*-2-pentene are inert toward secondary reactions during Fischer-Tropsch synthesis. 1-Decene undergoes isomerisation, hydrogenation and incorporation whereas ethene undergoes only the latter two conversions.	Tau *et al.*, 1990

2.4.2.2.1 Modeling Olefin re-adsorption

Detailed kinetic modeling to account for the above-mentioned secondary reactions of olefins has been reviewed by Claeys and Van Steen [2004]. Schulz and Claeys [1999] developed an extended model (see Figure 2.10), in which olefins can re-adsorb yielding a variety of product compounds. The model puts particular emphasis on the solubility of olefins in the liquid phase.

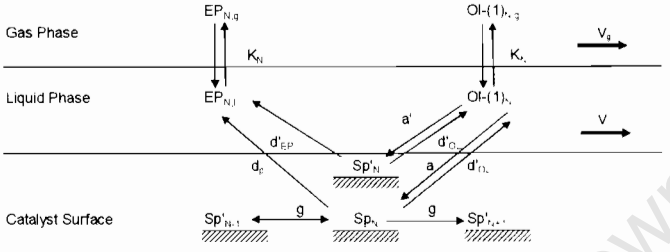

Figure 2.10 Kinetic scheme of the secondary olefin reactions taking into account the solubility of olefins in liquid FT product [Schulz and Claeys, 1999].

2.4.2.3 Effect of recycling alcohols

The tail gas contains also some alcohols, which may undergo secondary reactions. Table 2.7 summarizes the reported findings on secondary reactions of alcohols in the Fischer-Tropsch synthesis.

Tau *et al.* [1992] co-fed normal and iso-alcohols at 264ºC and 6.8bar over a fused iron catalyst. They reported that the n-alcohols initiate chains to produce n-alkanes. Iso-alcohols initiate chains that produce branched hydrocarbons. Furthermore, both alcohols dehydrogenate to aldehydes and ketones. In earlier contrasting work Tau, *et al.* [1991] reported that the n-alcohols undergoes two additional reactions: one is decarboxylation to produce CO_2 and the other is hydrogenation to produce the alkane with the same carbon number. In this work done at similar conditions (260ºC and 7bar) they also concluded that alcohols

Table 2.7 Summary of published research on co-feeding alcohol during Fischer-Tropsch Synthesis (on Fe catalysts)

Investigation	Experimental conditions	Conclusions	Reference
Co-feeding ethanol	Slurry reactor with fused magnetite catalyst at 248°C and 7.8-15 bar.	CH_4 formation decreased and olefin/paraffin ratio increased when ethanol was added. No effect on chain growth probability.	Hanlon and Satterfield, 1998
Co-feeding of normal and isoalcohols.	1L stirred autoclave reactor with fused Fe catalyst and octacosane solvent at 264°C and 6.8 bar.	n-Alcohol initiation leads to n-hydrocarbons whereas iso-alcohol initiates chain growth that leads to iso-hydrocarbons. Both alcohols dehydrogenate to aldehyde or ketone. n-alcohols produce normal alkanes and alkenes in greater yield than iso-products.	Tau *et al.*, 1992
Addition of methanol or ethanol	Tubular fixed bed reactor with CuO/ZnO catalyst at 330°C and 40-70 bar	C3+ alcohols increased with small traces of methane.	Lachowska and Skrzypek, 1998
Addition of ethanol	1L stirred autoclave reactor with Fe-SiO_2 catalyst and octacosane solvent at 265°C and 6-7 bar	Ethanol was dehydrogenated to acetaldehyde.	Tau *et al.*, 1987
Co-feeding small oxygenates	Fixed bed micro-reactor with Fe catalyst at 270°C and 20 bar.	Both dimethyl and diethyl ether lead to an increase in activity while acetaldehyde suppressed activity. No significant change in the α value.	Snel and Espinoza, 1989a
Addition of n-alcohols	Both fixed bed and CSTR at 260°C and 7 bar with fused and precipitated catalysts.	Alcohols initiates but does not propagate chain growth. The alcohol undergoes 2 additional reactions: one is decarboxylation to produce CO_2 and the other is hydrogenolysis to produce the alkane with the same carbon number.	Tau *et al.*, 1991

can serve as chain initiators but do not lead to significant chain propagation.

Most work up to date has been performed with ethanol, which is like ethene the most reactive of the n-alcohols. The exact extent of this reactivity relative to the reactivity of olefins is not known yet.

2.5 REACTION KINETICS

2.5.1 Rate of the Fischer-Tropsch Reaction

Both simple and detail Fischer-Tropsch reaction kinetics have been developed. Huff and Satterfield [1984], Zimmerman and Bukur [1990] and van der Laan and Beenackers [1999] review of the kinetic equations for iron-based catalysts. They concluded that the kinetic rate expressions reported for the Fischer-Tropsch process don't illustrate a uniform picture.

Anderson [1956], proposed a rate expression which includes water inhibition:

$$r_{FT} = \frac{k \cdot p_{CO} \cdot p_{H_2}}{p_{CO} + a \cdot p_{H_2O}} \tag{2.1}$$

This equation was also derived by Dry [1976] from the enol/carbide mechanism, assuming the hydrogenation of chemisorbed CO was the rate-determining step. Furthermore, it assumed that CO and H_2O adsorbed more strongly than either H_2 or CO_2. Shen *et al.* [1990] and Zimmerman *et al.* [1990] used this expression for a precipitated commercial Fe/Cu/K catalyst.

Huff and Satterfield [1984] modified equation (2.1) to include a linear decrease in the adsorption parameter, *a*, with the partial pressure of hydrogen:

$$r_{FT} = \frac{k \cdot p_{CO} \cdot p_{H_2}^2}{p_{CO} \cdot p_{H_2} + a \cdot p_{H_2O}} \tag{2.2}$$

Equation (2.2) can also be derived from either the carbide or enol/carbide mechanism. In the carbide mechanism, the rate-determining step is assumed to

be the hydrogenation of surface carbon whereas in the enol/carbide mechanism, it is the hydrogenation of the surface enol. Zimmerman *et al.* [1990] show that equations [2.1] and [2.2] have the same form if the constant *a* in equation [2.1] depends on the hydrogen partial pressure, i.e. $a_1 = a_2 / p_{H_2}$. Shen *et al.* [1995] obtained the same activation energy with equation (2.2) for their data than that with equation (2.1).

Ledakowicz *et al.* [1985] included CO_2 inhibition in their equation which is also a modification to equation [2.1]:

$$r_{FT} = \frac{k \cdot p_{CO} \cdot p_{H_2}}{p_{CO} + a \cdot p_{CO_2}} \tag{2.3}$$

This equation can be derived from the enol mechanism with hydrogenation of surface CO as the rate-determining step.

Van Steen and Schulz [1999] disputed the need of a rate-determining step in the derivation of a kinetic expression for the Fischer-Tropsch synthesis. They presented a new equation for describing the kinetics of consumption of CO for the formation of organic compounds in the Fischer-Tropsch synthesis for both Fe and Co based catalysts.

$$r_{c,org} = \frac{k \cdot \frac{p_{H_2}^{1.5} \cdot p_{CO}}{p_{H_2O}}}{\left(1 + a \cdot \frac{p_{H2} \cdot p_{CO}}{p_{H_2O}}\right)^2} \tag{2.4}$$

2.5.2 Rate of CO_2-Formation under Fischer-Tropsch Conditions

The Fischer-Tropsch synthesis can be formulated with water as the main co-product. With iron-based catalysts, carbon dioxide is formed as well. This may occur through a consecutive reaction of water with carbon monoxide through the water gas shift reaction. Carbon dioxide might be viewed as an alternative

way to remove adsorbed oxygen formed through the dissociation of carbon monoxide, from the catalyst surface.

Zimmerman and Bukur [1990] tested a number of models to fit their experimental WGS rates. Some of their kinetic expressions contain the same functional form of the denominator as used in their kinetic expressions to describe the rate of the Fischer-Tropsch synthesis implying that CO_2 is formed on the same sites as the Fischer-Tropsch synthesis occurs. One of their expressions is presented here:

$$r_{CO_2} = \frac{k_w \cdot \left(p_{H_2O} \cdot p_{CO} - p_{CO_2} \cdot p_{H_2} / K_P\right)}{p_{CO} \cdot p_{H_2} + a \cdot p_{H_2O}} \tag{2.5}$$

Van der Laan and Beenackers [1999] concluded in their literature review that only a few studies have considered the kinetics of the water gas shift reaction over iron-based catalysts in the Fischer-Tropsch synthesis. Van der Laan and Beenackers [2000] formulated a rate expression for the formation of CO_2 in the Fischer-Tropsch synthesis starting with elementary reactions. They assumed that the water gas shift reaction takes place on different sites than the Fischer-Tropsch reaction. They assumed that the formation of the formate species is the rate-determining step. If formate is through the reaction of adsorbed carbon monoxide and a surface hydroxyl species, the rate of formation of CO_2 can be expressed as:

$$r_{CO_2} = \frac{k_w \cdot \left(p_{H_2O} \cdot p_{CO} - p_{CO_2} \cdot p_{H_2} / K_P\right)}{\left(1 + a \cdot p_{CO} + b \cdot p_{H_2O}\right)^2} \tag{2.6}$$

If the formate species is formed by a reaction between adsorbed carbon monoxide and adsorbed water, the rate of formation of CO2 can be expressed as:

$$r_{CO_2} = \frac{k_w \cdot \left(\frac{p_{H_2O} \cdot p_{CO}}{\sqrt{p_{H_2}}} - p_{CO_2} \cdot \sqrt{p_{H_2}} / K_P\right)}{\left(1 + a \cdot p_{CO} + b \cdot p_{H_2O}\right)^2} \tag{2.7}$$

All three proposed rate expressions for the formation of CO_2 take into account the limitation through the water gas shift equilibrium. The equilibrium constant of the water gas shift reaction can be determined from:

$$K_P = 0.0102 \cdot e^{\frac{4730}{T}} \qquad [2.8]$$

2.6. CHAPTER SUMMARY AND RELATION TO PRESENT STUDY

There are currently two Fischer-Tropsch modes. The high temperature (300–350ºC) process (HTFT), with iron-based catalysts, is used for the production of gasoline and linear low molecular mass olefins. The low temperature (200–240ºC) process (LTFT), with either iron or cobalt catalysts, is used for the production of diesel and high molecular mass linear waxes [Dry, 2002].

The purified synthesis gas production in a typical Fischer-Tropsch plant normally accounts for 60-70% of costs of the end products [Dry, 2002]. Synthesis gas production accounts for more than half the capital cost investment and a disproportionate share of the operating costs for a Gas-to-Liquid complex. Therefore efficient use of the synthesis gas is imperative for the overall economics when constructing a Fischer-Tropsch plant.

It is beneficial from a hydrocarbon productivity standpoint to limit the synthesis gas conversion in the reactor to a lower value [Raje *et al.*, 1997a), due to the inhibition of the rate of the Fischer-Tropsch synthesis by product water [e.g. Huff and Satterfield, 1984]. This also results in a lower water-gas shift reaction rate. Furthermore, high conversion, with the resulting high partial pressure of water, may lead to catalyst deactivation due to oxidation [Davis, 2003, Biel, 2004]. The unconverted synthesis gas in the tail gas can either be recycled back to the reformer or, as is studied here, recycled back to the reactor to obtain a higher overall synthesis gas conversion. Recycling the tail gas back to

the reactor would lead to a lower load on the reformer and improve the overall energy efficiency of the Fischer-Tropsch plant.

If the usage ratio of the catalyst matches the H_2/CO ratio in the fresh feed, then recycling the tail-gas isn't complicated. The usage ratio for an iron-based catalyst in a fixed bed reactor at 225ºC is *ca*. 1.65 for a synthesis gas with a H_2/CO in the fresh feed of ca. 2.0 [Dry, 2003]. Since the rate of H_2 conversion can be different from that of CO, the exit H_2/CO ratio can be lower or higher than the initial H_2/CO ratio at the inlet of the reactor, depending on whether the initial H_2/CO ratio is lower or higher than the usage ratio.

The tail-gas from the Fischer-Tropsch reactor contains un-reacted synthesis gas, carbon dioxide, water vapour and lower hydrocarbons (olefins, paraffins and oxygenates). Controversies about the proper use of the tail-gas from a FT plant still exist. Literature shows that olefins, alcohols and even CO_2, all of which are present in a typical tail-gas stream from a FT reactor, can participate in secondary reactions.

3

EXPERIMENTAL APPARATUS AND PROCEDURES

3.1 REACTOR SET-UP

The experimental system (see Figure 3.1) consisted of gas delivery system, reactor system, hot and cold traps, a recycle line, back pressure regulator, on-line gas chromatograph (TCD and FID) for the analysis of the tail gas and vent system.

Synthesis gas was either delivered from gas bottles (H_2, 99.999%; CO: 99.97%) or came directly from the commercial reformers. Commercial APG gas was used for the experiments with a fresh feed H_2/CO ratio of 2. Argon is co-fed as an internal standard for the gas analysis. The gases are fed using mass flow controllers. A side stream can be taken from the gas feed line to analyze the feed gas composition. The fresh feed gas is mixed with the recycle stream.

A stirred reactor was used in this study with a volume of 500ml. The reactor has a double-blade stirrer to ensure good mixing of both the liquid and the gas phase under reaction conditions. The feed line enters the reactor at the top and reaches all the way down to 5 mm above the bottom stirrer. Both the gaseous and liquid products leave the reactor through a filter to ensure that the catalyst remains in the reactor. The temperature in the reactor is measured by two thermocouples, one of which measures the temperature in the liquid phase and the other one is

inserted between the heating mantle and the reactor wall. The temperature of the liquid phase is controlled.

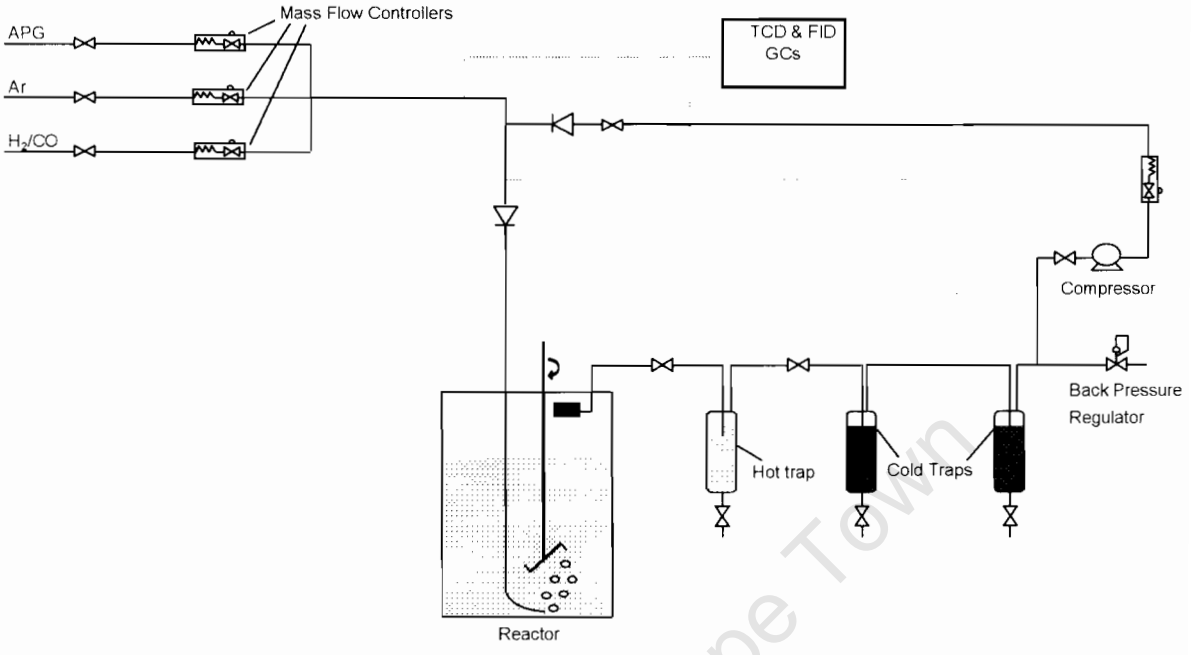

Figure 3.1 Flow Scheme of Micro-Slurry Reactor with recycle

The mixed product stream from the reactor passes a hot trap where the liquid, which is carried with the product stream, is separated from the vapour stream. The hot trap was kept at 200°C. The vapour stream then passes through two cold traps, which are kept at room temperature, in which water and organic product compounds are condensed out. From the cold traps, the water phase and the oil phase are taken for product analysis. The second cold trap was put in place to ensure equilibrium conditions. The tail gas composition can be determined using an on-line gas chromatograph. The amount of water in the tail gas can be neglected, since equilibrium water partial pressure of water at the conditions of the cold trap is very low (saturation water partial pressure at 25°C: 0.03 bar) in comparison to the water partial pressure in the reactor (typically in excess of 1 bar).

After the cold traps, the stream can be split into a recycle stream and a tail gas stream. The recycle stream is compressed. The flow rate of the recycled gas is controlled using a Brooks mass flow controller.

3.1.1 Catalyst loading

The catalyst used in this study is a precipitated iron catalyst (the same catalyst used in Sasol's LTFT process in Sasolburg). Before loading the catalyst, the reactor is heated to 150ºC to melt the wax medium. 20g of the catalyst is added to the wax medium. The reactor is then sealed and pressurized to 20bar using argon. The temperature increased to 240ºC.

3.1.2 Reduction and start-up of the Fischer-Tropsch synthesis

The catalyst is reduced *in-situ* using synthesis gas at 240ºC and 20bar for 24hr using a gas hourly space velocity (GHSV) of 6000ml/(g_{cat}·hr). Thereafter the knock-out pots are drained and the space velocity (GHSV) is reduced to ca. 5000ml/(g_{cat}·hr). The temperature and pressure are kept constant.

3.1.3 Start-up of recycle

After the catalyst has reached stable activity, the recycle line is pressurised and flushed with argon. The tail-gas from the reactor is then recycled. Due to the excess argon, the system is allowed to another 24hr to reach stability before accurate analysis can be obtained. The flow rate of the recycled gas is controlled using a Brooks mass flow controller. The actual flow rate of the recycle stream is determined by mass balances using Ar as the internal standard. Upon introduction of the recycle stream the fresh feed stream was reduced to ensure that the total feed stream through the reactor remained constant (i.e. a constant residence time in the reactor).

3.2 PRODUCT ANALYSIS

Two online gas chromatographs (GC's) were used to analyse the gases (feed, total feed and tail-gas). A gas chromatograph equipped with a thermal conductivity detector (TCD) was used to analyse for the permanent gases H_2, CO, CO_2, Ar, CH_4 and N_2 whilst a gas chromatograph equipped with a flame ionisation detector (FID) was used to analyse the hydrocarbons in the gases, including CH_4.

The liquid samples were analysed using off-line gas chromatographs. The wax sample, collected from the hot condensate pot (200°C), was analysed on one FID. The aqueous phase, collected at room temperature, was separated into a water and oil fraction and these were analysed on the other FID.

The details of the gas chromatographic separations used in this study are summarised in Table 3.1 and plots of various chromatograms are illustrated in Figures 3.2-3.6. Standard samples were used to ensure linearity of the detectors.

Table 3.1 Summary of the details for the GC's utilised.

Species	GC	Column details	Temperature [°C]	Detector
H_2	Gow-Mac 600	Restek PPQ Molecular Sieve 5Å, Packed 1m x 45.7mm	25-120	TCD
CO, CO_2, CH_4, Ar, N_2	Gow-Mac 600	Restek Shin Carbon 80/100 µ, Packed 2m x 45.7mm	25-120	TCD
Hydrocarbons in tail gas	HP 6890	Varian CP Sil 5 CP, Capillary 25m x 150µm x 20µm	25-150	FID
Water fraction	HP 6890	Varian CP Sil Pona, Capillary 50m x 210µm x 0.50µm	25-120	FID
Oil Fraction	HP 6890	Varian CP Sil Pona, Capillary 50m x 210µm x 0.50µm	25-200	FID
Wax	Shimadzu 17A	Restek MXT1 50635, Capillary 15m x 280µm x 150µm	60-400	FID

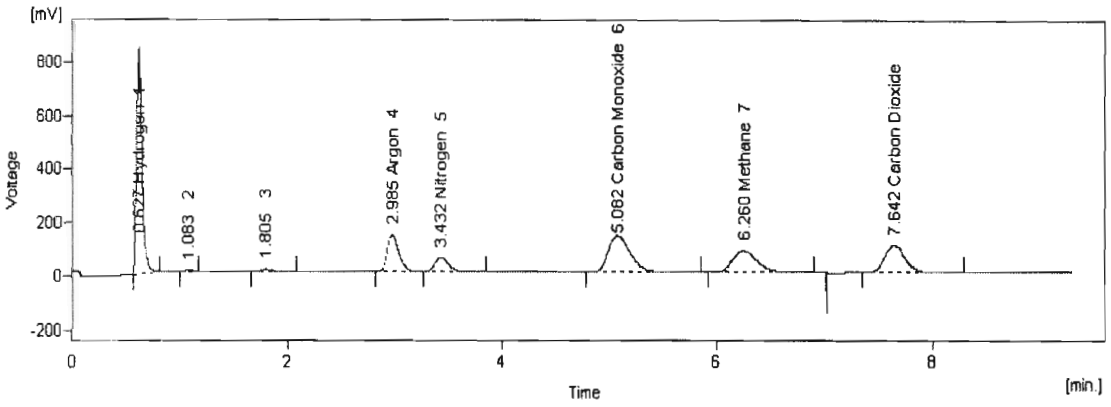

Figure 3.2: TCD-analysis of calibration gas on Gow-Mac 600 showing analysis of H_2, Ar, N_2, CO, CH_4 and CO_2

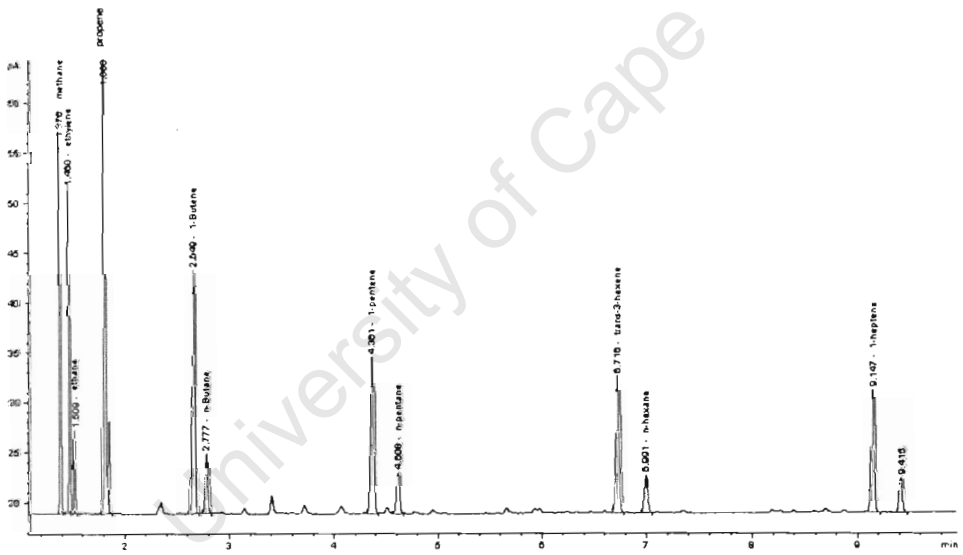

Figure 3.3: FID-analysis of organic product compounds in tail gas

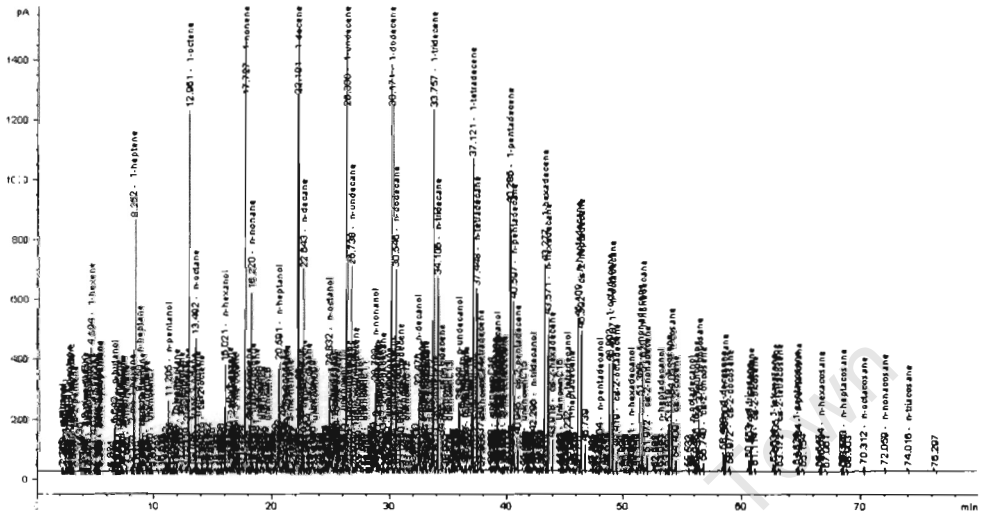

Figure 3.4: FID-analysis of organic product compounds in the oil phase

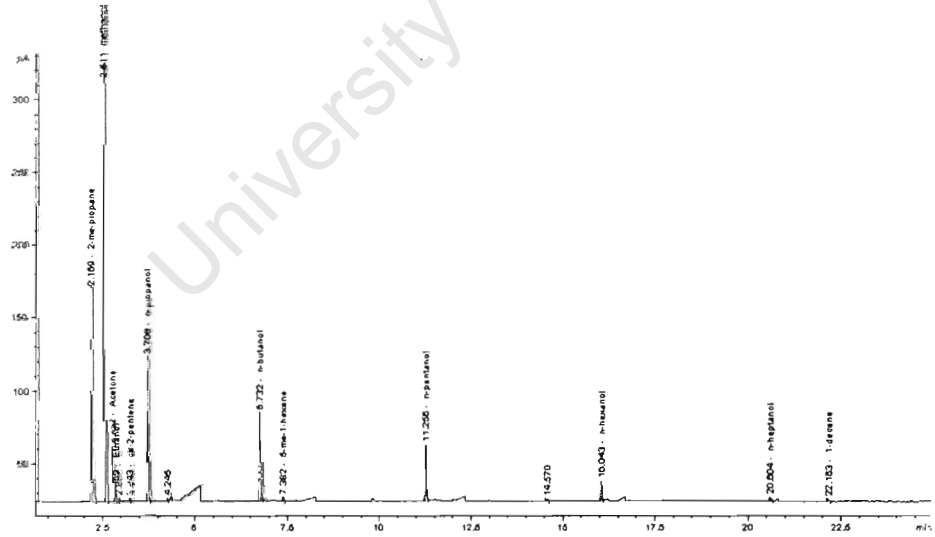

Figure 3.5: FID-analysis of organic product compounds in the water phase

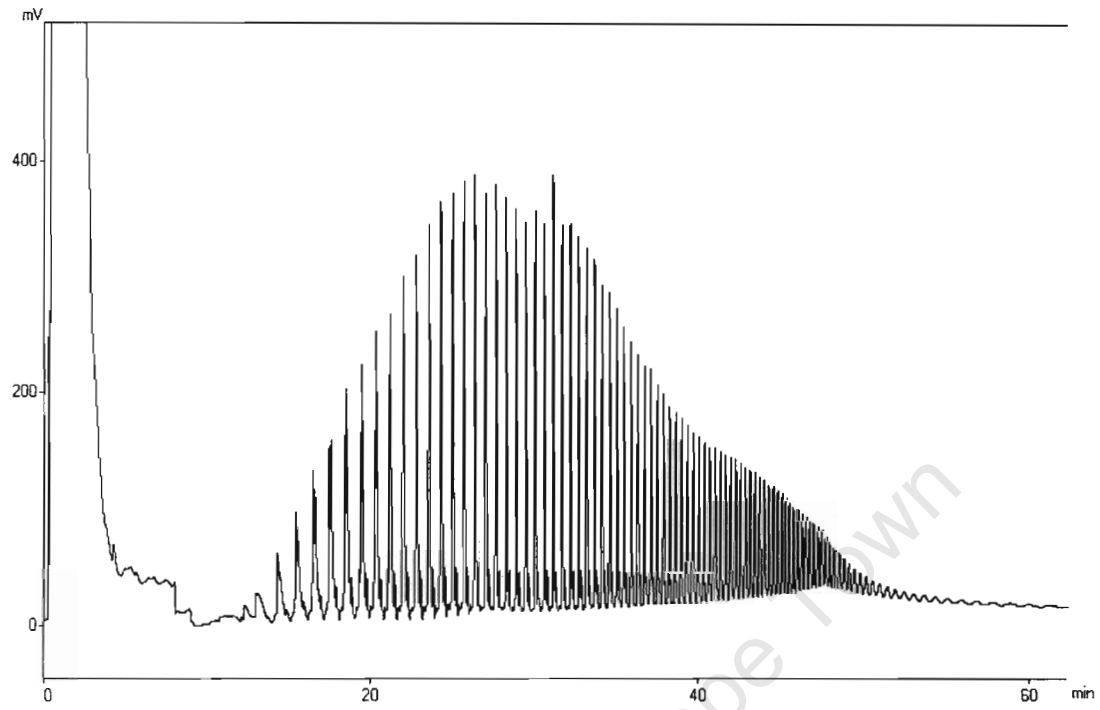

(d)

Figure 3.6: FID-analysis of liquid organic product compounds in the hot trap (200°C)

3.3 DATA EVALUATION

3.3.1 Calculation of flow rates of various compounds from gas chromatographic analysis

Argon is added to the fresh feed at a known flow rate, which is used as a basis for all flow rate calculations. The flow rates of the inorganic compounds (hydrogen, carbon monoxide and carbon dioxide) and methane can be calculated using the peak areas obtained in the gas chromatographic analysis with a TCD.

$$F_j = f_j \cdot \frac{A_j}{A_{Ar}} \cdot F_{Ar} \qquad (3.1)$$

where F_j = flow rate of compound j

F_{Ar} = flow rate internal standard, argon

f_j = compound specific calibration factor

A_j = peak area for compound j in GC trace

A_{Ar} = peak area for argon in GC trace

In the recycle experiments, argon is recycled as well. The total argon flow rate to the reactor (TF) is the sum of the argon flow rate in the fresh feed (FF) and the argon flow rate in the recycle flow (RF).

$$F_{Ar,TF} = F_{Ar,FF} + F_{Ar,RF} \tag{3.2}$$

The measured variables in those experiments are the fresh flow rate of the argon the flow rate of the recycle stream and the composition of the recycle stream. Thus, the total argon flow rate is given by:

$$F_{Ar,TF} = F_{Ar,FF} + y_{Ar} \cdot F_{RF} \tag{3.3}$$

It can be reasonably assumed that the recycle stream contains mainly H_2, CO and CO_2.

$$F_{Ar,TF} = F_{Ar,FF} + \frac{n_{Ar}}{n_{Ar} + n_{H_2} + n_{CO} + n_{CO_2}} \cdot F_{RF} \tag{3.4}$$

The total argon flow rate can thus be determined using a gas chromatographic analysis of the recycle stream:

$$F_{Ar,TF} = F_{Ar,FF} + \frac{1}{1 + f_{H_2} \cdot \frac{A_{H_2}}{A_{Ar}} + f_{CO} \cdot \frac{A_{CO}}{A_{Ar}} + f_{CO_2} \cdot \frac{A_{CO_2}}{A_{Ar}}} \cdot F_{RF} \tag{3.5}$$

The flow rate of water is calculated from an oxygen balance, i.e. the flow rates of CO and CO_2 in the feed and reactor outlet streams.

$$F_{H_2O} = F_{CO,feed} - F_{CO,tail} + 2 \cdot F_{CO_2,feed} - 2 \cdot F_{CO_2,tail} \tag{3.6}$$

The flow rate of organic product compounds can be found by relating it to the flow rate of methane, which can be linked to the flow rate of argon. This procedure can be prone to severe errors. Hence, the analysis of the organic product compounds will be limited to the selectivity within a certain fraction.

3.3.2 Calculation of partial pressures in the reactor

The partial pressures of each component is calculated by assuming the reactor to be well-mixed and therefore using the composition of the reactor outlet stream as the same as within the reactor.

$$p_i = \frac{p_i}{\sum_i p_i} \cdot p_{reactor} \tag{3.7}$$

where p_i = the partial pressure of component i

$p_{reactor}$ = total reactor pressure

3.3.3 Calculation of conversion and rate of reaction

The conversion of component i per pass and the overall conversion are calculated from the flow rate of a component i in the tail gas (TG) using the total feed flow rate (TF) and fresh feed flow rate (FF) respectively minus the tail-gas flow rate.

$$X_{i,per\ pass} = \frac{F_{i,TF} - F_{i,TG}}{F_{i,TF}} \tag{3.8}$$

$$X_{i,overall} = \frac{F_{i,FF} - F_{i,TG}}{F_{i,FF}} \tag{3.9}$$

The usage ratio, U, of H_2 to CO is defined as the amount of hydrogen consumed relative to the amount of CO consumed.

$$U = \frac{F_{H_2,FF} - F_{H_2,TG}}{F_{CO,FF} - F_{CO,TG}} \tag{3.10}$$

The rate of formation of organic Fischer-Tropsch products can be calculated from the amount of CO consumed minus the amount of CO_2 formed.

$$r_{FT} = \frac{(F_{CO,feed} - F_{CO_2,feed}) - (F_{CO,tail} - F_{CO_2,tail})}{m_{catalyst}} \tag{3.11}$$

where $m_{catalyst}$ = mass of the unreduced catalyst

The rate of the water gas shift reaction is determined from the amount of CO_2 formed.

$$r_{WGS} = r_{CO_2} = \frac{F_{CO_2,feed} - F_{CO_2,tail}}{m_{catalyst}} \quad (3.12)$$

3.3.4 Calculation of selectivity

The selectivity of component *i* is calculated relative to the amount of carbon converted. The amount of carbon is determined from the amount of CO converted to FT products, which is (CO+CO_2) conversion.

$$S_i = \frac{F_i}{(F_{CO,FF} + F_{CO_2,FF}) - (F_{CO,TG} + F_{CO_2,TG})} \quad (3.13)$$

3.4 EXPERIMENTS

The reaction conditions of the experiments are shown in Table 3.2. All the experiments are carried out at 20bar, 240°C and a total gas hourly space velocity of 5000ml/(g_{cat}·min). In all series, the reference conditions (recycle ratio = 0) were first obtained before introducing recycled tail-gas into the reactor. Furthermore, these reference conditions were checked before changing to different recycle ratios to determine if there was any catalyst deactivation. Upon the introduction of the recycle stream, the fresh feed was reduced to keep the residence time in the reactor constant.

Sampling was performed on a daily basis and a full mass balance was performed when stable conditions, based on a constant conversion value, were obtained. A minimum of two mass balances were performed before switching to another condition.

Table 3.2: Experimental conditions for the varying H_2/CO ratio in the fresh feed and varying recycle ratios in a micro-slurry reactor.

Experiment number	Run number	$(H_2/CO)_{fresh\ feed}$, mol/mol	Recycle Ratio (RR)	Fresh feed flow rate, ml(STP)/min
1	R005	2.0	0	1840
2	R005	2.0	0.8	960
3	R005	2.0	1.8	680
4	R007	1.5	0	1710
5	R007	1.5	0.8	910
6	R007	1.5	1.8	590
7	R008	1.3	0	1690
8	R008	1.3	1.7	620
9	R011	1.1	0	1750
10	R011	1.1	0.8	930
11	R012	1.4	0	1740
12	R012	1.4	0.9	930

4

RESULTS

In the experiments the effect of direct recycle of the tail gas back to the reactor after condensation of the condensable products was investigated. The catalyst was first stabilised using only the fresh feed with a specified hydrogen to carbon monoxide ratio. After stabilisation, tail gas was recycled back to reactor at a specified recycle ratio. The residence time in the reactor was kept constant by adjusting the space velocity.

4.1 FEED TO THE REACTOR

4.1.1 Molar H_2/CO Ratios

The fresh synthesis gas of all experiments, except for those with a hydrogen to carbon monoxide ratio equals two, was delivered from gas bottles. The synthesis gas for the fresh feed with a H_2/CO ratio of 2.0 was supplied by the commercial Autothermal Reformers at Sasol 1 in Sasolburg. This fresh feed also contained CO_2, and trace amounts of CH_4 and N_2.

Figure 4.1 shows the hydrogen to carbon monoxide ratio in the fresh feed, the feed to the reactor and the tail gas. The experiments were performed initially without recycle (RR=0). After stabilisation of the catalyst a part of the tail gas was recycled back to the reactor. The recycle ratio (RR) was set to 0.8 – 0.9. In some experiments a higher recycle ratio of 1.8 was tested. At the end of each experiment, the recycle ratio was reduced to zero to check for permanent deactivation of the catalyst during the recycle test.

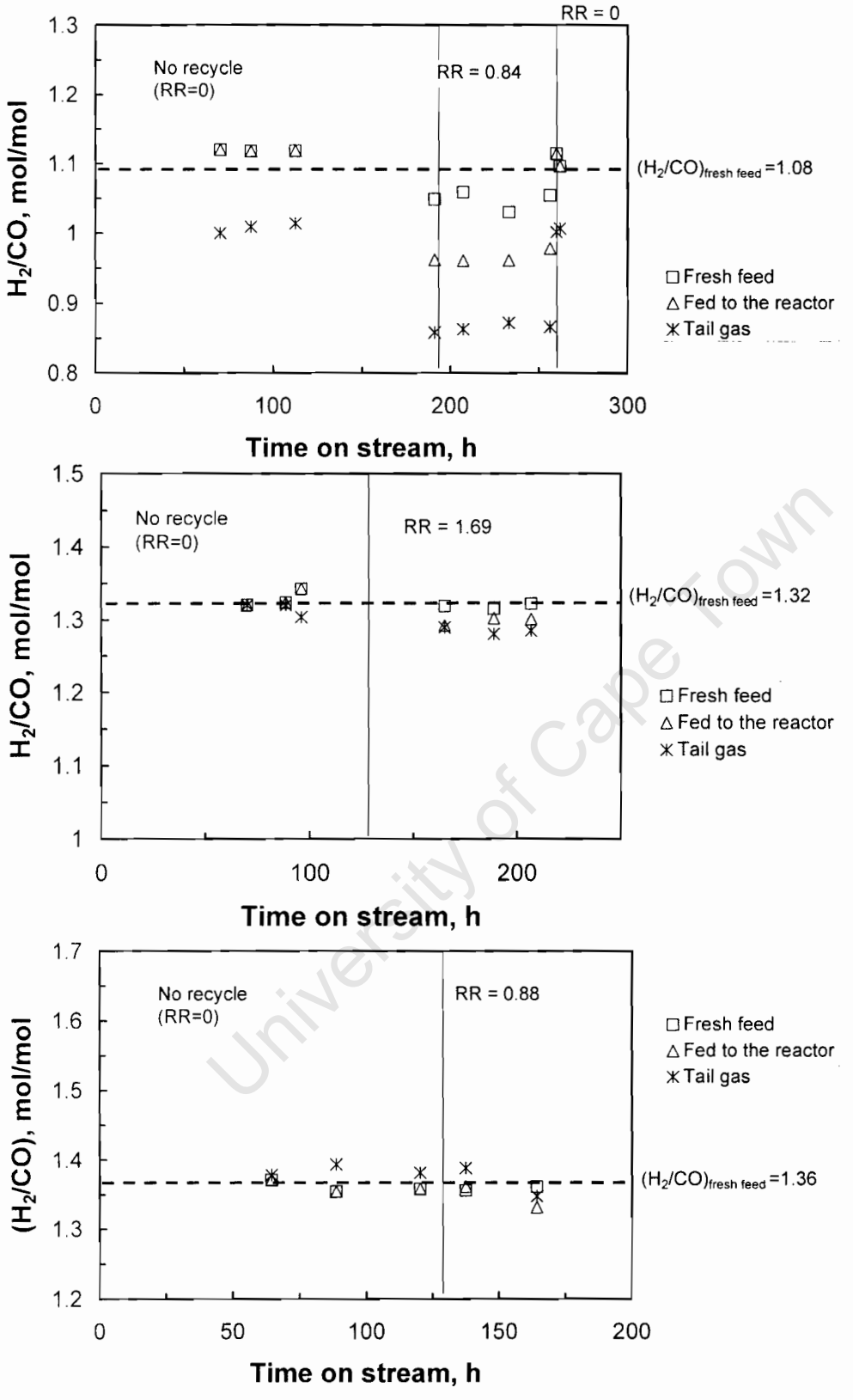

Figure 4.1: Molar H_2/CO ratio in the fresh feed, the gas fed to the reactor, and the tail gas as a function of time-on-stream

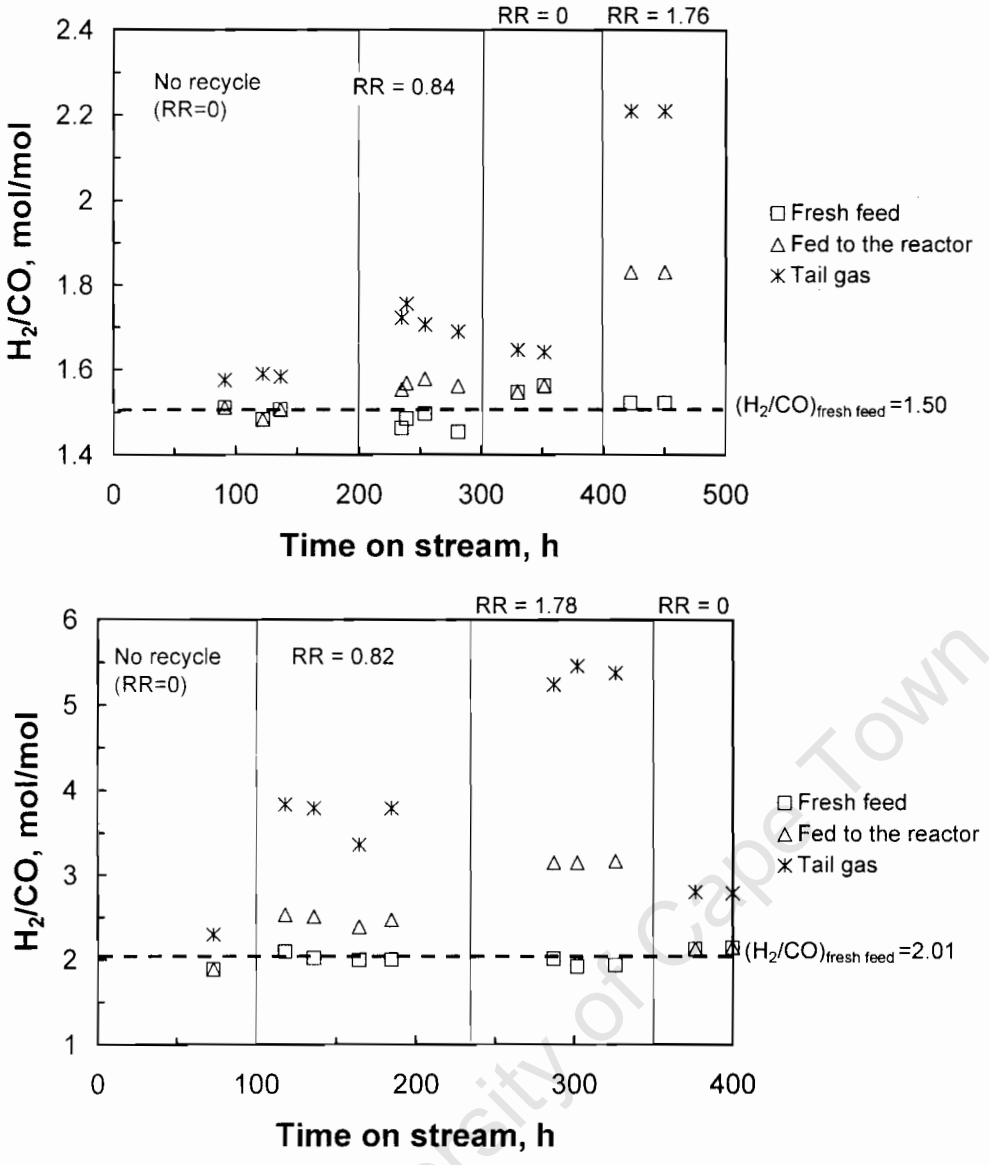

Figure 4.1 (continued): Molar H_2/CO ratio in the fresh feed, the gas fed to the reactor, and the tail gas as a function of time-on-stream

The synthesis gas with a H_2/CO ratio of 1.08 produced a tail gas, which had an even lower H_2/CO-ratio. As a consequence the H_2/CO ratio in the gas fed to the reactor dropped upon recycling the tail gas. The drop in the H_2/CO ratio in the fresh feed during the time, in which the non-condensable tail gas was recycled, can be attributed to errors in the analytical procedure. Upon reducing the recycle ratio back to zero, the performance of the system was identical to that before the introduction of the recycle. This indicates that permanent deactivation did not occur upon introduction of a recycle.

The H_2/CO-ratio did not change significantly upon introduction of a recycle for a fresh feed synthesis gas with a H_2/CO ratio of approximately 1.36. The tail gas has approximately the same H_2/CO ratio indicating that the usage ratio of H_2/CO in this system was ca. 1.4.

Fresh feed with a H_2/CO ratio of larger than 1.4 yielded a tail gas with a higher H_2/CO ratio. Hence, the feed to the reactor had a higher H_2/CO ratio upon recycling the non-condensable material in the tail gas. With increasing recycle ratio the H_2/CO ratio in the feed to the reactor becomes higher (up to 5.5 mol/mol for a synthesis gas with a H_2/CO=2.0 and a recycle ratio of 1.78). It can be seen that within the experimental error there is also no evidence for permanent deactivation upon recycling the tail gas for the fresh feed with a high H_2/CO ratio.

4.1.2 Organic Product Compounds Fed to the Reactor

Upon recycling tail gas, non-condensable organic product compounds are also recycled back to the reactor. Figure 4.2 shows the concentration of the organic product compounds in the cold tail gas and in the feed to the reactor in the synthesis with a synthesis gas with a H_2/CO ratio of 1.50 and a recycle ratio of 0.84. The concentration of the organic product compounds is low. The concentration of the organic product compounds in the feed to the reactor is even lower, since this stream is diluted with fresh feed. The ratio of the concentration of C1-C6 in the cold tail gas to the concentration of these compounds in the feed to the reactor is ca. 2.09, which corresponds well with the recycle ratio (based on the recycle ratio of 0.84, a value of 2.19 was expected).

Figure 4.3 shows the distribution of the various classes of products (paraffins, olefins and oxygenates) as a function of carbon number in the feed to the reactor (which corresponds well with the distribution in the cold tail gas). The organic products contain paraffins, olefins and oxygenates. The main oxygenate is methanol (8 mole-% in the C1-fraction).

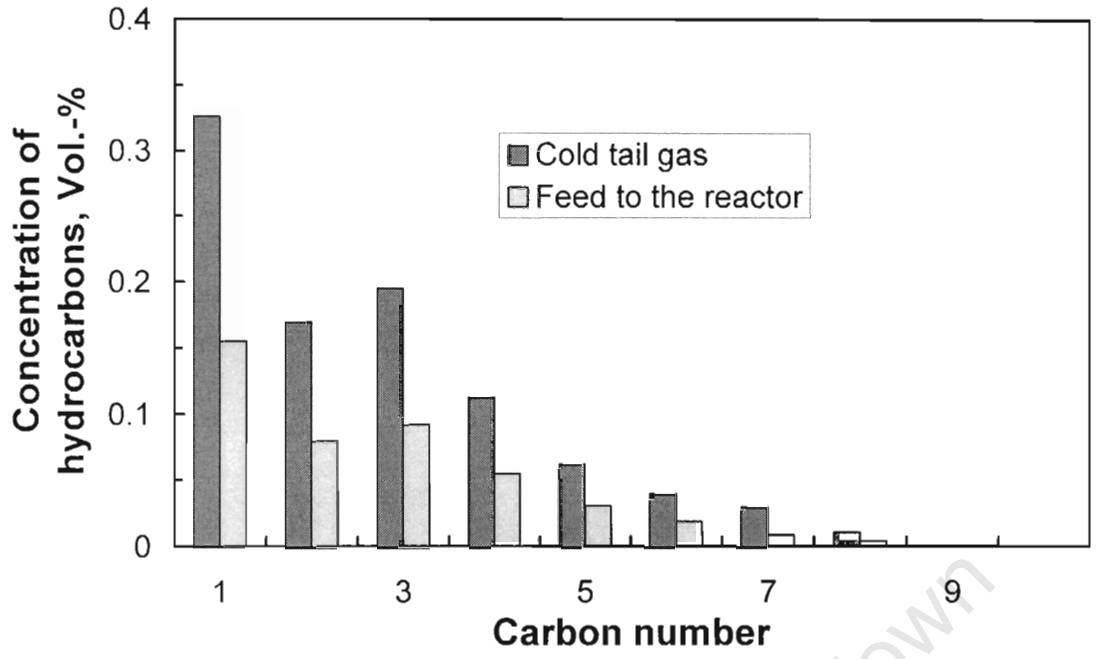

Figure 4.2: Concentration of organic product compounds as a function of carbon number in the cold tail gas and in the feed to the reactor for a fresh feed with $H_2/CO=1.50$ and a recycle ratio of 0.84

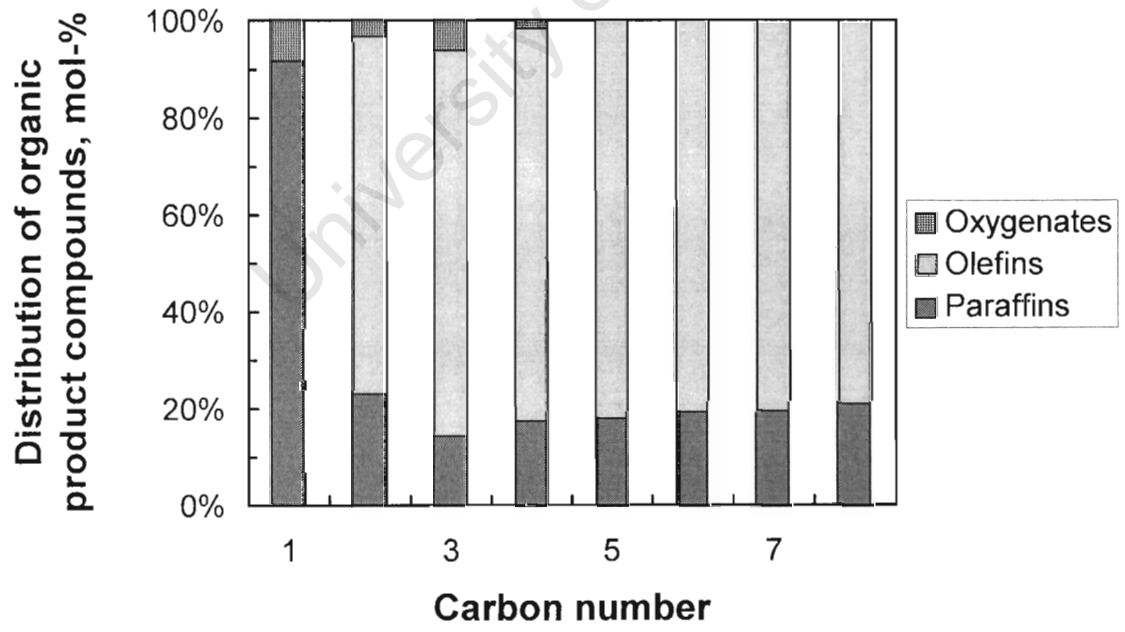

Figure 4.3: Distribution of organic product compounds as a function of carbon number in the feed to the reactor for a fresh feed with $H_2/CO=1.50$ and a recycle ratio of 0.84

The olefin content in the higher hydrocarbons, defined as the amount of olefins relative to the amount of olefins plus paraffins, is between 75 and 85 mole-% (see Figure 4.4). It can be concluded that the composition of the feed to the reactor corresponds to the composition of the cold tail gas. Hydrogenation in the feed line and a separation between organic product compounds in the splitter can be neglected.

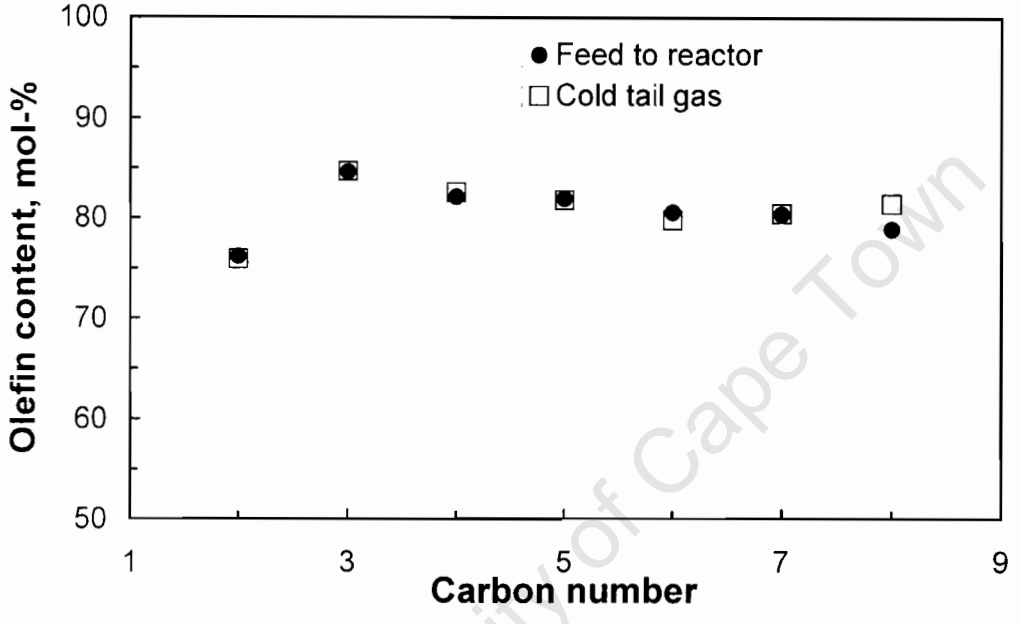

Figure 4.4: Olefin content in the fraction of linear olefins and paraffins as a function of carbon number in the cold tail gas and in the feed to the reactor for a fresh feed with $H_2/CO=1.50$ and a recycle ratio of 0.84.

4.2 INFLUENCE OF RECYCLE ON CONVERSION

4.2.1 Conversion of Carbon Monoxide

Carbon monoxide is consumed in iron-catalysed Fischer-Tropsch synthesis for the formation of organic product compounds and for the formation of carbon dioxide. Figure 4.5 shows the CO-conversion as a function of time-on-stream for the various fresh feed ratios of hydrogen to carbon monoxide and for the

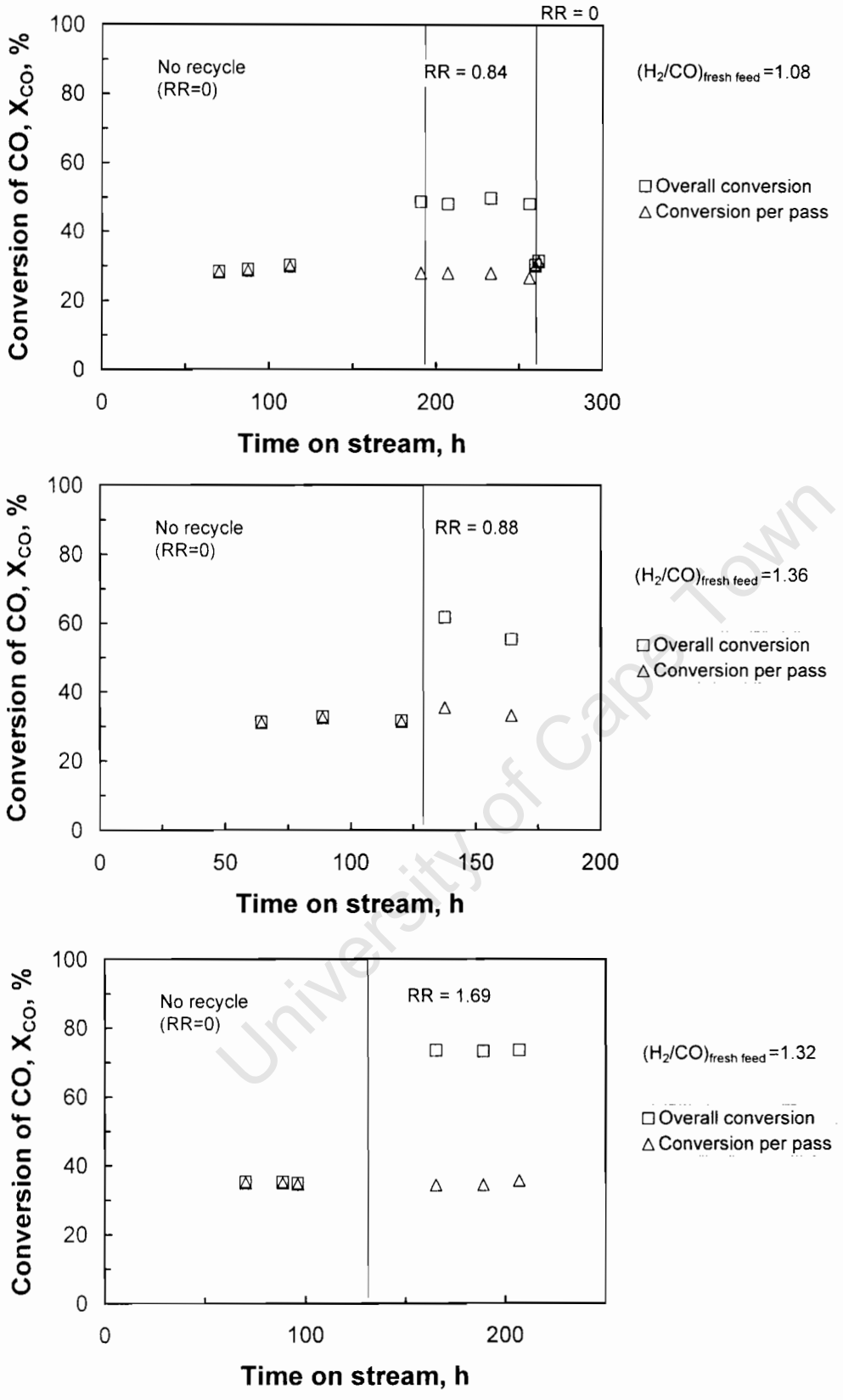

Figure 4.5: Overall conversion of carbon monoxide and the conversion of carbon monoxide per pass as a function of time-on-stream

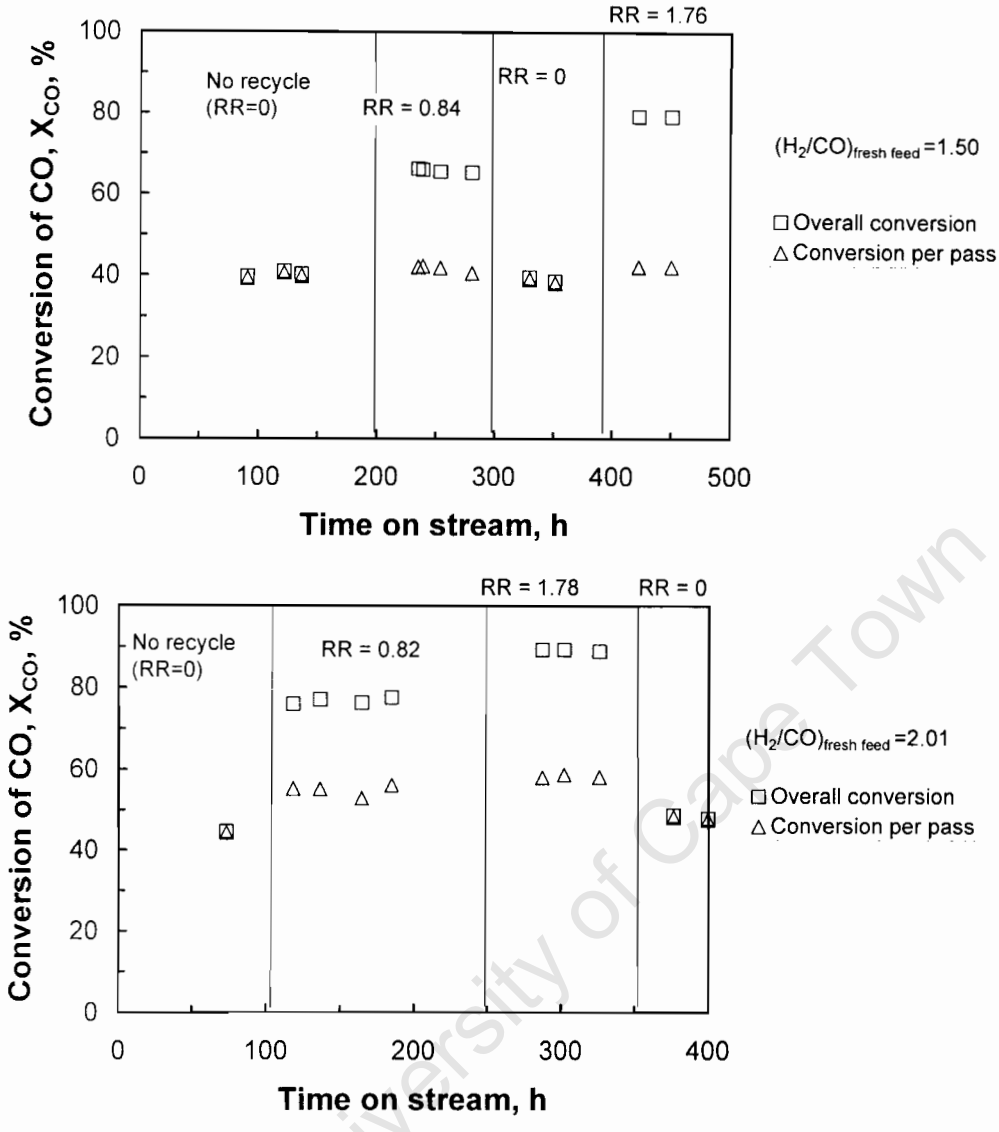

Figure 4.5 (continued):

Overall conversion of carbon monoxide and the conversion of carbon monoxide per pass as a function of time-on-stream

various recycle ratios. The residence time in the reactor was kept constant in these experiments (i.e. the overall space velocity was reduced, when tail gas was recycled back to the reactor) and thus the increase must be attributed to the change in the partial pressures within the reactor.

The CO-conversion per pass increases with increasing hydrogen content in the fresh feed gas. The CO-conversion per pass hardly changes upon the recycling

tail gas back to the reactor. A significant increase in the CO-conversion per pass is only observed with a synthesis gas with a high H_2/CO ratio of 2.0. This might be attributed to the low carbon monoxide partial pressures achieved under these conditions, since under these conditions the partial pressure of carbon monoxide in the reactor changed significantly upon recycling the tail gas (see section 4.3).

Recycling tail gas back to the reactor increases the overall conversion of carbon monoxide significantly. The overall conversion of CO increases further upon increasing the recycle ratio. The benefit of recycling the tail gas is more pronounced for a synthesis gas with a higher H_2/CO-ratio than for a synthesis gas with a low H_2/CO ratio.

4.2.2 CO-Conversion for the Formation of Organic Product Compounds

A part of the converted carbon monoxide is converted to organic product compounds. This can easily be measured by determining the conversion of carbon monoxide plus carbon dioxide (see chapter 3.3). The conversion of carbon monoxide plus carbon dioxide follows in essence the same trend as observed for the conversion of carbon monoxide (see Figure 4.6). The conversion per pass is a strong function of the hydrogen to carbon monoxide ratio in the fresh feed, but is hardly affected by the recycle of the tail gas.

4.2.3 Selectivity for the Formation of Carbon Dioxide

Iron is well known to catalyse not only the formation of hydrocarbons from mixtures of carbon monoxide and hydrogen, but also the water gas shift reaction. Thus, carbon monoxide is not only converted into organic product compounds, but also into carbon dioxide. This reaction pathway leads to a loss of the valuable carbon monoxide and the effect of recycle tail gas on the selectivity for the formation of CO_2 is therefore of importance.

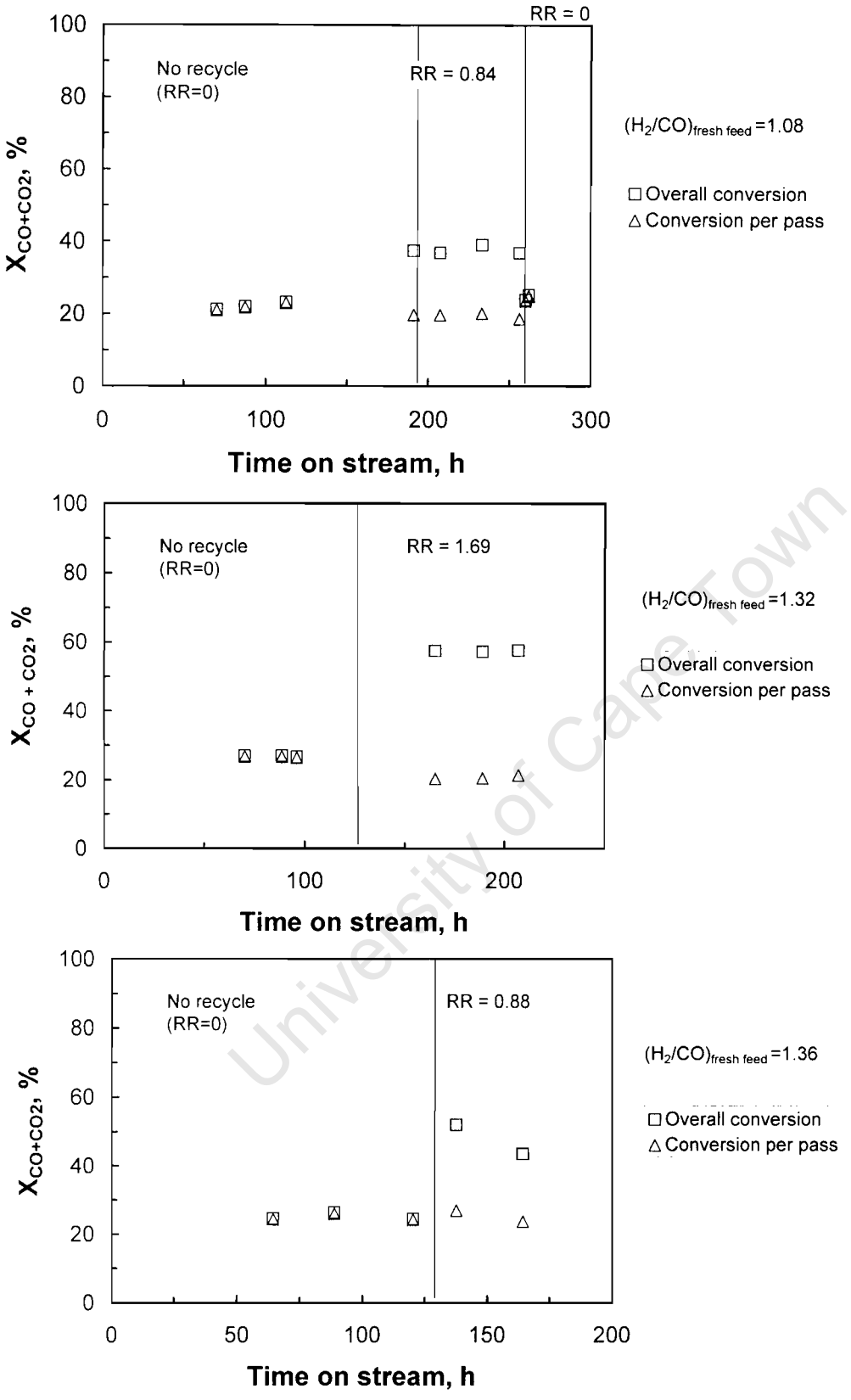

Figure 4.6: Overall conversion of carbon monoxide and the conversion of carbon monoxide per pass as a function of time-on-stream

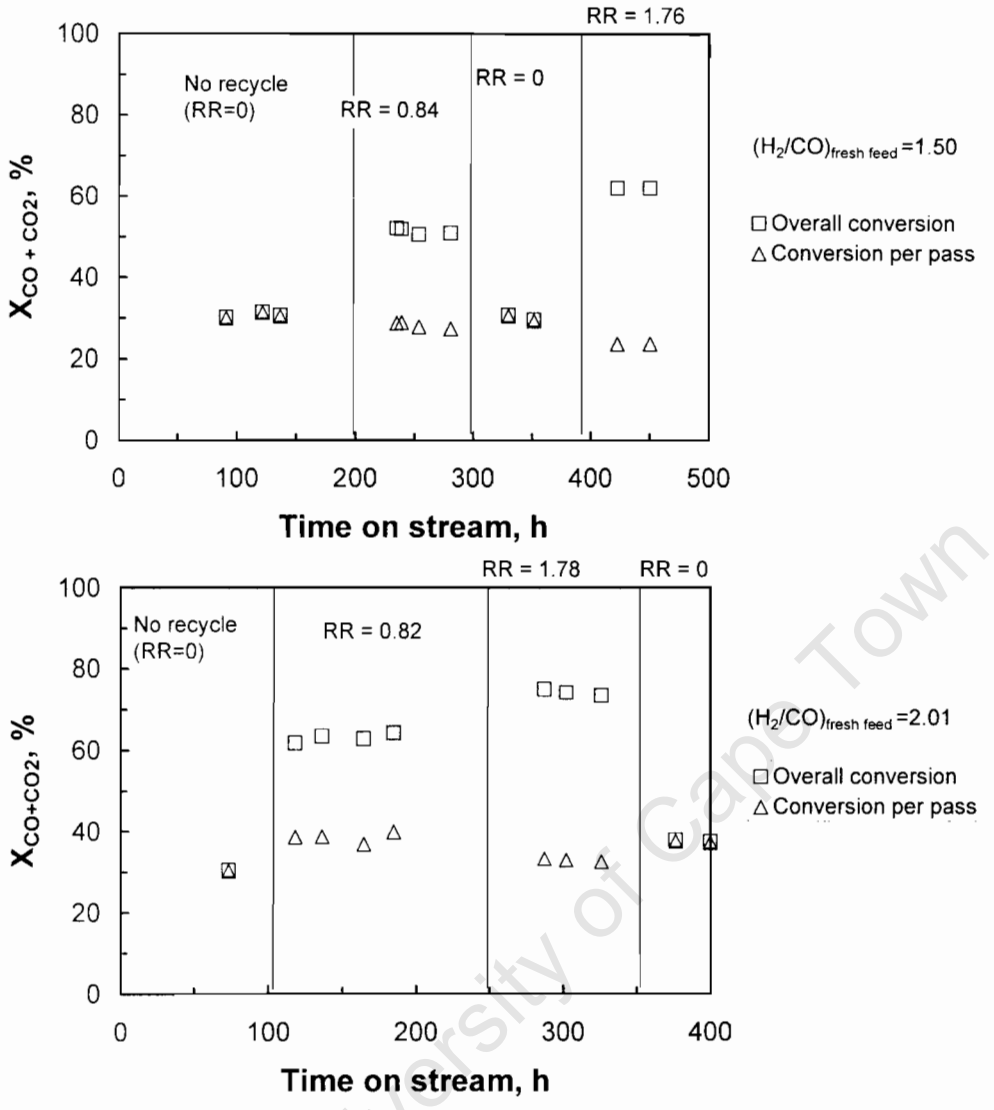

Figure 4.6 (continued):

Overall conversion of carbon monoxide and the conversion of carbon monoxide per pass as a function of time-on-stream

The selectivity for the formation of CO_2 is not a strong function of either the hydrogen to carbon monoxide ratio in the fresh feed or the extent of recycling tail gas back to the reactor (see Figure 4.7). The selectivity for CO_2 for a fresh feed with a H_2/CO=1.36 seems to be a little bit too low. At high hydrogen to carbon monoxide ratio (H_2/CO=2.01) the selectivity for the formation of CO_2 is slightly reduced. The average selectivity for the formation of CO_2 is ca. 21%.

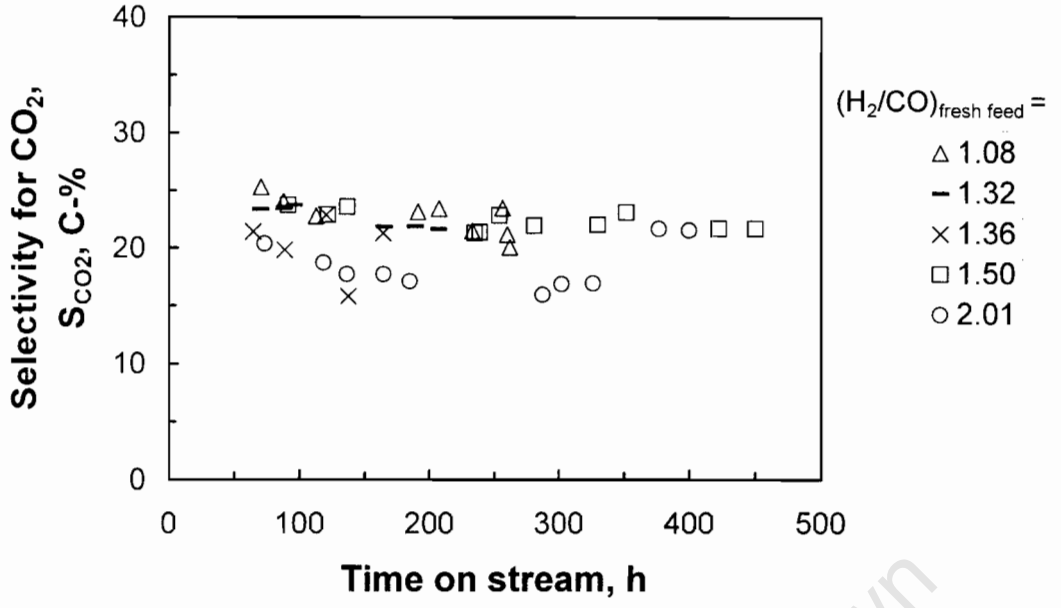

Figure 4.7: Selectivity for the formation of CO_2 as a function of time-on-stream

$(H_2/CO)_{fresh\ feed}$ mol/mol	1.08		1.32		1.36		1.50		2.01	
	TOS[1]	RR[2]	TOS[1]	RR[2]	TOS[1]	RR[2]	TOS[1]	RR[2]	TOS[1]	RR[2]
	0–125	0	0-140	0	0–125	0	0–150	0	0–80	0
	125-257	0.84	140-200	1.69	125–164	0.88	150–280	0.84	80–185	0.82
	257-270	0			257-270	0	280-360	0	185-330	1.78
							360-450	1.76	330-400	0

[1]TOS: Time on stream in hr; [2]RR: recycle ratio

Boelee (1988) defines *z* as the fraction of product water, which is converted by the water gas shift reaction. This translates in the factor z being defined as:

$$z = \frac{S_{CO_2}}{1 - S_{CO_2}} \qquad (4.1)$$

Approximately 30% of the water produced by the Fischer-Tropsch synthesis is consumed in the water gas shift reaction yielding CO_2 (see Figure 4.8). The fraction of water consumed in the water gas shift reaction decreases slightly with increasing hydrogen to carbon monoxide ratio in the feed and with increasing recycle ratio. This might be attributed to the low partial pressure of carbon monoxide in these systems.

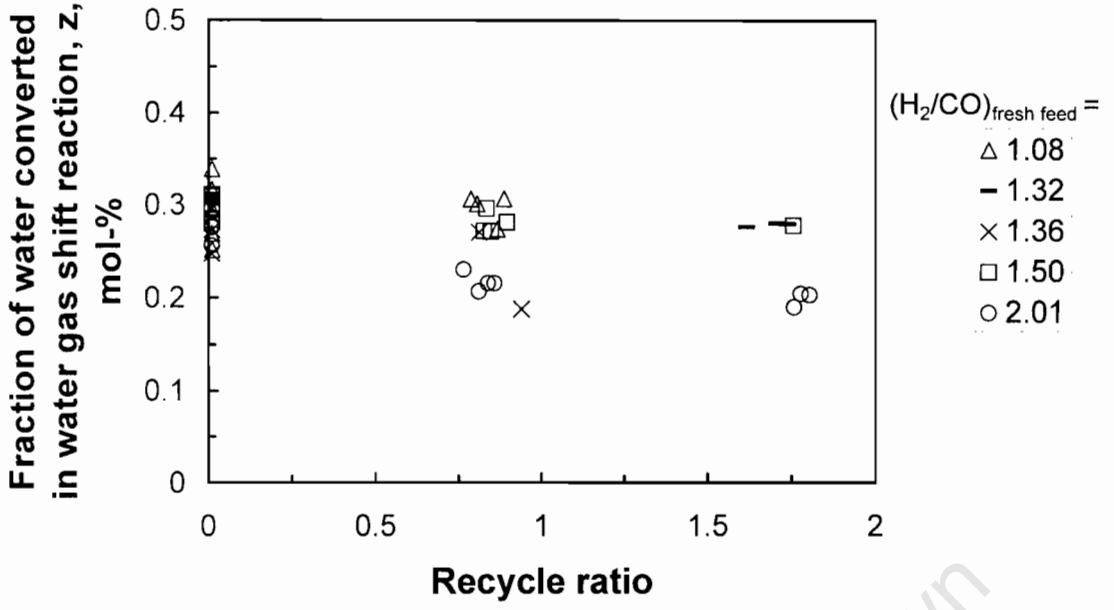

Figure 4.8: Fraction of water being converted in the water-gas shift reaction as a function of the recycle ratio

$(H_2/CO)_{fresh\ feed}$ mol/mol	1.08		1.32		1.36		1.50		2.01	
	TOS[1]	RR[2]	TOS[1]	RR[2]	TOS[1]	RR[2]	TOS[1]	RR[2]	TOS[1]	RR[2]
	0–125	0	0-140	0	0–125	0	0–150	0	0–80	0
	125-257	0.84	140-200	1.69	125–164	0.88	150–280	0.84	80–185	0.82
	257-270	0			257-270	0	280-360	0	185-330	1.78
							360-450	1.76	330-400	0

[1]TOS: Time on stream in hr; [2]RR: recycle ratio

Another way of evaluating the conversion of water to carbon dioxide is to look at the ratio of the product of the partial pressures of hydrogen and carbon dioxide relative to the product of the partial pressures of water and carbon monoxide. The value for this ratio should approach 102, if the reaction approaches equilibrium (see equation 2.8, page 35). It can be seen that the water gas shift reaction is far from equilibrium (see Figure 4.9), but the ratio increases with increasing hydrogen to carbon monoxide ratio in the fresh feed and with increasing recycle ratio.

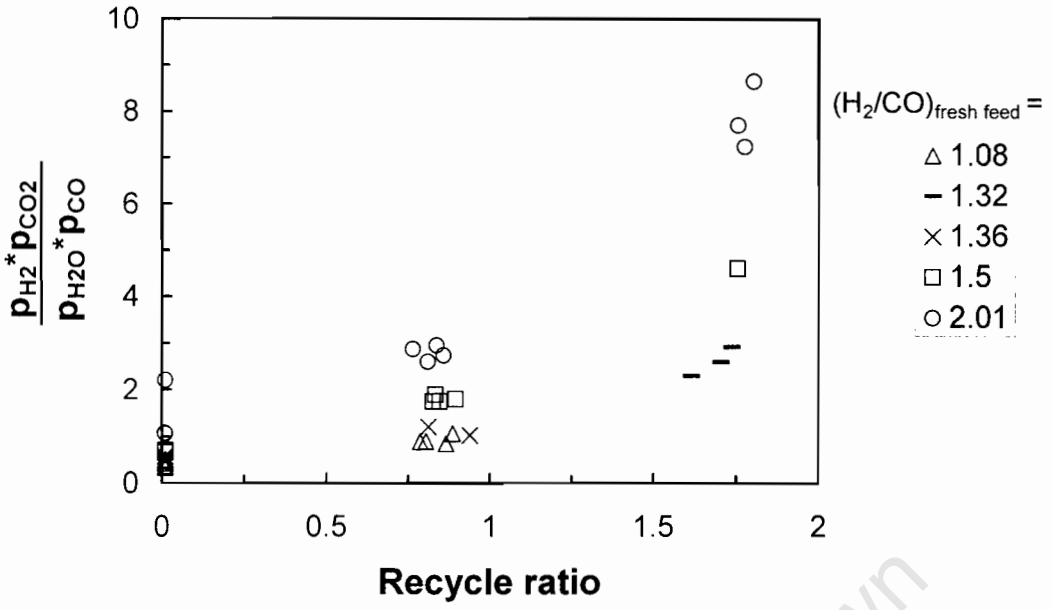

Figure 4.9: Water-gas shift reaction product ratio as a function of the recycle ratio

$(H_2/CO)_{fresh\ feed}$ mol/mol	1.08		1.32		1.36		1.50		2.01	
	TOS[1]	RR[2]	TOS[1]	RR[2]	TOS[1]	RR[2]	TOS[1]	RR[2]	TOS[1]	RR[2]
	0–125	0	0-140	0	0–125	0	0–150	0	0–80	0
	125-257	0.84	140-200	1.69	125–164	0.88	150–280	0.84	80–185	0.82
	257-270	0			257-270	0	280-360	0	185-330	1.78
							360-450	1.76	330-400	0

[1]TOS: Time on stream in hr; [2]RR: recycle ratio

4.2.4 Usage Ratio

The usage ratio is defined as the net molar ratio, in which CO and H_2 are consumed in the reaction. The usage ratio depends on the conversion of the reactants (H_2 and CO) as well as the water gas shift activity [Espinoza, 2004; Boelee, 1988]. A usage ratio of 2 is expected, if the Fischer-Tropsch synthesis only produces olefins and alcohols. The formation of paraffins (especially methane) in the Fischer-Tropsch synthesis will increase the usage ratio. The usage ratio is significantly reduced by the water-gas shift reaction. A usage ratio of 0.5 can be expected, if the Fischer-Tropsch synthesis produces only olefins and alcohols and all product water is converted to CO_2. The usage ratio increases with an increase in the hydrogen to carbon monoxide ratio in the fresh feed and with an increase in the recycle ratio (see Figure 4.10).

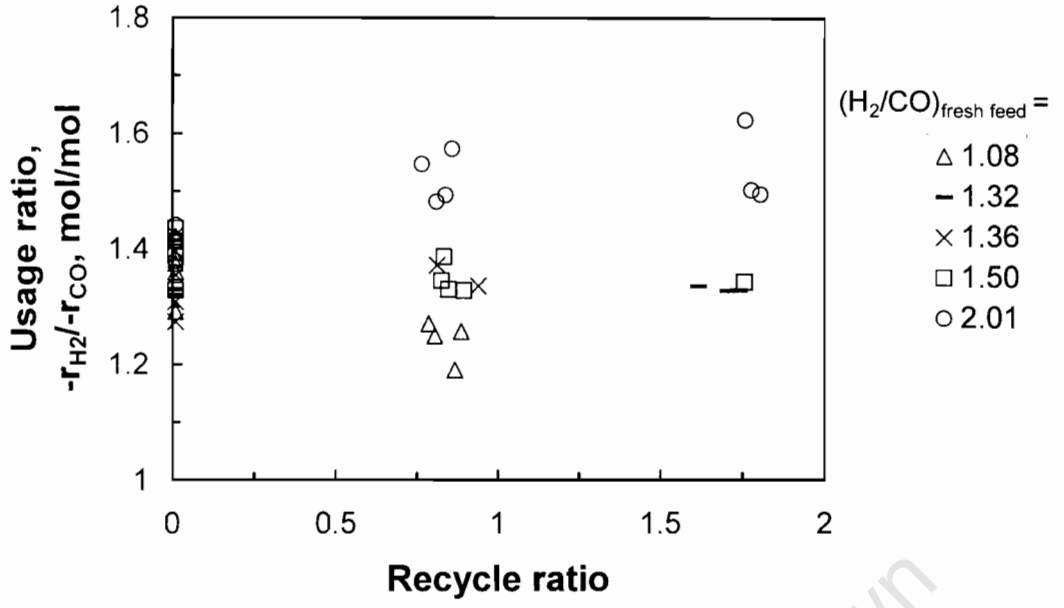

Figure 4.10: Usage ratio, defined as the amount of hydrogen consumed relative to the amount of carbon monoxide consumed, as a function of the recycle ratio

$(H_2/CO)_{fresh\ feed}$ mol/mol	1.08		1.32		1.36		1.50		2.01	
	TOS[1]	RR[2]	TOS[1]	RR[2]	TOS[1]	RR[2]	TOS[1]	RR[2]	TOS[1]	RR[2]
	0–125	0	0-140	0	0–125	0	0–150	0	0–80	0
	125-257	0.84	140-200	1.69	125–164	0.88	150–280	0.84	80–185	0.82
	257-270	0			257-270	0	280-360	0	185-330	1.78
							360-450	1.76	330-400	0

[1]TOS: Time on stream in hr; [2]RR: recycle ratio

A useful insight is obtained when looking at the usage ratio relative to the hydrogen to carbon monoxide ratio in the fresh feed. The relative usage ratio should in the ideal case approximate 1, indicating a feed composition comparable to the consumption of the two reactants. A value less than 1 indicates a higher consumption of carbon monoxide than hydrogen compared to the feed ratio.

Figure 4.11 shows the relative usage ratio as a function of the recycle ratio for the various feeds tested in this study. With increasing recycle ratio the relative usage ratio tend to 1, i.e. the relative usage ratio decreases with increasing recycle ratio for a fresh feed rich in carbon monoxide (H_2/CO =1.08) and increases for a feed rich in hydrogen (H_2/CO = 2.01).

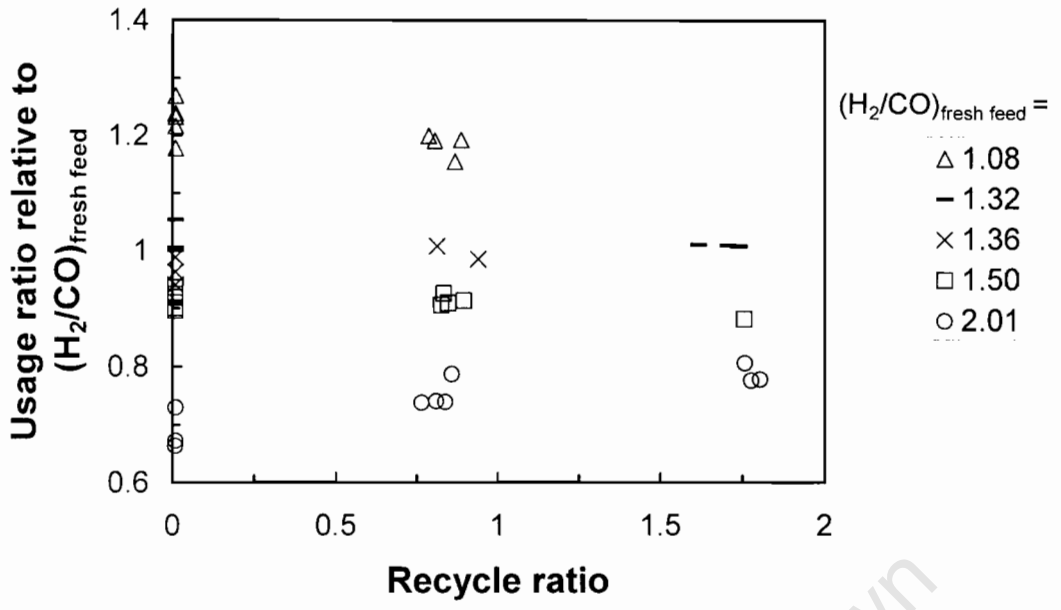

Figure 4.11: Usage ratio, defined as the amount of hydrogen consumed relative to the amount of carbon monoxide consumed, relative to the hydrogen to carbon monoxide ratio in the fresh feed as a function of the recycle ratio

$(H_2/CO)_{fresh\ feed}$ mol/mol	1.08		1.32		1.36		1.50		2.01	
	TOS[1]	RR[2]	TOS[1]	RR[2]	TOS[1]	RR[2]	TOS[1]	RR[2]	TOS[1]	RR[2]
	0–125	0	0-140	0	0–125	0	0–150	0	0–80	0
	125-257	0.84	140-200	1.69	125–164	0.88	150–280	0.84	80–185	0.82
	257-270	0			257-270	0	280-360	0	185-330	1.78
							360-450	1.76	330-400	0

[1]TOS: Time on stream in hr; [2]RR: recycle ratio

When recycling with a fresh feed H_2/CO above the usage ratio, the H_2/CO in the reactor increases, as illustrated in Figure 4.1. This change is negligible for H_2/CO ratios close to the usage ratio. Furthermore, a slight decrease is observed for H_2/CO ratios much smaller than the usage ratio. The latter trend needs to be confirmed with more data at higher recycle ratios.

4.3 PARTIAL PRESSURES IN THE REACTOR

The partial pressures in the reactor were calculated from the analysis of the tail gas and the total pressure in the reactor. The water content in the tail gas was not measured, and the partial pressure of water was determined using an oxygen balance. Figure 4.12 shows the partial pressure of the kinetically

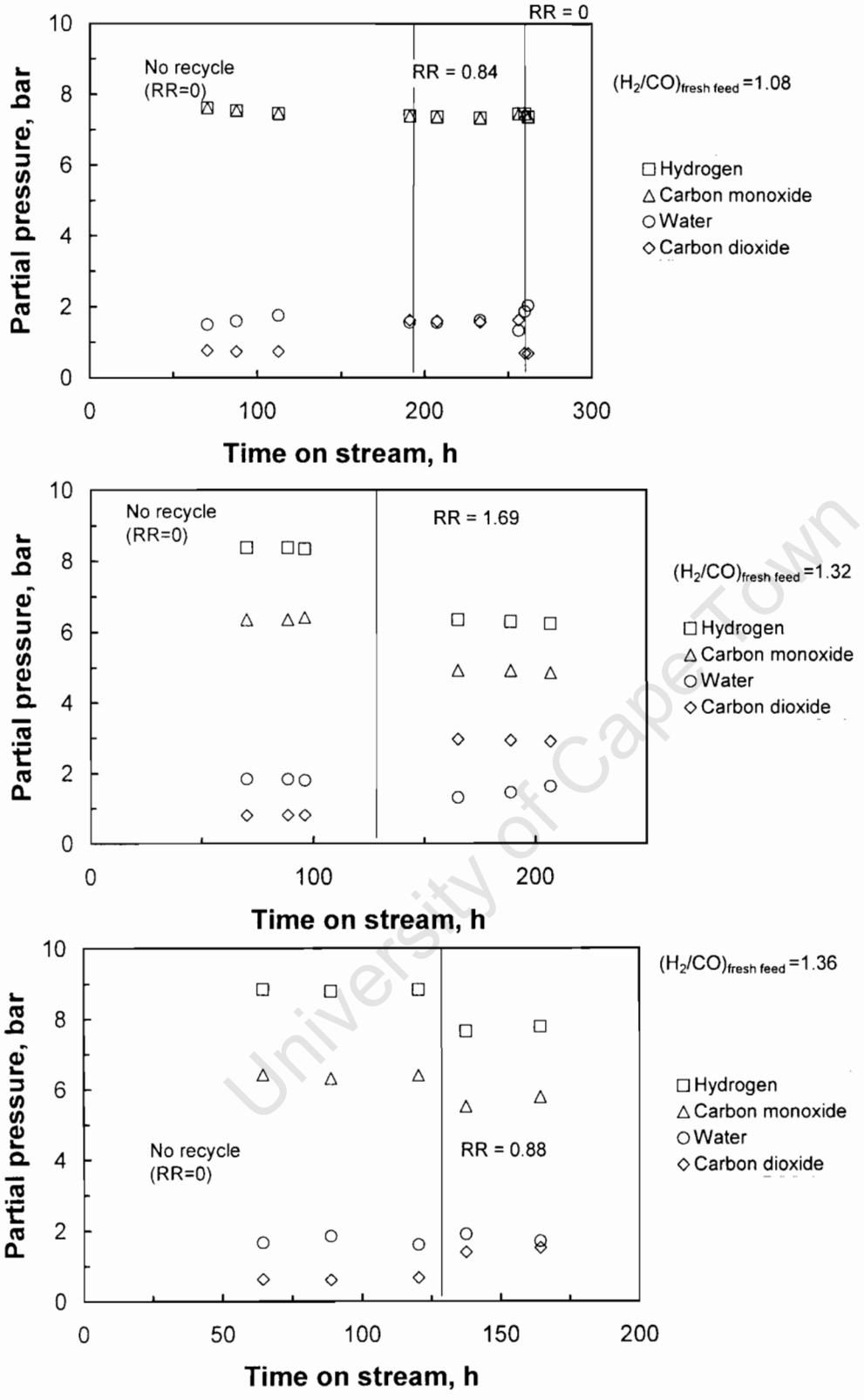

Figure 4.12: Partial pressure of hydrogen, carbon monoxide, water and carbon dioxide in the reactor as calculated from the tail gas composition as a function of time-on-stream

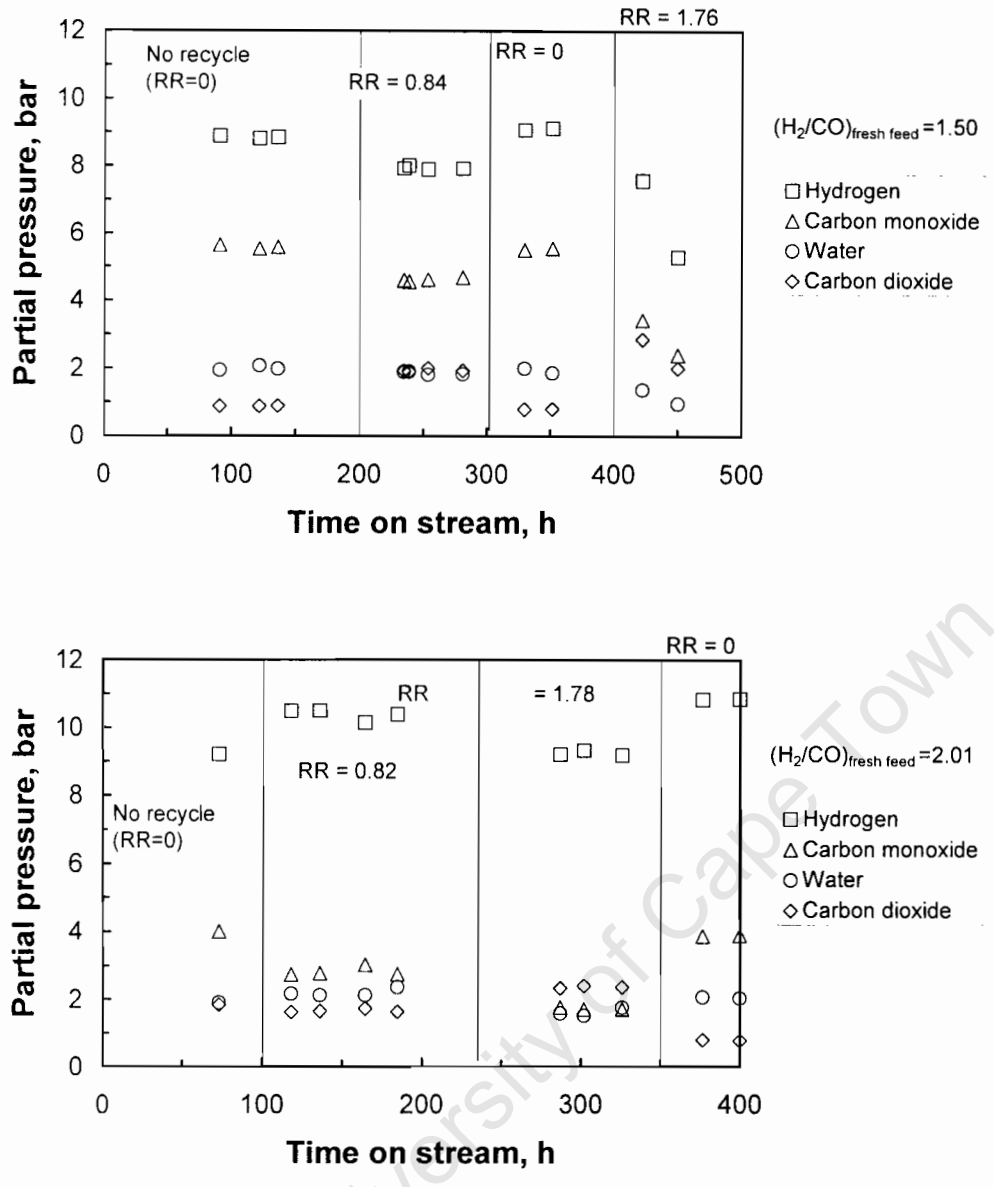

Figure 4.12 (continued):

Partial pressure of hydrogen, carbon monoxide, water and carbon dioxide in the reactor as calculated from the tail gas composition as a function of time-on-stream

important compounds (H_2, CO, H_2O and CO_2) as a function of time for the various feed streams used.

Table 4.1 summarises the average partial pressures obtained in the reactor. The partial pressures of hydrogen and carbon monoxide decrease upon recycling the tail gas, due to the dilution of the feed stream with product

compounds, such carbon dioxide (water is assumed to be almost completely condensed out and only a small fraction of water is recycled).

Table 4.1: Average partial pressures in the reactor as a function of the fresh feed composition and the recycle ratio

$(H_2/CO)_{fresh\ feed}$	Recycle ratio	p_{H2} bar	p_{CO} bar	p_{H2O} bar	p_{CO2} bar
1.08	0	7.5	7.5	1.7	0.7
	0.84	6.4	7.4	1.5	1.6
1.32	0	8.4	6.4	1.8	0.8
	1.69	6.3	4.9	1.5	2.9
1.36	0	8.8	6.4	1.7	0.6
	0.88	7.7	5.6	1.8	1.5
1.50	0	8.9	5.6	2.0	0.8
	0.84	7.9	4.6	1.9	1.9
	1.76	6.4	2.9	1.2	2.4
2.01	0	10.3	3.9	2.0	1.1
	0.82	10.4	2.8	2.2	1.7
	1.78	9.2	1.7	1.6	2.4

The partial pressure of water varies only slightly with increasing H_2/CO-ratio in the fresh feed, whereas the partial pressure of CO_2 increases dramatically. The introduction of the recycle increases the partial pressure of CO_2 in the reactor dramatically. This can be rationalised, because CO_2 is not condensed out and a part of the produced CO_2 is fed back to the reactor.

4.4 INFLUENCE OF RECYCLE ON PRODUCT SELECTIVITY

The distribution of organic product compounds in the Fischer-Tropsch synthesis as a function of carbon number is governed by the Anderson-Schulz-Flory distribution (as an example see Figure 4.13). The total product distribution was obtained by calculation together the analysis of the cold tail gas, the water phase and the oil phase.

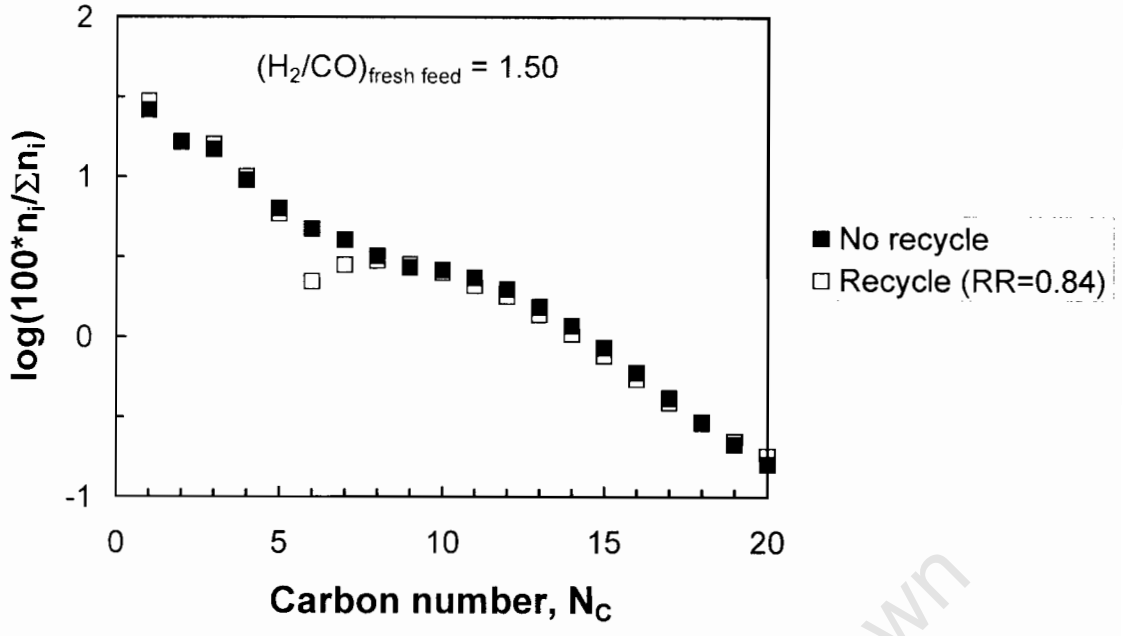

Figure 4.13: Anderson-Schulz-Flory distribution of C_1-C_{20} compounds calculated together from the analysis of the tail gas and the oil phase for the experiment with $H_2/CO)_{fresh\ feed}$ = 1.50 with and without recycle (recycle ratio equals 0.84)

The methane selectivity is higher than expected based on extrapolation of the Anderson-Schulz-Flory distribution as often described in literature [Claeys and van Steen, 2004]. Furthermore, the selectivity for the C_2-compounds is less than expected. This might be caused by the high reactivity of ethene for secondary reaction. In the range of C_5-C_{10} there seems to be a plateau in the Anderson-Schulz-Flory distribution. This is an artifact originating from the attempt to combine the analysis of the tail gas composition with that of the oil phase.

4.4.1 Methane Selectivity

Figure 4.14 shows the methane selectivity in C-% (as defined in chapter 3.3) as a function of the recycle ratio. The methane selectivity is in all experiments modest (less than 3.5 C-%). The methane selectivity increases with increasing H_2/CO-ratio in the fresh feed for H_2/CO ratios larger than 1.50. For smaller H_2/CO ratios in the fresh feed the methane selectivity shows a relative large scatter.

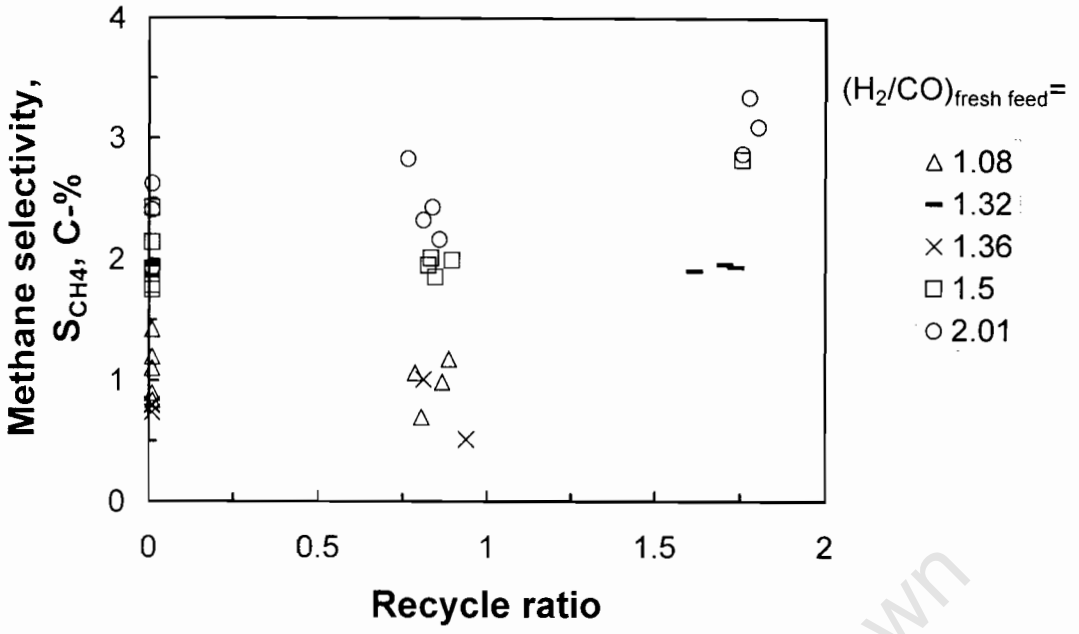

Figure 4.14: Methane selectivity in C-% as a function of recycle ratio for the various fresh feed ratios recycle

The methane selectivity seems to increase with increasing recycle ratio. The recycle stream contains also olefins. Based on co-feeding experiments by Hanlon and Satterfield [1998] and Snel and Espinoza [1987, 1989b, 1989c] a decrease in the methane selectivity was expected. The observed change in the methane selectivity might be better correlated with the change in the partial pressure of the kinetically relevant compounds in the reactor.

4.4.2 Chain Growth Probability

The carbon number range C_{15}-C_{20} was taken to evaluate the chain growth probability. Figure 4.15 shows the effect of recycle on the chain growth probability. With increasing recycle ratio the chain growth probability increases slightly. This might be caused by the recycling of reactive product compounds, which may have induced secondary chain growth [Claeys and van Steen, 2004].

The chain growth probability changes with carbon number. In the range of C_4-C_6 a chain growth probability between 0.64 and 0.75 was obtained. For the experiments with a fresh feed H_2/CO ratio of 1.50 and 2.01 the average chain

growth probability in the range of C_{30}-C_{50} could be determined to be 0.97 and 0.95, respectively.

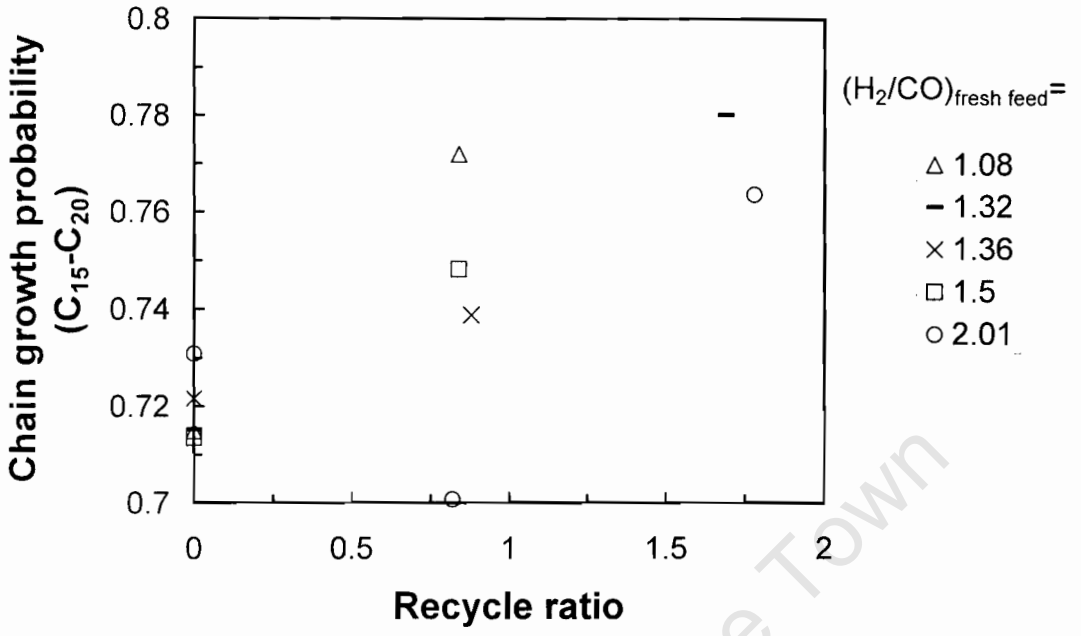

Figure 4.15: Chain growth probability in the range C_{15}-C_{20} as a function of recycle ratio for the various fresh feed ratios recycle

4.4.3 Secondary Reactions of Primarily Formed Olefins

Olefins are one of the major product compounds in the Fischer-Tropsch synthesis. They can however undergo secondary reactions, such as double bond isomerisation and secondary hydrogenation [Schulz and Claeys, 1999]. Figure 4.16 shows the olefin content (defined as the amount of n-olefins in the fraction of linear hydrocarbons) as a function of carbon number. The olefin content in the fraction of linear hydrocarbons is a measure of the extent to which n-olefins undergo secondary hydrogenation yielding n-paraffins.

The olefin content in the fraction of C_2–hydrocarbons is lower than the olefin content in the fraction of C_3-hydrocarbons, which can be attributed to the high reactivity of ethene for secondary reactions and in particular for secondary hydrogenation [Schulz and Claeys, 1999]. The olefin content in the fraction of C_2–hydrocarbons decreases strongly with increasing recycle ratio. The olefin content in the fraction of C_3-hydrocarbons is ca. 80% and decreases with increasing recycle ratio (albeit much less strong than the olefin content in the

fraction of C_2-hydrocarbons). The olefin content in the fraction of linear hydrocarbons decreases with increasing carbon number, especially for carbon numbers larger than 9, which might be attributed to the higher solubility of the long chain olefins in the wax [Schulz and Claeys, 1999].

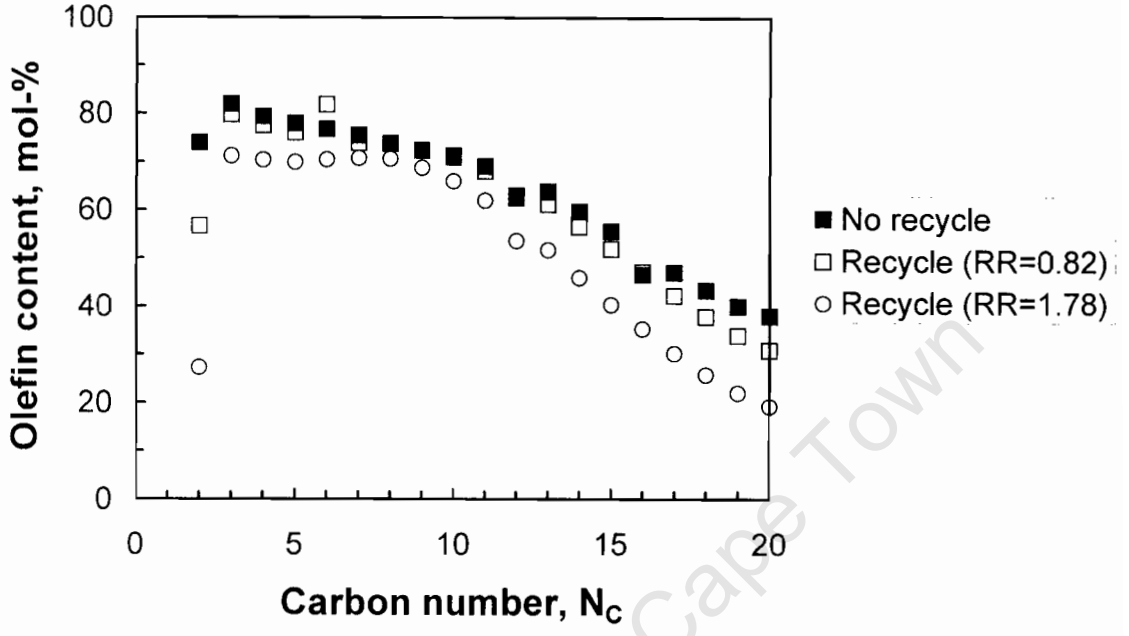

Figure 4.16: Olefin content defined as the amount of n-olefins in the fraction of linear hydrocarbons as a function of carbon number calculated together from the analysis of the tail gas and the oil phase for the experiment with $H_2/CO)_{fresh\ feed}$ = 2.01 with and without recycle (recycle ratios of 0.82 and 1.78)

Figure 4.17 shows the olefin content in the fraction of linear hydrocarbons as a function of the recycle ratio for C_2, C_3 and C_{10}. The olefin content in the fraction of linear hydrocarbons decreases with an increase in the hydrogen to carbon monoxide ratio in the fresh feed. The dependency of the olefin content in the fraction of linear hydrocarbons on the recycle ratio is modest. It seems that the olefin content in the fraction of linear hydrocarbons is more affected by the prevalent partial pressures in the reactor. Ethene is the most reactive compound and the olefin content in the fraction of C_2-hydrocarbons shows therefore the strongest dependency on the reaction conditions. Propene is rather unreactive and the olefin content in the fraction of C_3-hydrocarbons is therefore not a strong function of the reaction conditions.

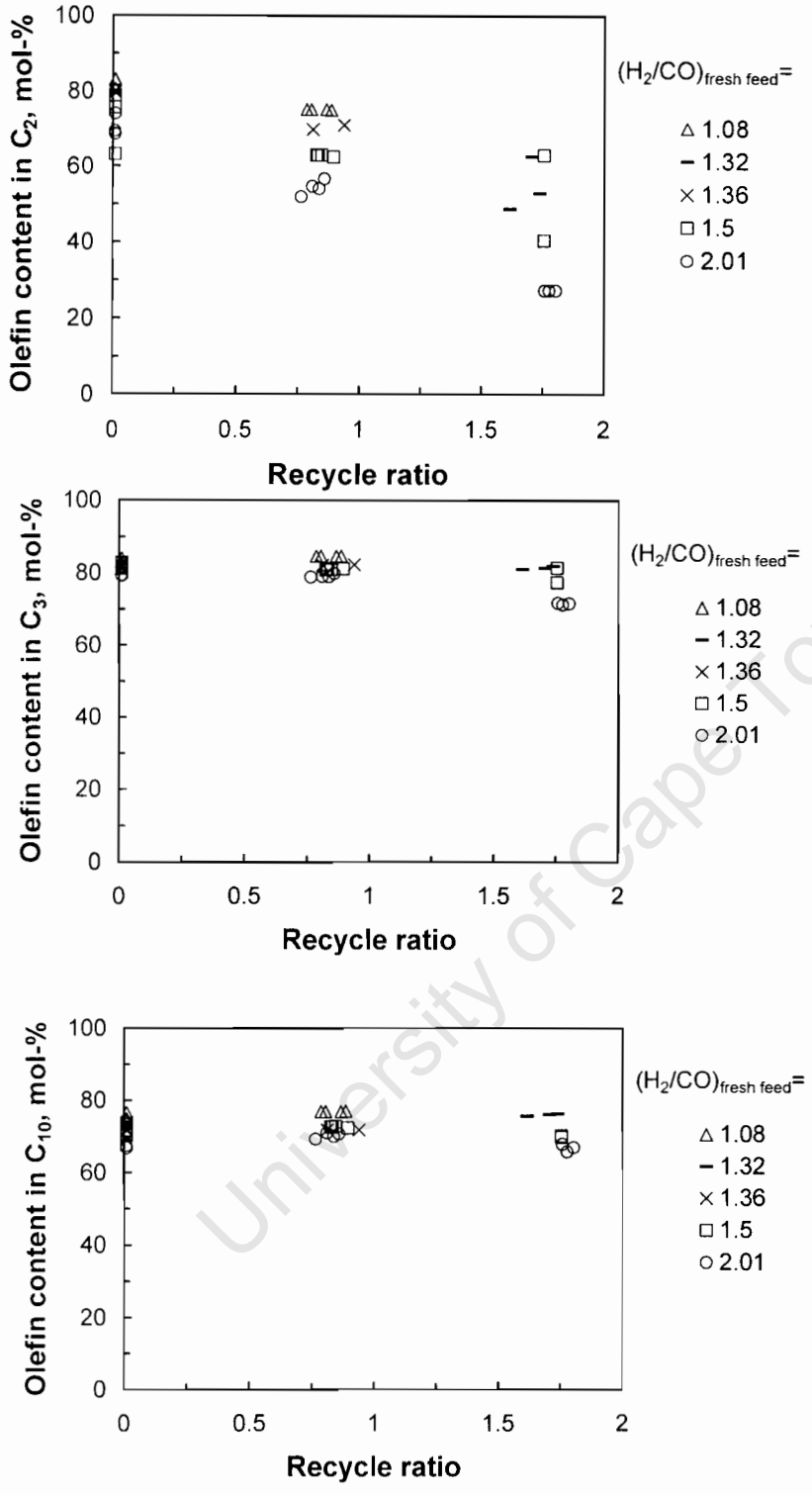

Figure 4.17: Olefin content defined as the amount of n-olefins in the fraction of linear hydrocarbons as a function of the recycle ratio

Top: olefin content in the fraction of C_2-hydrocarbons

Middle: olefin content in the fraction of C_3-hydrocarbons

Bottom: olefin content in the fraction of linear C_{10}-hydrocarbons

4.4.3.1 Double bond isomerisation

According to the alkyl-mechanism, 1- olefins are the primary olefins formed in the Fischer-Tropsch synthesis [Claeys and van Steen, 2004]. Readsorption of these primarily formed 1-olefins may lead to the formation of the double bond isomers. The 1-olefin content in the fraction of linear hydrocarbons is a measure for the extent to which the primarily formed 1-olefins undergo double bond isomerisation.

Figure 4.18 shows the 1-olefin content in the fraction of linear hydrocarbons as a function of carbon number. The 1-olefin content in the fraction of linear olefins is generally high (ca. 95 mol-% for C4) and decreases with increasing carbon number. This can be attributed to the increased solubility of long chain olefins in the liquid phase [Schulz and Claeys, 1999], which would increase the likelihood for secondary reactions.

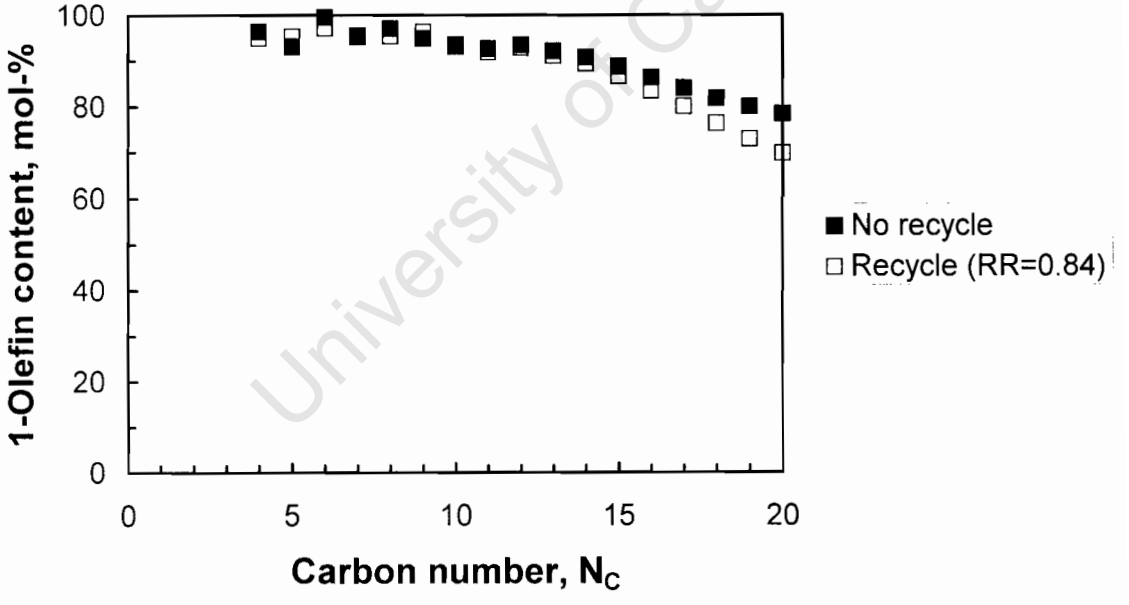

Figure 4.18: 1-Olefin content defined as the amount of 1-olefins in the fraction of linear olefins as a function of carbon number calculated together from the analysis of the tail gas and the oil phase for the experiment with $H_2/CO)_{fresh\ feed}$ = 1.50 with and without recycle (recycle ratios of 0.84)

Figure 4.19 shows the 1-olefin content in the fraction of linear olefins for C_4 and C_{10} as a function of the recycle ratio and the fresh feed hydrogen to carbon monoxide ratio. Generally, a high 1-olefin content in the fraction of linear olefins was obtained in the fraction of C_4 (larger than 95 mol-%) and C_{10} (larger than 87 mol-%). The 1-olefin content varies only slightly with the reactor conditions.

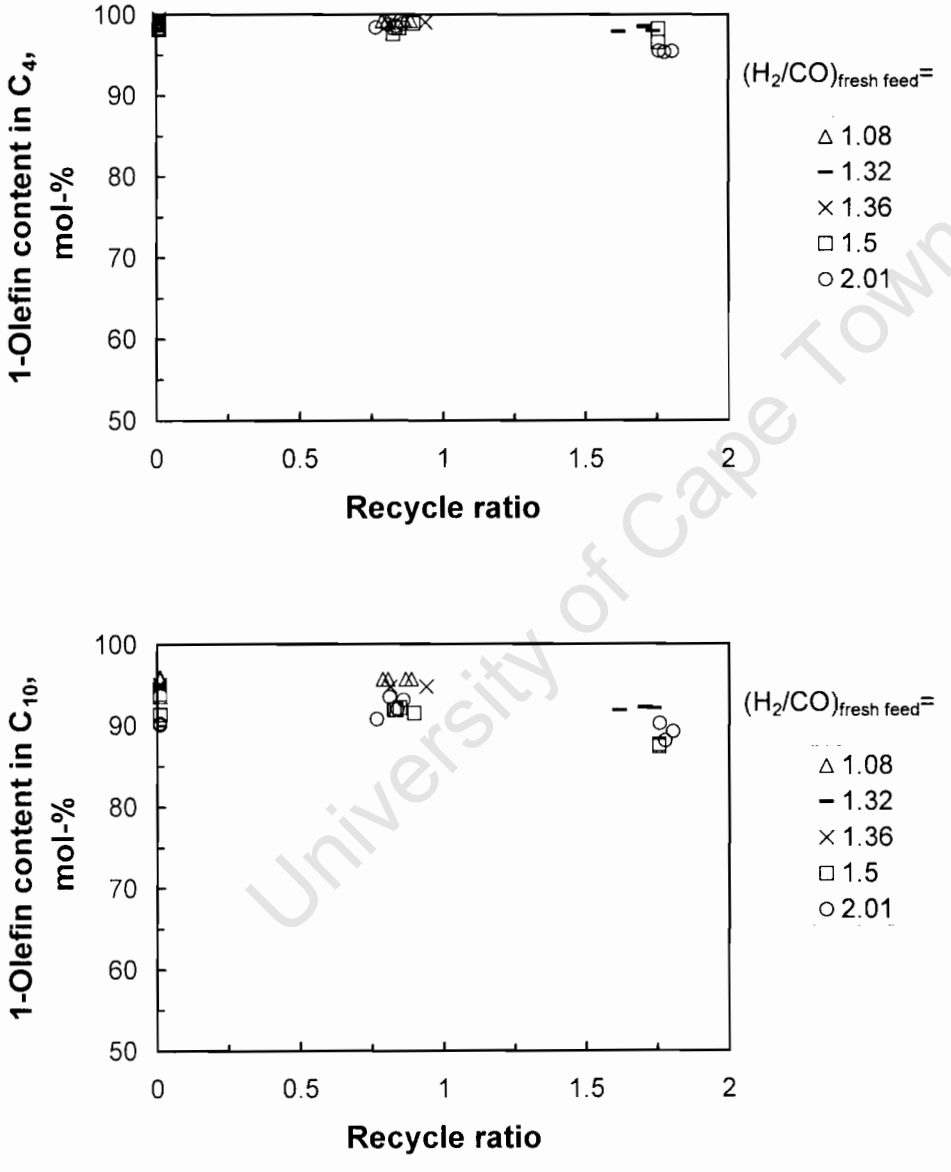

Figure 4.19: 1-Olefin content defined as the amount of 1-olefins in the fraction of linear olefins as a function of the recycle ratio

Top: 1-olefin content in the fraction of linear C_4-olefins

Bottom: 1-olefin content in the fraction of linear C_{10}-olefins

4.4.4 Formation of Oxygenates

The Fischer-Tropsch synthesis does not only produce olefins and paraffins. Alcohols, aldehydes and ketones form typically a minor part in the product of the Fischer-Tropsch synthesis. Figure 4.20 shows the oxygenate content (alcohols, aldehydes plus ketones) in the fraction of linear product compounds (oxygenates, olefins and paraffins) as a function of carbon number (as calculated together from the tail gas, water phase and oil phase analysis). The oxygenate content increases from C_1 to C_2 followed by a decline.

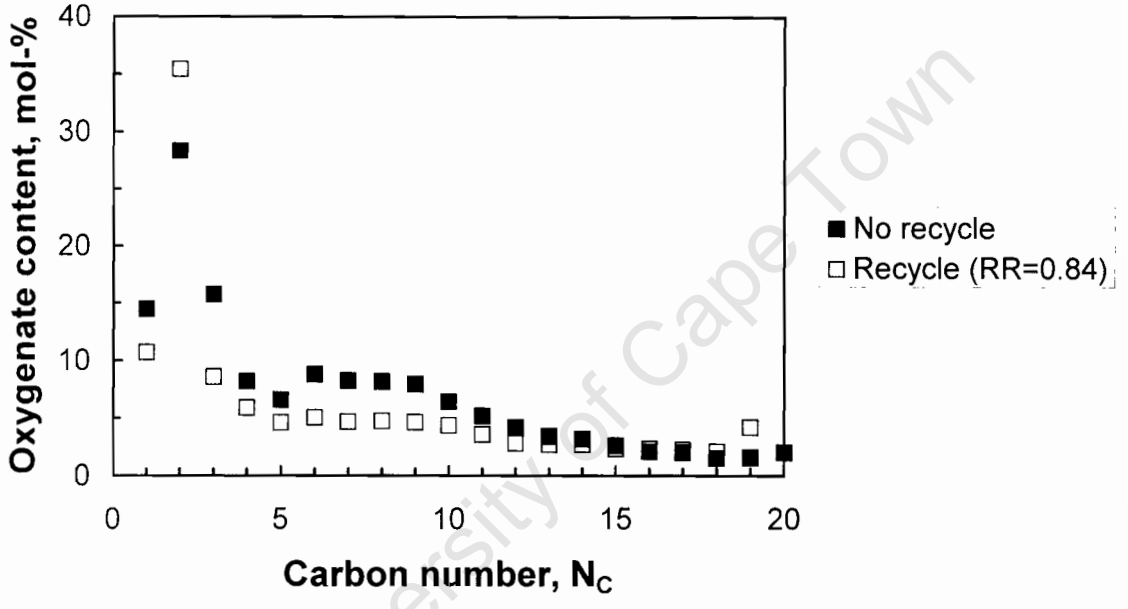

Figure 4.20: Oxygenate content in the fraction of linear product compounds content defined as the amount of oxygenates (alcohols, aldehydes plus ketones) in the fraction of linear product compounds ((oxygenates, olefins and paraffins) as a function of carbon number calculated together from the analysis of the tail gas, the water phase and the oil phase for the experiment with $H_2/CO)_{fresh\ feed}$ = 1.50 with and without recycle (recycle ratios of 0.84)

Figure 4.21 shows the alcohol content in the fraction of linear C_{10}-product compounds as a function of the recycle ratio and the hydrogen to carbon monoxide ratio in the fresh feed. In general, there seems to be a slight decrease in the alcohol content in the fraction of linear C_{10}-compounds with increasing

recycle ratio and with increasing hydrogen to carbon monoxide ratio in the fresh feed. This might be attributed to a secondary conversion of the alcohol.

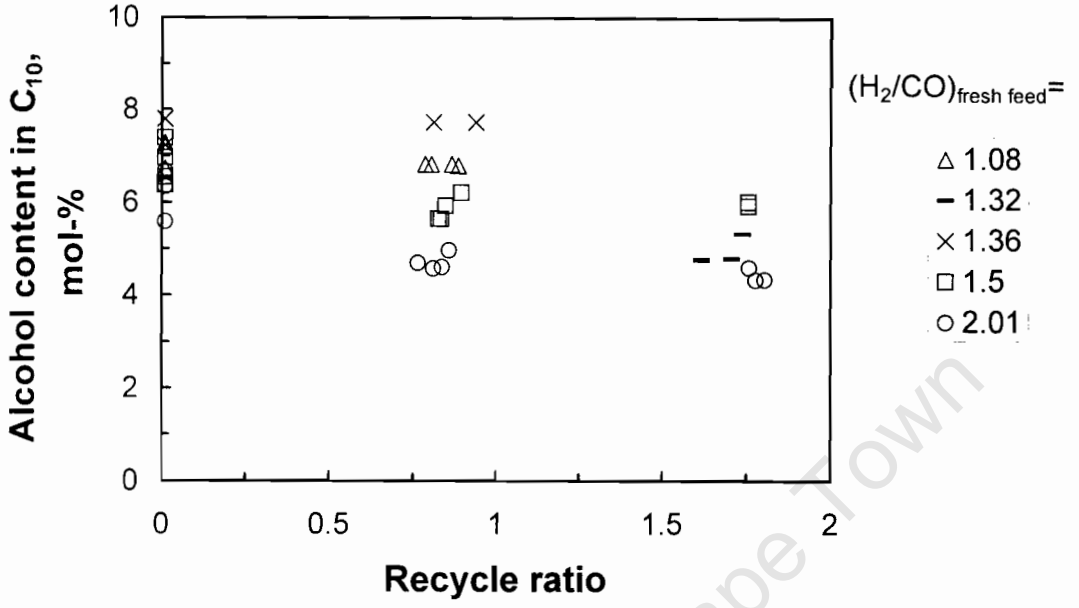

Figure 4.21: Alcohol content defined as the amount of n-alcohol in the fraction of linear C_{10}-product compounds

The selectivity for the lower alcohols (methanol, ethanol, propanol and butanol) is presented in Figure 4.22. The methanol selectivity seems to decrease with increasing recycle ratio for the H_2/CO ratios above the usage ratio. For the lower H_2/CO ratios, an increase in the methanol selectivity is observed. These observations were not so noticeable for the ethanol, butanol and propanol selectivites. This result was unexpected since other researchers, Hanlon [1998], Tau [1987, 1991 and 1992], and Lachowska [1998], reported decreases in the co-fed alcohol.

The methanol selectivity remained unchanged for H_2/CO ratios close to the usage ratio. Therefore the decrease in the methanol selectivity here was more a consequence of the changing H_2/CO ratio in the reactor rather than readsorption.

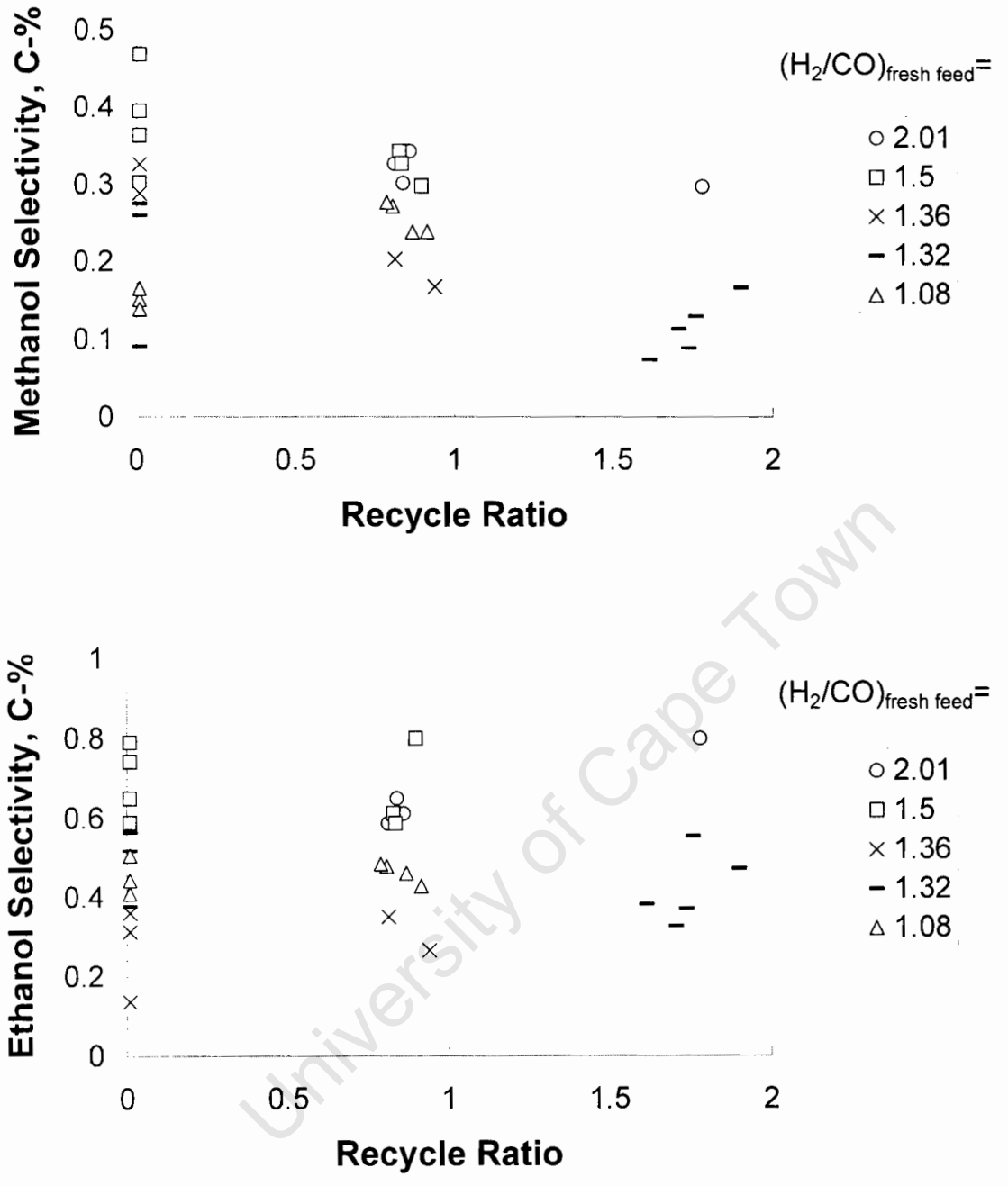

Figure 4.22: Alcohol Selectivity in C-% as a function of recycle ratio for the various fresh feed ratios

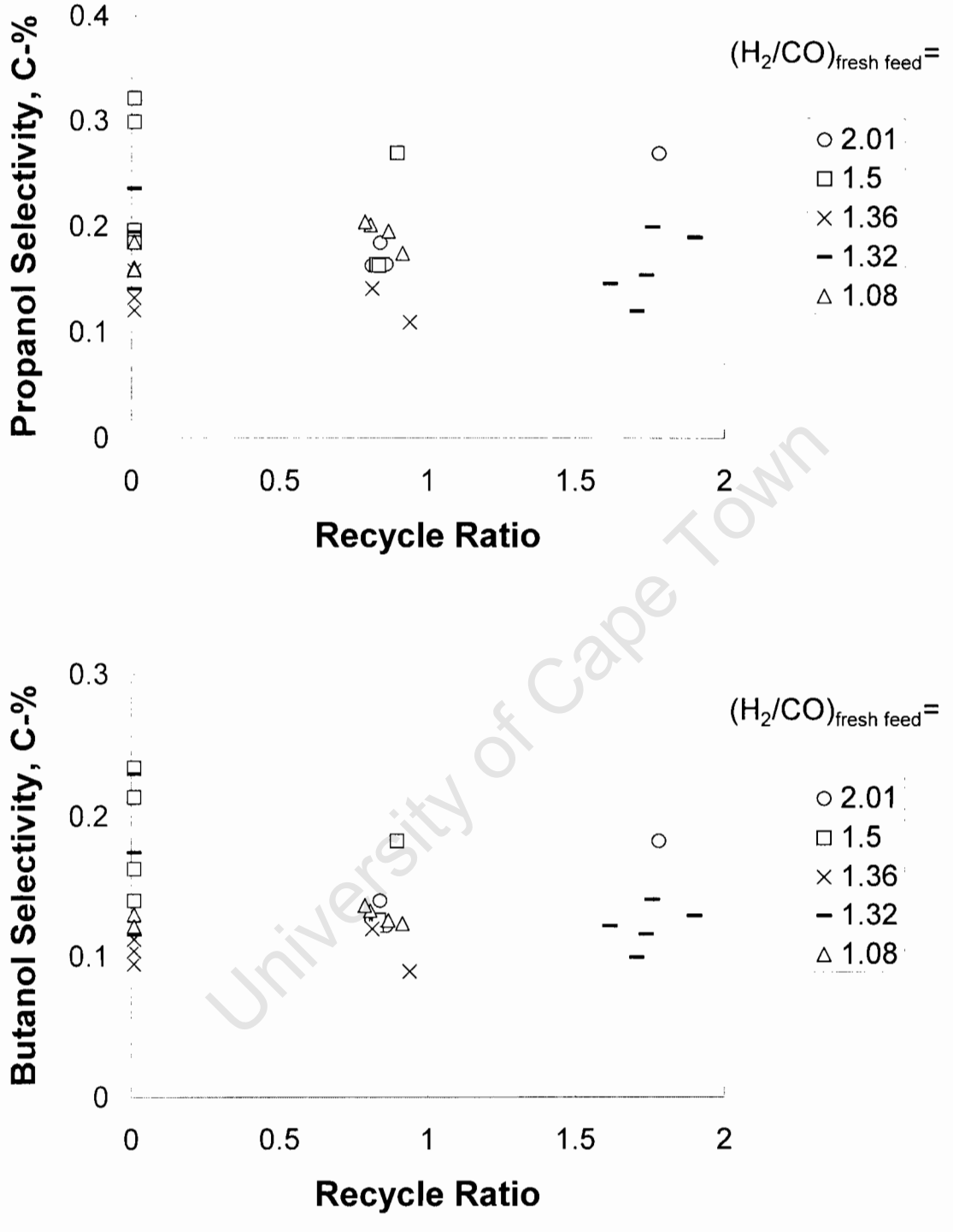

Figure 4.22 (continued):

Alcohol Selectivity in C-% as a function of recycle ratio for the various fresh feed ratios

5

DISCUSSION

In this study the effect of recycle of the tail gas back to the reactor was investigated for different ratios of hydrogen to carbon monoxide in the fresh feed. Thus, data was obtained at a large variety of partial pressures within the reactor. Product formation in the Fischer-Tropsch synthesis is determined by the partial pressures in the reactor.

5.1 MODELING THE FORMATION OF ORGANIC PRODUCT COMPOUNDS

In order to obtain more clarity on the effect of recycling the tail-gas on the Fischer-Tropsch activity, i.e. the formation of organic product compounds, various proposed rate expressions for the Fischer-Tropsch synthesis were tested (see section 2.5.1). The data from the different runs were lumped together and the parameters for the corresponding rate equations were optimised. The different rate expressions were linearised in the following form:

Anderson [1956]
$$\frac{p_{H_2}}{r_{FT}} = \frac{1}{k} + \frac{a}{k} \cdot \frac{p_{H_2O}}{p_{CO}} \tag{5.1}$$

Huff and Satterfield [1984]
$$\frac{k \cdot p_{H_2}}{r_{FT}} = \frac{1}{k} + a \cdot \frac{p_{H_2O}}{p_{CO} \cdot p_{H_2}} \tag{5.2}$$

Ledakowicz *et al.* [1985]
$$\frac{p_{H_2}}{r_{FT}} = \frac{1}{k} + \frac{a}{k} \cdot \frac{p_{CO_2}}{p_{CO}} \tag{5.3}$$

Van Steen and Schulz [1999]

$$\sqrt{\frac{p_{H_2}^{1.5} \cdot p_{CO}}{\frac{p_{H_2O}}{r_{FT}}}} = \frac{1}{\sqrt{k}} + \frac{a}{\sqrt{k}} \cdot \frac{p_{H2} \cdot p_{CO}}{p_{H_2O}} \qquad (5.4)$$

Figure 5.1 shows the linearised form of the various rate expressions. The obtained kinetic constants are given in Table 5.1. Figure 5.2 shows the parity plot for the various rate expressions.

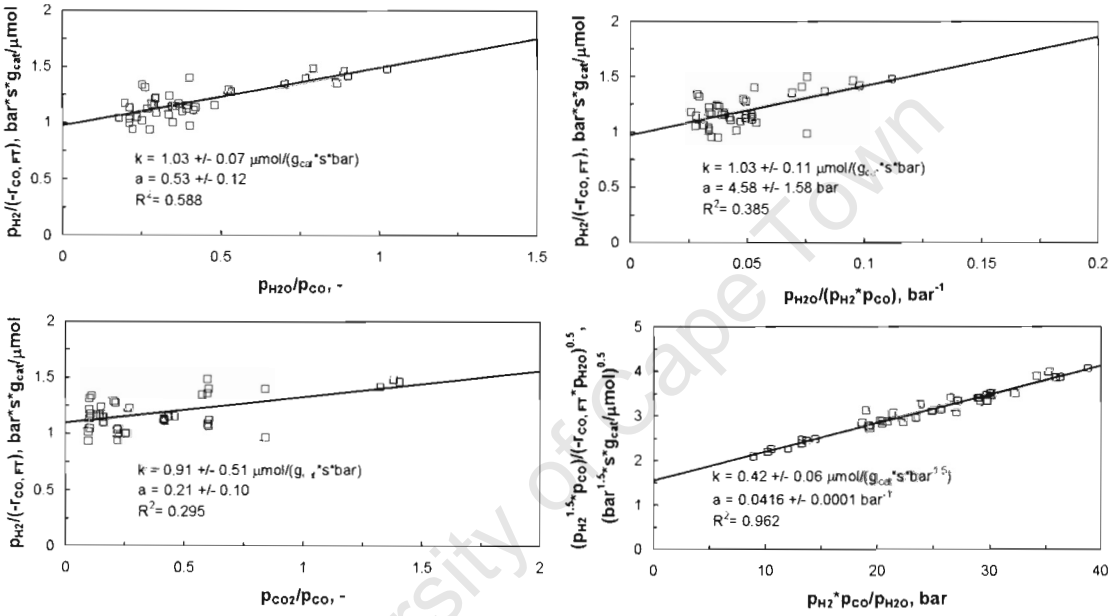

Figure 5.1: Fit of the experimental data to the linearised forms of the proposed rate expressions in literature to describe the rate of the Fischer-Tropsch synthesis, i.e. the rate of carbon incorporation in organic product compounds)

Top left: Fit to the expression proposed by Anderson [1956]

Top right: Fit to the expression proposed by Huff and Satterfield [1984]

Bottom left: Fit to the expression proposed by Ledakowicz *et al.* [1985]

Bottom right: Fit to the expression proposed by van Steen and Schulz [1999]

Table 5.1: Obtained kinetic parameters for the rate of the Fischer-Tropsch synthesis and goodness of fit (the kinetic coefficients as obtained from equations (5.1-5.4) with the 95% confidence interval)

	k	a	$R^{2,1}$	$Error^2$
Anderson [1956]	1.03±0.07	0.53±0.12	0.588	0.064
Huff and Satterfield [1984]	1.03±0.11	4.58±1.58	0.385	0.080
Ledakowicz et al. [1985]	0.91±0.51	0.21±0.10	0.295	0.192
Van Steen and Schulz [1999]	0.42±0.06	0.042±0.0001	0.962	0.047

[1] Correlation coefficient for the linear fit of the experimental data to the proposed rate expression

[2] Average error in the parity plot defined as:

$$error = \frac{1}{N-1} \cdot \sum_{i=1}^{i=N} \frac{\left| r_{FT,measured,i} - r_{FT,calculated,i} \right|}{r_{FT,measured,i}} \qquad (5.5)$$

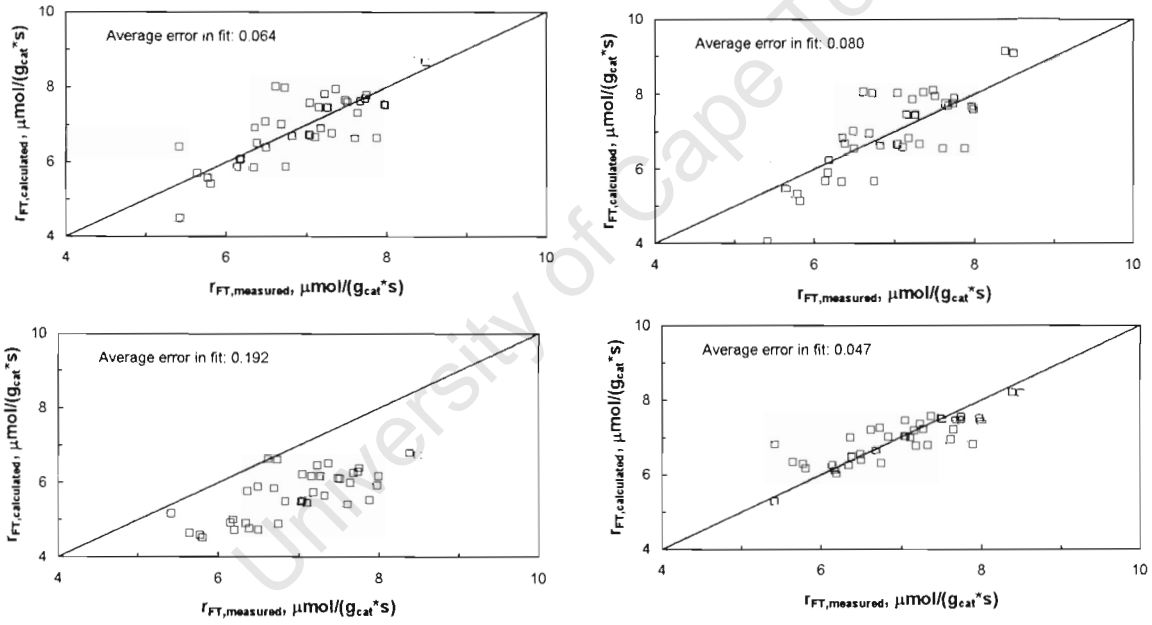

Figure 5.2: Parity plot of the calculated rate of the Fischer-Tropsch synthesis using the optimized kinetic constants (average error defined as the relative deviation of the calculated rate from the measured rate – see Table 5.1, equation 5.5)

Top left: Expression proposed by Anderson [1956]

Top right: Expression proposed by Huff and Satterfield [1984]

Bottom left: Expression proposed by Ledakowicz *et al.* [1985]

Bottom right: Expression proposed by van Steen and Schulz [1999]

The rate of the Fischer-Tropsch synthesis is best described by the rate expression proposed by van Steen and Schulz [1999]. The rate expression proposed by Anderson [1956] is the next best descriptor of the rate of the Fischer-Tropsch synthesis. The obtained correlation coefficient and the average error in the parity plot (as defined in Table 5.1) is significantly lower than those obtained for the fit to the rate expression proposed by van Steen and Schulz [1999]. The rate expression proposed by Ledakowicz *et al.* [1985] incorporates an inhibition by carbon dioxide instead of water (as was proposed by Anderson [1956]). The experiments performed in this study cannot be described adequately by an inhibition with carbon dioxide. The rate expression proposed by Huff and Satterfield, which was verified by those authors on a fused magnetite catalyst at 270°C, also fails results of the analyses for the FT rate expressions.

Table 5.2 compares the obtained kinetic coefficients for the kinetic expression developed by van Steen and Schulz on various iron-based catalysts as reported by different researchers. All researchers obtained good correlation coefficient in their determination of the kinetic coefficient (larger than 0.94). The obtained kinetic coefficient, *k*, indicates that this catalyst is more active than the other

Table 5.2: Comparison of the kinetic coefficients obtained from fitting experimental data to the rate expression proposed by Schulz and van Steen [1999]

Author(s)	catalyst	$T_{reaction}$ °C	k μmol/(g s $bar^{1.5}$)	a* 100 bar^{-1}
Van Steen and Schulz [1999]	100 Fe/3 Cu/2 K_2O/37 Al_2O_3	250	0.02	1.4
Claeys [1997]	100 Fe/10 Cu/13 Al_2O_3	250	0.14	7.9
	100 Fe/10 Cu/5 K_2O/13 Al_2O_3	250	0.27	5.1
Riedel [2002]	100 Fe/11 Cu/11 K_2O/13 Al_2O_3	205	0.06	4.7
		220	0.11	6.7
		235	0.26	9.8
		250	0.53	11.5
Biel [2004]	100Fe/5 Cu/4 K_2O/24 SiO_2	240	0.22±0.03	3.9±0.04
This study	Precipitated iron	240	0.42±0.06	4.2±0.01

ones reported up to now. This might originate from the actual catalyst composition or the catalyst pre-treatment. This study, the study by Biel [2004] and the study by Claeys [1997] all yield similar values for the inhibition coefficient.

5.2 MODELING THE FORMATION OF CARBON DIOXIDE

Carbon dioxide is often formed as a co-product in iron-catalysed Fischer-Tropsch synthesis. The formation of carbon dioxide is often formulated as a consecutive reaction, i.e. water, which is primarily formed in the Fischer-Tropsch synthesis, reacts further with carbon monoxide yielding carbon dioxide. Van der Laan and Beenackers [1999] developed a rate expression for the formation of CO_2, assuming that the water gas shift reaction takes place on a different site than the Fischer-Tropsch synthesis and thus implying a consecutive reaction. Zimmerman and Bukur [1990] tested a variety of rate expressions for the rate of formation of CO_2 in the Fischer-Tropsch synthesis. Their conclusion was that the rate of formation of CO_2 takes place on similar sites as the Fischer-Tropsch synthesis.

The obtained data in this study were fitted to a linearised form of the rate expressions proposed in literature:

Zimmerman and Bukur [1990]:

$$\frac{\left(\frac{p_{H_2O}}{p_{H_2}} - \frac{p_{CO_2}}{K_P \cdot p_{CO}}\right)}{r_{CO_2}} = \frac{1}{k_w} + \frac{a}{k_w} \cdot \frac{p_{H_2O}}{p_{CO} \cdot p_{H_2}} \qquad (5.6)$$

Van der Laan and Beenackers [2000]:

$CO^* + OH^* \rightarrow COOH^* + ^*$:

$$\sqrt{\frac{\left(p_{H_2O} \cdot p_{CO} - p_{CO_2} \cdot p_{H_2} / K_P\right)}{r_{CO_2}}} = \frac{1}{\sqrt{k_w}} + \frac{a}{\sqrt{k_w}} \cdot p_{CO} + \frac{b}{\sqrt{k_w}} \cdot p_{H_2O} \qquad (5.7)$$

$CO^* + H_2O^* \rightarrow COOH^* + H^*$:

$$\sqrt{\frac{\left(\frac{p_{H_2O}\cdot p_{CO}}{\sqrt{p_{H_2}}} - p_{CO_2}\cdot\sqrt{p_{H_2}}/K_P\right)}{r_{CO_2}}} = \frac{1}{\sqrt{k_w}} + \frac{a}{\sqrt{k_w}}\cdot p_{CO} + \frac{b}{\sqrt{k_w}}\cdot p_{H_2O} \qquad (5.8)$$

The obtained kinetic coefficients are given in Table 5.3 together with the correlation coefficient for the linear fit and the average error in the parity plot (as defined in equation 5.5). Figure 5.3 shows the parity plot for the three proposed rate expressions.

The rate expression proposed by van der Laan and Beenackers [2000], in which CO_2 is formed by the reaction of adsorbed CO and an adsorbed hydroxyl species fits the data best. However, the kinetic constants cannot be estimated with a great confidence.

Table 5.3: Obtained kinetic parameters for the rate of formation of CO_2 in the Fischer-Tropsch synthesis and goodness of fit (the kinetic coefficients as obtained from equations (5.6-5.8) with the 95% confidence interval)

	k_W	a	b	$R^{2,1}$	Error[2]
Zimmerman and Bukur [1990]	10.2±1.9	3.5±4.3		0.123	0.131
Van der Laan and Beenackers [2000]					
CO* + OH* → COOH* +*	4.2±24.3	0.4±0.7	0.8±2.1	0.879	0.089
CO* + H_2O* → COOH* +H*	4.8±13.5	0.3±0.3	0.3±0.7	0.844	0.115

[1] Correlation coefficient for the linear fit of the experimental data to the proposed rate expression

[2] Average error in the parity plot defined as:

$$\text{error} = \frac{1}{N-1}\cdot\sum_{i=1}^{i=N}\frac{\left|r_{FT,measured,i} - r_{FT,calculated,i}\right|}{r_{FT,measured,i}} \qquad (5.5)$$

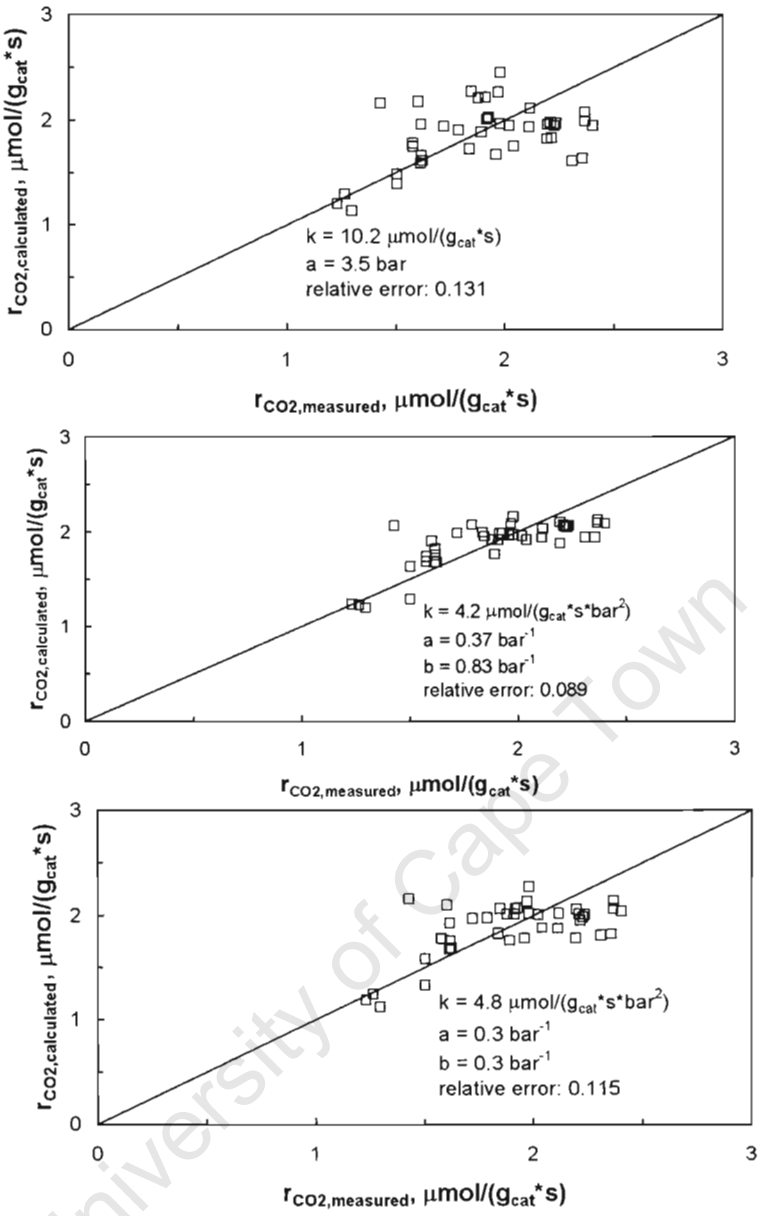

Figure 5.3: Parity plot of the proposed rate expressions in literature to describe the rate of formation of CO_2 in the Fischer-Tropsch synthesis

Top: Fit to the expression proposed by Zimmerman and Bukur [1990]

Middle: Fit to the expression proposed by van der Laan and Beenackers [2000] assuming the rate determining step to be the reaction between adsorbed CO and a surface hydroxyl species (equation (5.7))

Bottom: Fit to the expression proposed by van der Laan and Beenackers [2000] assuming the rate determining step to be the reaction between adsorbed CO and adsorbed water (equation (5.8))

In this rate expression it is assumed that the formation of CO_2 takes place on a different site from the site for the Fischer-Tropsch synthesis. The nature of this site is presently unknown. From the work by Biel [2004], it might be speculated that the site responsible for the formation of CO_2 is superparamagnetic Fe_3O_4. According to the rate expression proposed by van der Laan and Beenackers [2000], CO_2 is formed in a sequential reaction. However, CO_2 is always observed with iron-based catalysts, and the sequential nature of its formation might be questioned.

5.3 MODELING USAGE RATIO

The usage ratio, the ratio of the rate of consumption of hydrogen relative to the rate of consumption of carbon monoxide, can be modeled assuming that in the Fischer-Tropsch synthesis 2 mole of hydrogen is consumed per mole of carbon monoxide consumed and that hydrogen is co-produced in the formation of carbon dioxide. The assumption that the Fischer-Tropsch synthesis consumes 2 mole of hydrogen for each mole of carbon monoxide is reasonable for this study, since the methane selectivity is relatively low and the olefin content in the products is high. The usage ratio can thus be modeled as:

$$\text{usage ratio} = \frac{-r_{H_2}}{-r_{CO}} = \frac{2 \cdot r_{FT} - r_{CO_2}}{r_{FT} + r_{CO_2}} \tag{5.6}$$

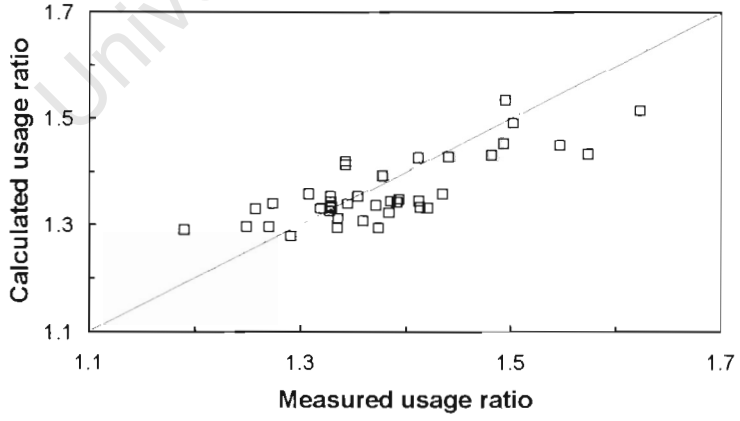

Figure 5.4: Parity plot for the usage ratio

Figure 5.4 shows the parity plot for the usage ratio. Despite the relative poor fit to describe the rate of CO_2-formation, the usage ratio can be estimated reasonably well with an average error, as defined by equation (5.5), of 3.4%.

5.4 MODELING ORGANIC PRODUCT SELECTIVITY

The product selectivity in the Fischer-Tropsch synthesis was evaluated according to the various characteristic features of the Fischer-Tropsch product slate, viz. methane selectivity, chain growth probability, olefin selectivity, and alcohol selectivity. For the purpose of this study the effect of recycled olefins on the olefin selectivity is of primary interest.

5.4.1 EFFECT OF RECYCLE RATIO ON 1-OLEFIN CONTENT

Schulz and Claeys [1999] developed an extended olefin-readsorption model, in which primarily formed 1-olefins can re-adsorb to undergo secondary hydrogenation, secondary double bond isomerisation and further chain growth. According to their model the ratio of the concentration of the so-called linear end-products (i.e. products which are not susceptible to consecutive reactions, n-paraffins and internal olefins) to the concentration of 1-olefins in the liquid phase for a given carbon number is given by:

$$\frac{C_{EP,L,N}}{C_{1-Ol,L,N}} = \frac{\left(\frac{k_{d,1-Ol}}{k_{d,P}}\right)^{-1} \cdot \left(\frac{k_a \cdot m_{Me}}{\dot{V}_g} + \frac{k'_a \cdot m_{Me}}{\dot{V}_g} \cdot \left(1 - \frac{1 - \left(\frac{k'_{d,1-Ol}}{k_{d,1-Ol}}\right) \cdot \left(\frac{k_{d,1-Ol}}{k_{d,P}}\right) \cdot \left(\frac{k'_{d,EP}}{k_{d,P}}\right)^{-1}}{1 + \left(\frac{k'_{d,1-Ol}}{k_{d,1-Ol}}\right) \cdot \left(\frac{k_{d,1-Ol}}{k_{d,P}}\right) \cdot \left(\frac{k'_{d,EP}}{k_{d,P}}\right)^{-1}} \right) + \frac{\dot{V}_L}{\dot{V}_g} + \frac{1}{K_N} \right)}{\frac{\dot{V}_L}{\dot{V}_g} + \frac{1}{K_N}} \tag{5.7}$$

The ratio of the concentration of the end product relative to the concentration of the 1-olefin is given by a set of dimensionless parameters:

$\frac{k_{d,Ol-(1)}}{k_{d,P}}$ expresses the ratio of the primary desorption as an olefin relative to the desorption as a paraffin and as such expresses the primary olefin selectivity

$\frac{k_a \cdot m_{Me}}{\dot{V}_g}$ expresses the rate of re-adsorption yielding a surface species Sp_N, which can grow further, relative to the removal of this species through the gas phase

$\frac{k'_a \cdot m_{Me}}{\dot{V}_g}$ expresses the rate of re-adsorption yielding a surface species Sp'_N, which cannot grow further (this surface species can desorb yielding either an end product or an 1-olefin)

$\frac{k'_{d,Ol-(1)}}{k_{d,Ol-(1)}}$ expresses the ratio of desorption as an 1-olefin from species Sp'_N relative to the desorption as an 1-olefin from species Sp_N

$\frac{k'_{d,EP}}{k_{d,P}}$ expresses the ratio of desorption as an end-product from species Sp'_N relative to the desorption as an end-product (n-paraffin) from species Sp_N

$\frac{\dot{V}_L}{\dot{V}_g}$ expresses the ratio of the liquid flow out of the reactor relative to the gas flow out of the reactor

K_N expresses the carbon number dependent partition coefficient of the product compounds between the liquid and the gas phase

The olefin content in the fraction of linear hydrocarbons is dependent on the carbon number (see Figure 4.16). The carbon number dependency originates in this model from the carbon number dependent distribution coefficient, K_N, and thus from the difference in the concentration of the 1-olefin in the liquid phase. Based on the values published by Schulz and Claeys [1999], the carbon number dependency of the partition coefficient was modeled as:

$$K_N = 1.52 \cdot (1.46)^{n-2} \tag{5.8}$$

Figure 5.5 shows the 1-olefin content in the fraction of linear hydrocarbons as a function of carbon number. The 1-olefin content was modeled with the model developed by Schulz and Claeys [1999]. Readsorption of ethene cannot lead to the formation of a species Sp'_N. Thus, for C_2 k'_a was put equal to zero. Furthermore, ethene is known to have a higher reactivity than the other hydrocarbons. The ratio of the concentration of the end-product relative to the 1-olefin for C_2 was thus modeled as:

$$\frac{C_{EP,L,N=2}}{C_{1-Ol,L,N=2}} = \frac{\left(\frac{k_{d,1-Ol}}{k_{d,P}}\right)^{-1} \cdot \left(\frac{a \cdot k_a}{\dot{V}_g} \cdot m_{Me} + \frac{\dot{V}_L}{\dot{V}_g} + \frac{1}{K_N}\right)}{\frac{\dot{V}_L}{\dot{V}_g} + \frac{1}{K_N}} \qquad (5.9)$$

with a the reactivity of ethene relative to the reactivity of longer 1-olefins.The model shows a good fit with the experimentally obtained 1-olefin content.

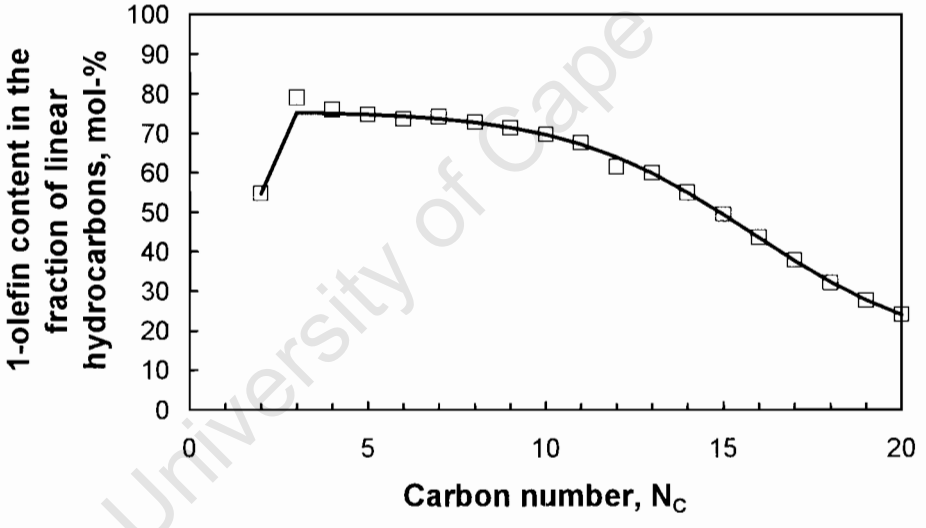

Figure 5.5: 1-Olefin content in the fraction of linear hydrocarbons as a function of carbon number for the experiment with $(H_2/CO)_{fresh\ feed}$ = 2.01 and a recycle ratio of 0.8 (solid line is model fit)

6 Dimensionless parameters were extracted from the experimental data using the model developed by Schulz and Claeys [1999] (the parameter describing the ratio of desorption as an 1-olefin from species Sp'_N and desorption from

species Sp_N and the parameter describing the ratio of desorption as an end-product from species Sp'_N and the desorption as an end-product from species Sp_N can only be determined together).

Figure 5.6 shows the ratio of the primary desorption as an olefin relative to desorption as a paraffin as a function of the recycle ratio and the hydrogen to carbon monoxide ratio in the fresh feed. The ratio decreases with hydrogen to carbon monoxide ratio in the fresh feed and with increasing recycle ratio.

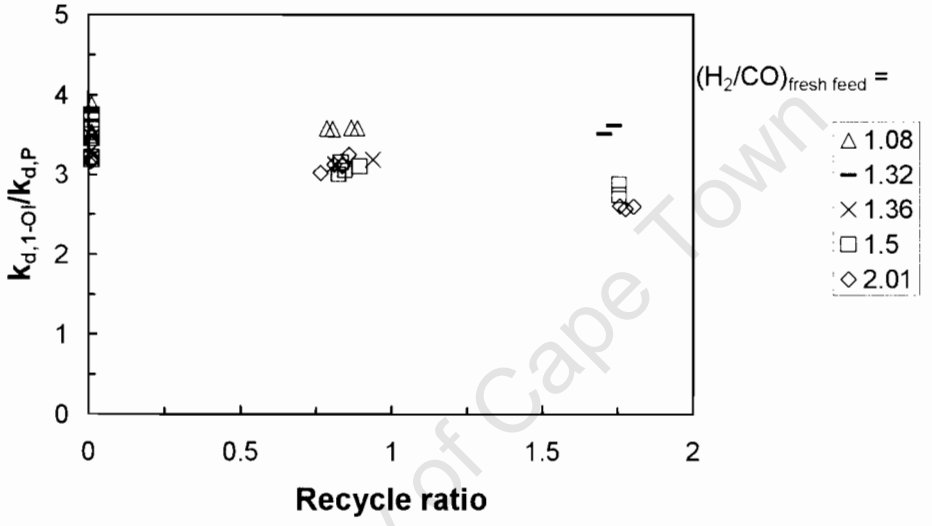

Figure 5.6: Ratio of rate of desorption as an olefin to the rate of desorption as a n-paraffin from a surface species Sp_N, which participates in chain growth, as a function of recycle ratio and the hydrogen to carbon monoxide ratio in the fresh feed

The primary formation of n-paraffin can be viewed as the H-addition to a surface alkyl species, whereas the formation of an 1-olefin can be viewed as the β-H-abstraction from a surface alkyl species [Claeys and van Steen, 2004]. Based on this mechanistic picture and assuming that the β-H-abstraction requires an adjacent vacant site, the ratio of the rate of desorption as a paraffin relative to the rate of desorption as an olefin should correlate with the square root of the hydrogen partial pressure. Figure 5.7 shows the ratio of the rate of desorption as a paraffin from Sp_N to the rate of desorption as an 1-olefin from Sp_N as a

function of the square root of the partial pressure of hydrogen. A reasonable correlation is observed. The correlation differs for the different recycle ratios. This might be attributed to the olefins in the feed, when tail gas is recycled back to the reactor.

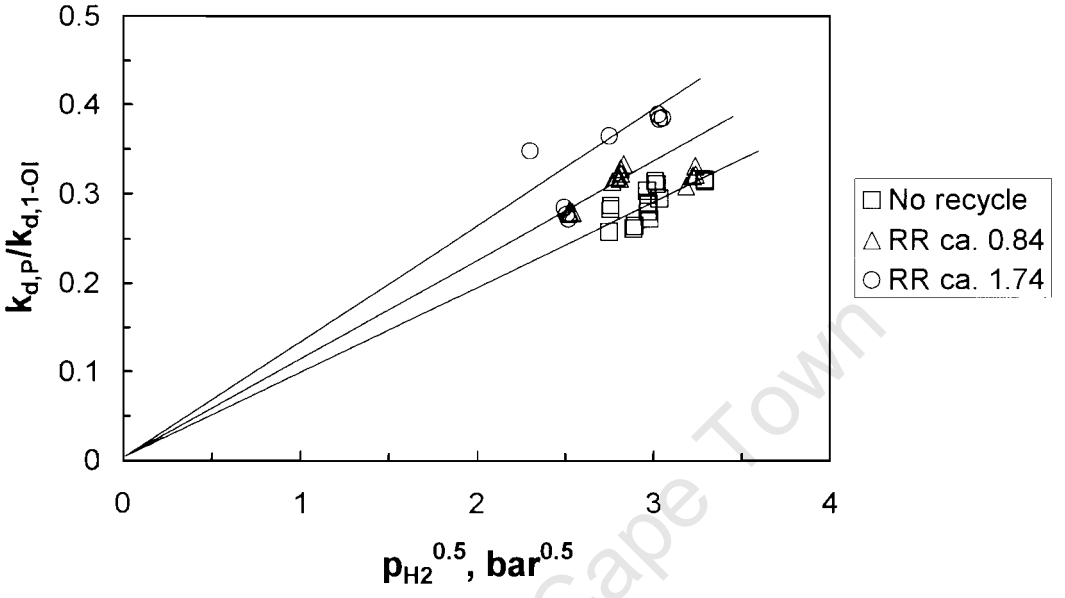

Figure 5.7: Ratio of rate of desorption as a n-paraffin to the rate of desorption as an 1-olefin from a surface species Sp_N, which participates in chain growth, as a function of the square root of the hydrogen partial pressure

The lumped parameter describing the ratio of the rate of desorption as an 1-olefin from species Sp'_N and the rate of desorption from species Sp_N and the parameter describing the ratio of the rate of desorption as an end-product from species Sp'_N and the rate of desorption as an end-product from species Sp_N as a function of the recycle ratio is shown in Figure 5.8. A value of 1 for this lumped parameter indicates, that the desorption probabilities of species Sp'_N is identical to the desorption probabilities for species Sp_N. A value of less than 1 is expected, since the β-H-abstraction of the species Sp'_N can also lead to internal olefins, which are end-products. For all experiments a value of less than 1 is obtained. The lumped parameter has a value of ca. 0.42 ± 0.06. It must however be noted that the optimization procedure used was not very sensitive to variations in the lumped parameter.

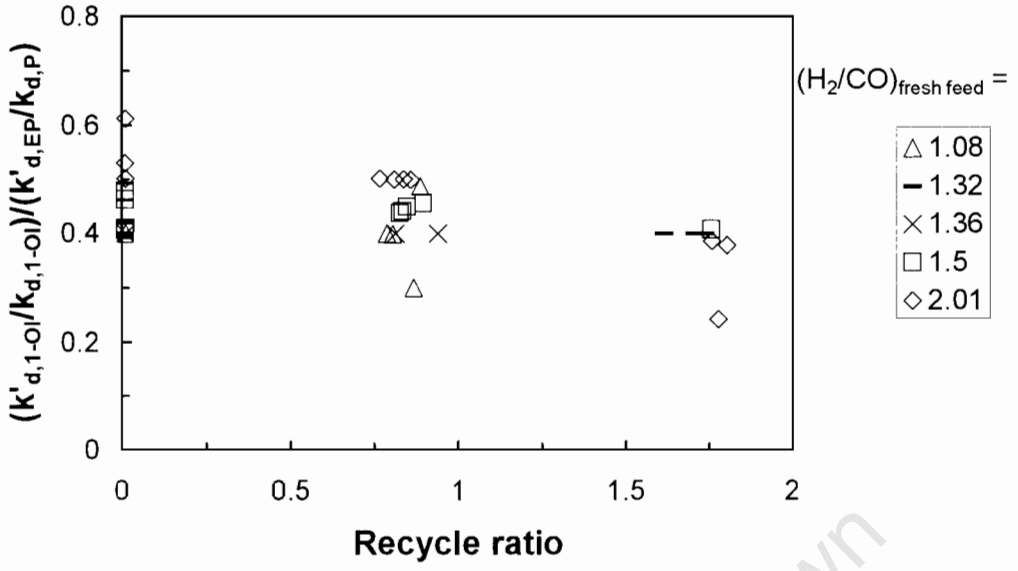

Figure 5.8: Lumped parameter describing the ratio of the rate of desorption as an 1-olefin from species Sp'_N and the rate of desorption from species Sp_N and the parameter describing the ratio of the rate of desorption as an end-product from species Sp'_N and the rate of desorption as an end-product from species Sp_N as a function of the recycle ratio

Re-adsorption of 1-olefins may lead to the formation of the species Sp_N from which the 1-olefin originally was formed. The influence of the recycle ratio on the parameter describing the rate of re-adsorption relative to the rate of transport out of the reactor through the gas phase is shown in Figure 5.9. The rate of re-adsorption seems to increase with increasing hydrogen to carbon monoxide ratio in the fresh feed (if the parameters estimated from the experiments with a hydrogen to carbon monoxide ratio in the fresh feed of 1.50 can be omitted). Re-adsorption of olefins involves the reaction of an 1-olefin with surface hydrogen [Claeys and van Steen, 2004]. Thus, an increase in the hydrogen to carbon monoxide ratio, which corresponds to an increase in the partial pressure of hydrogen in the reactor, should yield an increase in the rate of re-adsorption.

Furthermore, at going from a recycle ratio of ca. 0.8 to 1.7 the rate of re-adsorption relative to the rate of transport out of the reactor through the gas

phase seems to increase with increasing recycle ratio. This might be caused by the presence of olefins in the feed, when tail gas is recycled.

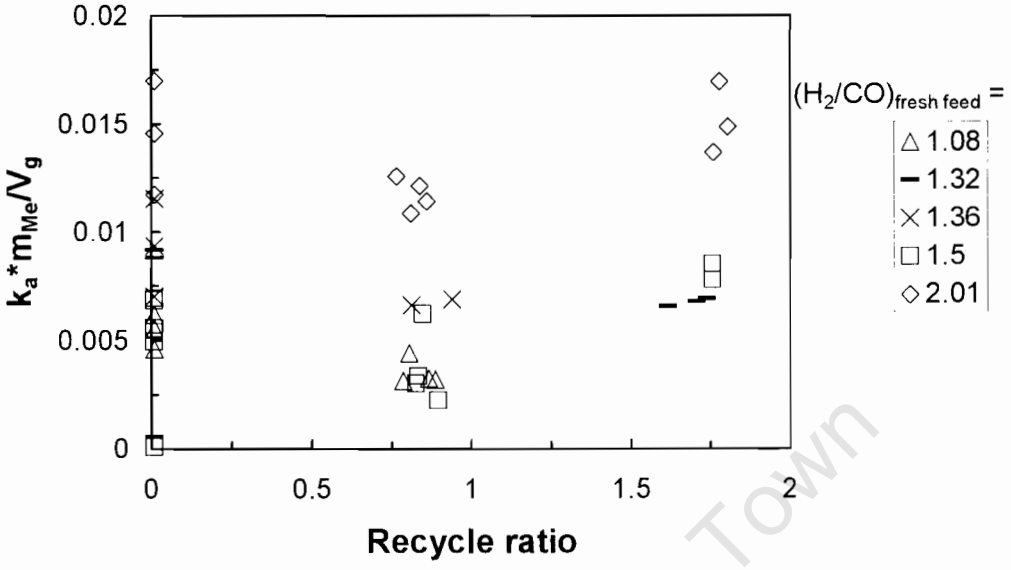

Figure 5.9: The rate of re-adsorption yielding surface species Sp_N relative to the rate of transport out of the reactor through the gas phase as a function of the recycle ratio

Re-adsorption of 1-olefins may also lead to the formation of the species Sp'_N, which does not participate in chain growth. The influence of the recycle ratio on the parameter describing the rate of re-adsorption yielding this species relative to the rate of transport out of the reactor through the gas phase is shown in Figure 5.10. The parameters estimated from the experiments with hydrogen to carbon monoxide ratio in the fresh feed of 1.50 yielded much larger values than the parameters estimated from the other experiments. The parameters estimated from the experiments with hydrogen to carbon monoxide ratio in the fresh feed of 2.01 are higher than that for the other experiments. The re-adsorption yielding a surface species Sp'_N is between 10 and 100 times less likely than the re-adsorption yielding a surface species Sp_N. This might be related to the space requirements for re-adsorption on a surface covered with surface carbon.

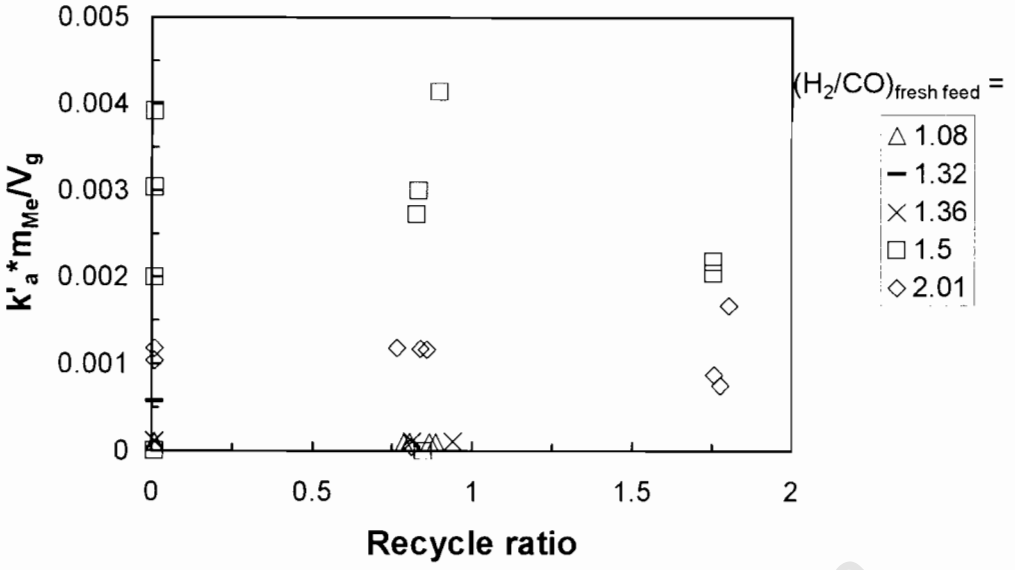

Figure 5.10: The rate of re-adsorption yielding surface species Sp'_N relative to the rate of transport out of the reactor through the gas phase as a function of the recycle ratio

The volumetric flow rate of the liquid relative to the volumetric flow rate of the gas phase was also estimated as a parameter in the model. The ratio of the liquid to gas volumetric flow rate shows a good correlation with time-on-stream indicating that it might be more related with the experimental procedure than with the production of liquid hydrocarbons (see Figure 5.11).

Ethene is known to be much more reactive than the other olefins [Schulz and Claeys, 1999]. The reactivity of ethene relative to the reactivity of the other 1-olefins was obtained as a model parameter as well. Figure 5.12 shows the reactivity of ethene relative to the reactivity of the other olefins as a function of the recycle ratio. Without recycle ethene is ca. 12 times more reactive than the other olefins. Schulz and Claeys [1999] reported a similar value. With increasing recycle ratio the ethene reactivity is increased. This might be attributed to the increase in ethene concentration, since ethene is fed back to the reactor as was.

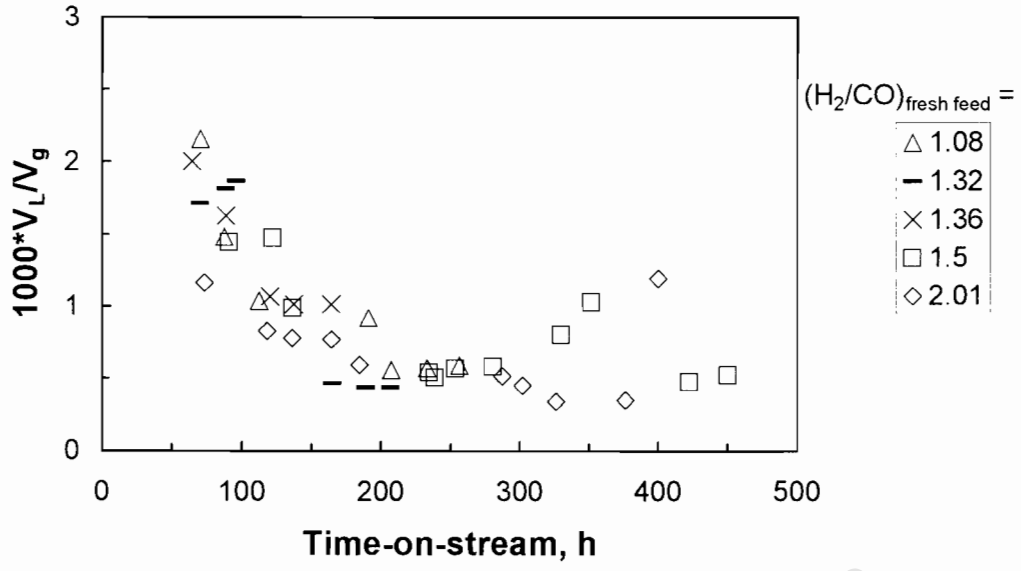

Figure 5.11: Ratio of the volumetric flow rate of the liquid leaving the reactor relative to the volumetric flow rate of the gas phase leaving the reactor as a function of time-on-stream

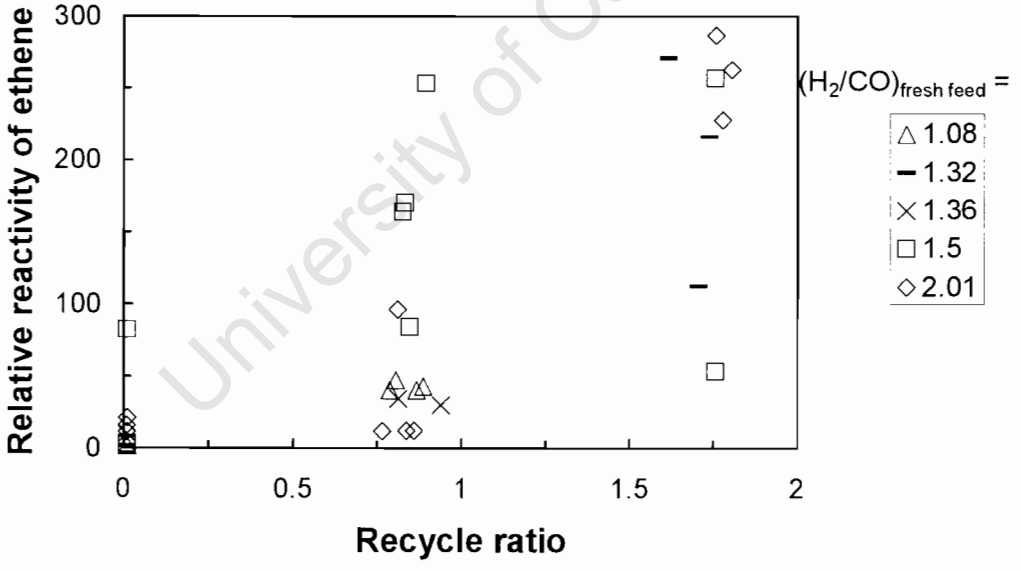

Figure 5.12: Reactivity of ethene relative to the reactivity of other 1-olefins as a function of recycle ratio

6

CONCLUSIONS

The effect of recycling the tail-gas back to the reactor, during the low temperature Fischer-Tropsch process, was investigated for different H_2/CO ratios in the fresh feed on a precipitated iron catalyst using a micro-slurry reactor.

Recycling the tail gas back to the reactor increases the overall conversion of carbon monoxide significantly. The overall conversion of CO increases further upon increasing the recycle ratio. The benefit of recycling the tail gas is more pronounced for a synthesis gas with a higher H_2/CO-ratio than for a synthesis gas with a low H_2/CO ratio.

The usage ratio of H_2/CO in this system was ca. 1.4. Consequently, the H_2/CO-ratio in the gas fed to the reactor did not change significantly upon introduction of recycle for a fresh feed synthesis gas with a H_2/CO ratio of approximately 1.36. The synthesis gas with a H_2/CO ratio of 1.08 produced a tail gas with lower H_2/CO-ratio and upon recycling the tail gas, the H_2/CO ratio in the gas fed to the reactor dropped. The fresh feed with a H_2/CO ratio of larger than 1.4 yielded a tail gas with a higher H_2/CO ratio. Hence, the feed to the reactor had a higher H_2/CO ratio upon recycling the tail gas. With increasing recycle ratio the H_2/CO ratio in the feed to the reactor becomes higher (up to 5.5 mol/mol for a synthesis gas with a $H_2/CO=2.0$ and a recycle ratio of 1.78). These trends compare well with that reported by Espinoza [2004] and Boelee [1989] on a cobalt-based and iron-based catalyst respectively.

Upon reducing the recycle ratio back to zero, the performance of the system was identical to that before the introduction of the recycle. This indicates that permanent deactivation did not occur upon introduction of a recycle.

Approximately 30% of the water produced by the Fischer-Tropsch synthesis is consumed in the water gas shift reaction yielding CO_2. The fraction of water consumed in the water gas shift reaction decreases slightly with increasing hydrogen to carbon monoxide ratio in the feed and with increasing recycle ratio.

The methane selectivity increases with increasing H_2/CO-ratio in the fresh feed for H_2/CO ratios larger than 1.50. For smaller H_2/CO ratios in the fresh feed the methane selectivity shows a relative large scatter. This was due to the analytical technique, which produces greater errors for very small concentrations of methane. With increasing recycle ratio the chain growth probability increases slightly. The recycling of reactive product compounds, which may have induced secondary chain growth, might have caused this.

For the FT rate expressions tested, the rate expression proposed by van Steen and Schulz [1999] describes the data the best. The rate expression proposed by Anderson [1956] is the next best descriptor of the rate of the Fischer-Tropsch synthesis. The rate expression proposed by Ledakowicz *et al.* [1985] incorporates an inhibition by carbon dioxide instead of water (as was proposed by Anderson [1956]). The experiments performed in this study cannot be described adequately by an inhibition with carbon dioxide. The rate expression proposed by Huff and Satterfield also fails results of the analyses for the FT rate expressions.

For the two WGS rate expression tested, the rate expression proposed by van der Laan and Beenackers [2000], in which CO_2 is formed by the reaction of adsorbed CO and an adsorbed hydroxyl species describes the data better.

The 1-olefin content was modeled with the model developed by Schulz and Claeys [1999] and showed a good fit with the experimental data obtained in this

study. With increasing recycle ratio, the ethene reactivity increased. Ethene is the most reactive compound and the olefin content in the fraction of C_2-hydrocarbons shows therefore the strongest dependency on the reaction conditions. Propene is rather unreactive and the olefin content in the fraction of C_3-hydrocarbons is therefore not a strong function of the reaction conditions.

The oxygenates (alcohols, ketones and aldehydes) also showed a similar trend to the olefins suggesting secondary reactions. However, the extent of this was not as strong as that of the olefins. The methanol selectivity seems to decrease with increasing recycle ratio for the H_2/CO ratios above the usage ratio. For the lower H_2/CO ratios, an increase in the methanol selectivity is observed. These observations were not so noticeable for the ethanol, butanol and propanol selectivites. The methanol selectivity remained unchanged for H_2/CO ratios close to the usage ratio.

References

Anderson, R.B.
in *Catalysis,* Vol. 4 (Emmett P.H., Ed.), Reinhold, New York (1956).

Ando, H., Xu, Q., Fujiwara, M., Matsumura, Y., Tanaka, M., Souma, Y.
Hydrocarbon synthesis from CO_2 over Fe–Cu catalysts
Catalysis Today **45** (1998), 229-234.

Arcuri, K.B., Agee, K.I., Agee, M.A.
Structured Fischer-Tropsch catalyst system and method
US 6262131 (2001) assigned to Syntroleum Corporation

Asian Tribune
India, China will drive global energy use increase
http://www.asiantribune.com/show_news.php?id=4059 (2003)

Biel, H.B.
The effect of water partial pressure on low temperature iron Fischer-Tropsch reaction rate, selectivity and catalyst structure
MSc thesis, University of Cape Town (2004)

Boelee, J.H., Custers, J.M.G., van der Wiele, K.
Influence of reaction conditions on the effect of co-feeding ethene in the Fischer-Tropsch synthesis on a fused-iron catalyst in the liquid-phase
Applied Catalysis **53** (1989), 1-13.

Benham, C.B., Bohn, M.S., Yakobson, D.L.
Process for the production of hydrocarbons
US 5620670 (1997) assigned to Rentech Inc.

Bohn, M.S., Benham, C.B.
Process for the production of hydrocarbons, power and carbon dioxide from carbon-containing materials
US 6036917 (2001) assigned to Rentech Inc.

Clark, G.L., Walker, D.G.
Multiple reactor system and method for Fischer-Tropsch synthesis
US 6156809 (2000) to Reema International Corporation

Claeys, M.
Selektivität, Elementarschritte und kinetische Modellierung bei der Fischer-Tropsch Synthess
PhD thesis, University of Karlsruhe (1997)

Claeys, M. van Steen, E.
Fischer-Tropsch synthesis: fundamentals
Studies in Surface Science and Catalysis **152** (2004), 601-680.

Davis, B.H.
Fischer-Tropsch synthesis: relationship between iron catalyst composition and process variables
Catalysis Today **84** (2003), 83-98.

Dry, M.E.
Advances in Fischer-Tropsch chemistry
Industrial & Engineering Chemistry Product Research and Development **15** (1976), 282-285

Dry, M.E.,
The Fischer-Tropsch synthesis
in "*Catalysis Science and Technology*", Vol. 15-255, p. 1 (Anderson, R.B and Boudart, M., Eds.), Springer-Verlag, Berlin (1981).

Dry, M.E.
Fischer-Tropsch reactions and the environment
Applied Catalysis A: General **189** (1999), 185-190.

Dry, M.E.
The Fischer-Tropsch process: 1950-2000
Catalysis Today **71(3-4)** (2002), 227-241.

Dry, M.E.
Fischer-Tropsch synthesis – industrial
Encyclopaedia of Catalysis, Vol. 3, p. 347-403 (Horvath, I.T., Ed.),John Wiley and Sons, New York (2003).

Espinoza, R.L., Raje, A.P., Jack, D.
Recycling light olefins in multi-stage Fischer-Tropsch process
US Pat. App. Pub. 2004/0092609 (2004) assigned to ConocoPhilips Co.

Fiato, R.A., Soled, S.L., Rice, G.W.
Method for producing olefins from H_2 and CO_2 using an iron carbide based catalyst
US5140049 (1992) assigned to Exxon Research and Engineering Co.

Hanlon, R.T., Satterfield, C.N.
Reactions of ethanol and selected 1-olefins added during the Fischer-Tropsch synthesis
Energy & Fuels **2** (1998), 196-204.

Hong, J., Hwang, J.S., Jun, K.-W., Sur, J.C., Lee, K.-W.
Deactivation study on a co-precipitated Fe-Cu-K-Al catalyst in CO_2 hydrogenation
Applied Catalysis A: General **218** (2001), 53-59.

Huff, G.A., Satterfield, C.N.
Intrinsic kinetics of the Fischer-Tropsch synthesis on a reduced fused magnetite catalyst
Industrial & Engineering Chemistry Process Design and Development **23** (1984), 696-705.

Jess, A., Popp, R., Hedden, K.
Fischer-Tropsch synthesis with nitrogen-rich syngas: Fundamentals and reactor design aspects
Applied Catalysis A: General **186** (1999), 321-342.

Jun, K.W., Roh, H.-S., Kim, K.-S., Ryu, J.-S., Lee, K.-W.
Catalytic investigations for Fischer-Tropsch synthesis from bio-mass derived syngas
Applied Catalysis A: General **259** (2004), 221-226.

Kennedy, P.E.
Hydrocarbon conversion process using a plurality of synthesis gas sources
US 6512018 (2001) assigned to Syntroleum Corporation

Kölbel, H., et al.
US2692274 (1954) assigned to Rheinpreussen AG für Bergbau und Chemie

Lachowska, M., Skrszypek, J.
Synthesis of higher alcohols: Enhancement by the addition of methanol or ethanol to syngas
Studies in Surface Science and Catalysis **119** (1998), 473-479.

Ledakowicz, S., Nettelhoff, H., Kokuun, R., Deckwer, W.D.
Kinetics of the Fischer-Tropsch synthesis in the slurry phase on a potassium-promoted iron catalyst
Industrial & Engineering Chemistry Process Design and Development **24** (1985), 1043-1049.

Patzlaff, J., Liu, Y., Graffmann, C., Gaube, J.
Studies on product distributions of iron and cobalt catalysed Fischer-Tropsch synthesis
Applied Catalysis A: General **186** (1999), 109-119.

Patzlaff, J., Liu, Y., Graffmann, C., Gaube, J.
Interpretation and kinetic modelling of product distributions of cobalt catalysed Fischer-Tropsch synthesis
Catalysis Today **71** (2002), 381-394.

Raje, A., Inga, J.R. and Davis, B.H.
Fischer-Tropsch synthesis: considerations based on performance of iron-based catalysts
Fuel **76** (1997a), 273-280

Raje, A. and Davis, B.H.
Fischer-Tropsch synthesis over iron-based catalysts in a slurry reactor. Reaction rates, selectivity and implications for improving hydrocarbon productivity
Catalysis Today **36** (1997b), 335-345.

Riedel, T., Claeys, M., Schulz, H., Schaub, G., Nam, S.-S., Jun, K.-W., Choi, M.-J., Kishan, G. Lee, K.-W.
Comparative study of Fischer-Tropsch synthesis with H_2/CO and H_2/CO_2 syngas using Fe- and Co-based catalysts
Applied Catalysis A: General **186** (1999) 201-213.

Riedel, T.
Reaktionen von CO_2 bei der Fischer-Tropsch Synthese – Kinetik und Selektivität
PhD thesis University of Karlsruhe (2002)

Schanke, D., Hansen, R. Sogge, J., Hofstad, K.H., Wesenberg, M.H., Rytter, E.
Optimum integration of Fischer-Tropsch synthesis and syngas production
US Pat. App. Pub. US 2003/0134911 (2003)

Schulz, H.
Short history and present trends of Fischer-Tropsch synthesis
Applied Cataysis A: General **186** (1999), 3-12.

Schulz, H., Claeys, M.
Reactions of α-olefins of different chain length added during the Fischer-Tropsch synthesis on a cobalt catalyst in a slurry reactor
Applied Cataysis A: General **186** (1999), 71-90.

Shah, L.S., Thacker, P.S., Quintana, M.E., Lalit, Song, R.
Fischer-Tropsch tail-gas utilisation
US Pat. App. Pub. US2003/0083390 (2003)

Shen, W.J.; Zhou, J.L.; Zhang, B.J.,
Kinetics of Fischer-Tropsch synthesis over precipitated iron catalyst,
Journal of Natural Gas Chemistry ***4*** (1994), 385–400.

Slaghuis, J.H.
Fuel Science: A Study Guide for the National Diploma in Fuel Technology
Fuel Science III, Sasolburg: Sasol Technology R&D (1995).

Snel, R., Espinoza, R.L.
Secondary reactions of primary products of the Fischer-Tropsch synthesis. 1. The role of ethene
Journal of Molecular Catalysis **43** (1987), 237-247.

Snel, R., Espinoza, R.L.
Fischer-Tropsch synthesis on iron-based catalysts – the effect of co-feeding small oxygenates
Journal of Molecular Catalysis 54, (1989a), 103-117

Snel, R., Espinoza, R.L.
Secondary reactions of primary products of the Fischer-Tropsch synthesis. 2. The role of propene
Journal of Molecular Catalysis **54** (1989b), 103-117

Snel, R., Espinoza, R.L.
Secondary reactions of primary products of the Fischer-Tropsch synthesis. 3. The role of butene
Journal of Molecular Catalysis **54** (1989c), 119-130

Song, X., Gou, Z.
A new process for synthesis gas by co-gasifying coal and natural gas
Fuel **84** (2005), 525-531

Sorensen, J.C., Benedict, D.E., Tsao, T-C. R., Klosek, J.
Control scheme for conversion of variable composition synthesis gas to liquid fuels in a slurry bubble column reactor
US 6642280 (2003) assigned to Air Products and Chemicals, Inc.

Tau, L.M., Robinson, R., Ross, R.D., Davis, B.H.
Oxygenates formed from ethanol during Fischer-Tropsch synthesis
Journal of Catalysis **105** (1987), 335-341.

Tau, L.M., Dabbagh, H.A., Davis, B.H.
Fischer-Tropsch synthesis – C-14 tracer study of alkene incorporation
Energy and Fuels **4** (1990), 94-99.

Tau, L.M., Dabbagh, H.A., Davis, B.H.
Fischer-Tropsch synthesis – comparison of C-14-distribution when labelled alcohol is added to the synthesis gas
Energy and Fuels ***5*** (1991), 174-179.

Tau, L.M., Dabbagh, H.A., Halasz, J., Davis, B.H.
Fischer-Tropsch synthesis – incorporation of C-14-labelled normal and isoalcohols
Journal of Molecular Catalysis **71** (1992), 37-55.

Van Berge, P.J., Everson, R.C.
Cobalt as an alternative Fischer-Tropsch catalyst to iron for the production of middle distillates
Studies in Surface Science and Catalysis **107** (1997), 207-212

Van der Laan, G.P., Beenackers, A.A.C.M.
Kinetics and selectivity of the Fischer-Tropsch synthesis: a literature review
Catalysis Reviews- Science and Engineering **41** (1999), 255

Van der Laan, G.P., Beenackers, A.A.C.M.
Intrinsic kinetics of the gas-solid Fischer-Tropsch and water gas shift reactions over a precipitated iron catalyst
Applied Catalysis A: General **193** (2000), 39-53

Van Steen, E., Schulz, H.
Polymerisation kinetics of the Fischer-Tropsch CO hydrogenation using iron and cobalt based catalysts
Applied Cataysis A: General **186** (1999), 309-320.

Vosloo, A.C.
Fischer-Tropsch: a futuristic view
Fuel Processing Technology **71** (2001), 149-155.

Vosloo, A.C., Gibson, P. and Van Berge, P.J.
21st Annual International Pittsburgh Coal Conference (2004), Osaka, Japan.

Wender, I.
Reactions of synthesis gas
Fuel Processing Technology **48** (1996), 189-297.

Wilhelm, D.J., Simbeck, D.R., Karp, A.D., Dickenson, R.L.
Syngas production for gas-to-liquid applications: technologies, issues and outlook
Fuel Processing Technology **71** (2001), 139-148.

Wu, J., Fang, Y., Peng, H., Wang, Y.
A new integrated approach of coal gasification: the concept and preliminary experimental results
Fuel Processing Technology **86** (2004), 261-266.

Xu, L.G., Bao, S.Q., Houpt, D.J., Lamber, S.H., Davis, B.H.
Role of CO_2 in the initiation of chain growth and alcohol formation during the Fischer-Tropsch synthesis
Catalysis Today **36** (1997), 347-355.

Zhang, Y.Q., Jacobs, G., Sparks, D.E., Dry, M.E., Davis, B.H.
CO and CO_2 hydrogenation study on supported cobalt Fischer-Tropsch synthesis catalysts
Catalysis Today **71** (2002), 411-418.

Zimmerman, W.H., Bukur, D.B.
Reaction kinetics over iron catalysts used for the Fischer-Tropsch synthesis
Canadian Journal of Chemical Engineering **68** (1990), 292-301.

APPENDIX A

This section presents the data used for testing the FT and WGS rate expressions.

Table A1. Experimental data used for the testing of FT and WGS rate expressions.

Reactor & Run Name	Time on Stream [hr]	Syngas Conversion %	P_{H2} [bar]	P_{CO} [bar]	P_{H2O} [bar]	P_{CO2} [bar]	r_{FT} (observed) $x10^{-6}$ mole CO/ g-cat / s
RO10	41.28	29.98	7.72	7.54	1.36	0.73	5.74
RO10	166.75	31.13	7.54	7.69	1.47	0.75	5.86
RO10	161.75	31.12	7.54	7.69	1.47	0.75	5.86
RO12	120.33	30.93	8.86	6.41	1.61	0.68	5.98
RO12	64.50	31.02	8.86	6.43	1.67	0.63	6.10
RO12	88.75	31.57	8.80	6.32	1.85	0.61	6.20
ROO8	45.50	34.26	8.49	6.43	1.72	0.78	6.48
ROO8	88.58	35.32	8.39	6.36	1.83	0.81	6.68
ROO8	70.17	35.19	8.39	6.36	1.84	0.81	6.62
ROO7	329.83	37.08	9.07	5.51	2.00	0.79	7.19
ROO5	191.33	38.39	10.55	3.89	2.26	0.72	8.05
ROO5	231.67	38.95	10.56	3.78	2.21	0.85	8.08
ROO5	207.42	39.09	10.48	3.85	2.29	0.77	8.10
ROO5	95.58	39.57	9.09	2.69	2.54	1.17	6.70
ROO5	136.25	38.97	10.50	2.77	2.12	1.65	6.92
ROO5	118.25	39.32	10.49	2.74	2.16	1.62	6.72
ROO5	164.50	39.62	10.16	3.02	2.12	1.72	7.16
ROO5	112.25	39.95	10.28	2.79	2.21	1.65	6.93
ROO5	287.23	36.85	9.24	1.76	1.59	2.33	6.18
ROO5	302.08	35.61	9.35	1.71	1.52	2.41	5.82
ROO5	352.83	35.59	9.31	1.74	1.48	2.46	5.74
ROO5	326.17	35.68	9.20	1.71	1.75	2.36	5.64
ROO5	280.77	39.03	9.11	1.83	1.80	2.32	5.57
ROO5	263.00	40.59	8.97	1.73	1.94	2.19	5.90

APPENDIX B

The experimental data and catalytic performance results (from TCD analyses) for the different H_2/CO ratios in the fresh feed with and without recycle is summarised in this section.

Table B1. Experimental data and catalytic performance results for $H_2/CO = 1.0$.

Run number		R011	R011	R011	R011	R011	R011
Time on stream	[h]	70.42	87.58	112.58	207.33	233.08	256.33
Temperature	[oC]	240.00	240.00	240.00	240.00	240.00	240.00
Pressure	[bar]	20.00	20.00	20.00	20.00	20.00	20.00
GHSV	[ml/g-cat h]	5221.93	5193.06	5272.53	2771.38	2825.30	2777.34
H2/CO in feed		1.12	1.12	1.12	1.06	1.03	1.05
H2/CO in total feed		1.12	1.12	1.12	0.96	0.96	0.98
H2/CO in tail		1.00	1.01	1.01	0.86	0.87	0.87
Recycle ratio		0.01	0.01	0.01	0.79	0.87	0.89
Reactor partial pressure							
H2	[bar]	7.61	7.61	7.56	6.36	6.40	6.46
CO	[bar]	7.61	7.54	7.46	7.37	7.33	7.45
H2O	[bar]	1.49	1.59	1.75	1.56	1.61	1.32
CO2	[bar]	0.76	0.74	0.73	1.60	1.56	1.62
Conversion overall							
CO	[mol %]	28.41	28.93	30.12	48.06	49.75	48.09
CO + H2	[mol %]	32.45	32.58	33.56	53.00	53.66	52.84
CO + CO2	[mol %]	21.22	21.98	23.26	36.79	39.05	36.79
Conversion per pass							
CO	[mol %]	28.14	28.66	29.83	27.97	28.03	26.66
CO + H2	[mol %]	32.16	32.28	33.25	32.13	31.29	30.54
CO + CO2	[mol %]	21.00	21.75	23.02	19.63	20.12	18.59
CO2 selectivity	[% C atom]	25.30	24.02	22.78	23.45	21.52	23.48
CH4 selectivity	[% C atom]	1.42	1.19	1.10	1.06	0.99	1.18
H2/CO usage ratio		1.42	1.38	1.36	1.27	1.19	1.26

Table B2. Experimental data and catalytic performance results for $H_2/CO = 1.3$

Run number		R008	R008	R008	R008	R008	R008	R008
Time on stream	[h]	45.50	70.17	88.58	143.33	165.17	188.92	206.92
Temperature	[oC]	240.00	240.00	240.00	240.00	240.00	240.00	240.00
Pressure	[bar]	20.00	20.00	20.00	20.00	20.00	20.00	20.00
GHSV	[ml/g-cat h]	5056.23	5035.49	5055.91	1836.81	1838.78	1885.33	1887.68
H2/CO in feed		1.34	1.32	1.32	1.32	1.32	1.32	1.32
H2/CO in total feed		1.34	1.32	1.32	1.29	1.29	1.30	1.30
H2/CO in tail		1.32	1.32	1.32	1.29	1.29	1.28	1.28
Recycle ratio		0.01	0.01	0.01	1.76	1.74	1.71	1.62
Reactor partial pressure								
H2	[bar]	8.48	8.38	8.38	6.35	6.34	6.29	6.23
CO	[bar]	6.42	6.35	6.35	4.92	4.92	4.91	4.84
H2O	[bar]	1.71	1.84	1.83	1.31	1.31	1.45	1.62
CO2	[bar]	0.78	0.81	0.81	2.95	2.96	2.93	2.90
Conversion overall								
CO	[mol %]	33.81	35.19	35.23	73.29	73.38	73.14	73.42
CO + H2	[mol %]	34.26	35.19	35.32	73.62	73.71	73.55	73.84
CO + CO2	[mol %]	25.74	26.98	26.94	57.30	57.34	57.13	57.52
Conversion per pass								
CO	[mol %]	33.50	34.88	34.91	33.97	34.24	34.35	35.53
CO + H2	[mol %]	33.95	34.88	35.01	34.36	34.62	34.82	36.03
CO + CO2	[mol %]	25.48	26.71	26.66	20.11	20.25	20.39	21.27
CO2 selectivity	[% C atom]	23.86	23.35	23.54	21.82	21.85	21.89	21.66
CH4 selectivity	[% C atom]	2.00	1.86	1.97	1.94	1.94	1.96	1.91
H2/CO usage ratio		1.37	1.32	1.33	1.33	1.33	1.33	1.34

Table B3. Experimental data and catalytic performance results for H_2/CO = 1.4.

Run number		R012	R012	R012	R012	R012	R012
Time on stream	[h]	40.42	64.50	88.75	120.33	137.58	164.33
Temperature	[oC]	240.00	240.00	240.00	240.00	240.00	240.00
Pressure	[bar]	20.00	20.00	20.00	20.00	20.00	20.00
GHSV	[ml/g-cat h]	5180.47	5245.16	5237.32	5161.40	2787.30	2785.43
H2/CO in feed		1.37	1.37	1.35	1.36	1.36	1.36
H2/CO in total feed		1.37	1.37	1.35	1.36	1.36	1.33
H2/CO in tail		1.38	1.38	1.39	1.38	1.39	1.35
Recycle ratio		0.01	0.01	0.01	0.01	0.94	0.81
Reactor partial pressure							
H2	[bar]	8.95	8.84	8.79	8.84	7.65	7.79
CO	[bar]	6.50	6.42	6.31	6.40	5.51	5.78
H2O	[bar]	1.44	1.66	1.85	1.60	1.90	1.70
CO2	[bar]	0.63	0.63	0.61	0.68	1.40	1.52
Conversion overall							
CO	[mol %]	29.41	31.23	32.68	31.60	61.59	55.18
CO + H2	[mol %]	29.15	31.02	31.57	30.93	61.07	55.43
CO + CO2	[mol %]	22.52	24.53	26.19	24.37	51.85	43.42
Conversion per pass							
CO	[mol %]	29.04	30.95	32.39	31.31	35.37	33.06
CO + H2	[mol %]	28.79	30.73	31.28	30.64	34.86	33.28
CO + CO2	[mol %]	22.21	24.29	25.94	24.13	26.87	23.54
CO2 selectivity	[% C atom]	23.43	21.45	19.85	22.87	15.82	21.31
CH4 selectivity	[% C atom]	0.89	0.79	0.73	0.80	0.51	1.01
H2/CO usage ratio		1.35	1.35	1.27	1.31	1.34	1.37

Table B4. Experimental data and catalytic performance results for $H_2/CO = 1.5$.

Run number		R007	R007	R007	R007	R007	R007	R007	R007	R007
Time on stream	[h]	122.00	136.50	208.17	215.75	234.92	239.00	253.83	280.92	305.67
Temperature	[°C]	240.00	240.00	240.00	240.00	240.00	240.00	240.00	240.00	240.00
Pressure	[bar]	20.00	20.00	20.00	20.00	20.00	20.00	20.00	20.00	20.00
GHSV	[ml/g-cat h]	5068.46	5048.39	2676.64	2745.60	2708.94	2721.07	2720.37	2733.26	5103.50
H_2/CO in feed		1.48	1.51	1.46	1.50	1.46	1.48	1.50	1.45	1.54
H_2/CO in total feed		1.48	1.51	1.56	1.58	1.55	1.57	1.58	1.56	1.54
H_2/CO in tail		1.59	1.58	1.74	1.79	1.72	1.76	1.71	1.69	1.65
Recycle ratio		0.01	0.01	0.95	0.81	0.85	0.83	0.83	0.90	0.01
Reactor partial pressure										
H_2	[bar]	8.80	8.83	7.84	7.94	7.92	8.01	7.89	7.92	9.06
CO	[bar]	5.54	5.58	4.51	4.43	4.60	4.56	4.62	4.69	5.49
H_2O	[bar]	2.08	1.98	1.78	2.01	1.89	1.90	1.81	1.82	1.99
CO_2	[bar]	0.88	0.88	2.06	1.95	1.92	1.89	2.00	1.94	0.80
Conversion overall										
CO	[mol %]	40.91	40.20	67.66	67.35	66.21	66.01	65.49	65.28	39.56
$CO + H_2$	[mol %]	38.37	38.37	64.10	63.54	62.64	62.30	62.59	61.94	36.91
$CO + CO_2$	[mol %]	31.55	30.72	52.87	53.00	52.07	51.89	50.54	50.94	30.76
Conversion per pass										
CO	[mol %]	40.56	39.86	41.79	43.85	42.03	42.19	41.78	40.53	39.22
$CO + H_2$	[mol %]	38.03	38.03	38.00	39.75	38.29	38.31	38.75	37.10	36.59
$CO + CO_2$	[mol %]	31.24	30.41	27.80	29.92	28.68	28.84	27.87	27.34	30.47
CO_2 selectivity	[% C atom]	22.89	23.60	21.86	21.31	21.35	21.39	22.84	21.97	22.24
CH_4 selectivity	[% C atom]	1.78	1.91	1.69	1.85	1.85	1.95	2.01	1.99	1.73
H_2/CO usage ratio		1.33	1.39	1.33	1.36	1.33	1.35	1.39	1.33	1.37

Table B5. Experimental data and catalytic performance results for $H_2/CO = 2.0$

Run number		R005	R005	R005	R005	R005	R005	R005	R005	R005
Time on stream	[h]	64.17	73.33	112.25	118.25	136.25	164.50	184.75	191.33	207.42
Temperature	[oC]	240.00	240.00	240.00	240.00	240.00	240.00	240.00	240.00	240.00
Pressure	[bar]	20.00	20.00	20.70	20.70	20.80	20.90	20.90	20.00	20.00
GHSV	[ml/g-cat h]	5142.44	5227.97	2873.54	2849.80	2876.22	2893.29	2874.69	5583.21	5524.30
H2/CO in feed		1.85	1.89	2.03	2.10	2.02	2.00	2.00	2.09	2.07
H2/CO in total feed		1.85	1.89	2.48	2.53	2.51	2.39	2.47	2.09	2.07
H2/CO in tail		2.24	2.30	3.68	3.83	3.79	3.36	3.79	2.71	2.72
Recycle ratio		0.01	0.01	0.79	0.76	0.84	0.86	0.81	0.01	0.01
Reactor partial pressure										
H2	[bar]	9.09	9.20	10.27	10.48	10.49	10.15	10.39	10.55	10.48
CO	[bar]	4.06	4.00	2.79	2.74	2.77	3.02	2.74	3.89	3.85
H2O	[bar]	1.95	1.91	2.21	2.16	2.12	2.11	2.36	2.26	2.29
CO2	[bar]	1.81	1.83	1.65	1.62	1.65	1.72	1.62	0.72	0.77
Conversion overall										
CO	[mol %]	44.30	44.60	76.54	75.95	77.07	76.27	77.55	48.78	49.86
CO + H2	[mol %]	36.75	36.72	63.80	62.48	63.63	65.49	64.15	38.39	39.09
CO + CO2	[mol %]	30.60	30.54	62.67	61.72	63.40	62.75	64.26	39.28	39.85
Conversion per pass										
CO	[mol %]	43.96	44.26	55.04	55.20	55.08	52.76	56.06	48.42	49.50
CO + H2	[mol %]	36.44	36.41	39.80	39.38	38.97	39.73	39.80	38.05	38.75
CO + CO2	[mol %]	30.31	30.25	38.65	38.61	38.73	36.92	39.91	38.94	39.50
CO2 selectivity	[% C atom]	19.79	20.39	18.12	18.73	17.74	17.72	17.13	19.48	20.08
CH4 selectivity	[% C atom]	2.02	1.92	3.06	2.83	2.43	2.16	2.32	2.00	1.96
H2/CO usage ratio		1.37	1.38	1.53	1.55	1.49	1.57	1.48	1.43	1.40

Table B5. (continued): Experimental data and catalytic performance results for $H_2/CO = 2.0$

Run number		R005	R005	R005	R005	R005	R005	R005	R005
Time on stream	[h]	231.67	280.77	287.23	302.08	326.17	352.83	376.50	399.83
Temperature	[oC]	240.00	240.00	240.00	240.00	239.90	240.00	240.00	240.00
Pressure	[bar]	20.00	20.00	20.00	20.00	20.00	20.00	20.00	20.00
GHSV	[ml/g-cat h]	5531.03	1965.92	2102.83	2026.06	1986.98	2008.38	5644.88	5663.89
H2/CO in feed		2.06	1.87	2.01	1.92	1.94	1.92	2.13	2.14
H2/CO in total feed		2.06	2.84	3.15	3.15	3.17	3.10	2.13	2.14
H2/CO in tail		2.79	4.98	5.24	5.46	5.38	5.36	2.80	2.79
Recycle ratio		0.01	1.48	1.76	1.80	1.78	1.78	0.01	0.01
Reactor partial pressure									
H2	[bar]	10.56	9.09	9.20	9.32	9.17	9.28	10.82	10.84
CO	[bar]	3.78	1.83	1.76	1.71	1.71	1.73	3.86	3.89
H2O	[bar]	2.21	1.80	1.58	1.51	1.75	1.48	2.06	2.03
CO2	[bar]	0.85	2.31	2.33	2.40	2.35	2.45	0.79	0.77
Conversion overall									
CO	[mol %]	50.79	88.21	89.25	89.26	88.82	88.98	48.50	47.88
CO + H2	[mol %]	38.95	75.44	77.73	76.25	75.73	75.96	37.40	37.18
CO + CO2	[mol %]	39.76	73.27	75.01	74.18	73.49	73.39	37.96	37.53
Conversion per pass									
CO	[mol %]	50.42	60.82	58.01	58.72	58.02	58.50	48.16	47.53
CO + H2	[mol %]	38.60	38.92	36.75	35.47	35.17	35.54	37.08	36.85
CO + CO2	[mol %]	39.41	36.25	33.32	32.96	32.53	32.49	37.64	37.20
CO2 selectivity	[% C atom]	21.71	16.94	15.96	16.90	16.97	17.44	21.73	21.61
CH4 selectivity	[% C atom]	1.73	2.89	2.87	3.10	3.34	3.24	2.41	2.62
H2/CO usage ratio		1.34	1.45	1.62	1.50	1.50	1.49	1.41	1.44

APPENDIX C

The results of the selectivity calculations for the different H_2/CO ratios in the fresh feed with and without recycle is summarised in this section.

Table C1. Normal-and iso-Paraffn Selectivity results for H_2/CO = 1.08

Run	R011	R011	R011	R011	R011	R011	R011
TOL [hr]	70.4	87.6	112.6	161.0	191.0	207.3	233.1
RR	0.0	0.0	0.0	0.9	0.8	0.8	0.9
Carbon No.	***n-Paraffin Selectivity [% C-atom]***						
1	1.479	0.854	0.957	0.969	1.073	1.111	1.018
2	0.334	0.166	0.181	0.249	0.292	0.302	0.277
3	0.574	0.302	0.286	0.271	0.304	0.315	0.289
4	0.545	0.293	0.288	0.256	0.301	0.312	0.285
5	0.412	0.226	0.247	0.203	0.252	0.263	0.237
6	0.332	0.196	0.246	0.180	0.238	0.252	0.220
7	0.091	0.077	0.111	0.091	0.105	0.119	0.089
8	0.176	0.150	0.166	0.136	0.156	0.178	0.132
9	0.248	0.210	0.203	0.167	0.189	0.216	0.160
10	0.287	0.242	0.222	0.182	0.205	0.234	0.174
11	0.317	0.266	0.240	0.197	0.212	0.242	0.180
12	0.324	0.269	0.242	0.199	0.222	0.254	0.189
13	0.289	0.239	0.214	0.176	0.197	0.225	0.167
14	0.268	0.221	0.201	0.165	0.183	0.209	0.156
15	0.232	0.195	0.182	0.149	0.166	0.190	0.141
16	0.192	0.162	0.159	0.130	0.146	0.167	0.124
17	0.144	0.130	0.137	0.112	0.128	0.147	0.109
18	0.110	0.104	0.120	0.099	0.115	0.131	0.097
19	0.085	0.083	0.106	0.087	0.104	0.118	0.088
20	0.068	0.069	0.095	0.078	0.095	0.108	0.080
Carbon No.	***iso-Paraffin Selectivity [% C-atom]***						
4	0.000	0.000	0.000	0.000	0.000	0.000	0.000
5	0.002	0.000	0.007	0.006	0.001	0.001	0.001
6	0.172	0.008	0.028	0.007	0.024	0.026	0.021
7	0.038	0.027	0.022	0.018	0.021	0.024	0.018
8	0.018	0.015	0.019	0.016	0.019	0.022	0.016
9	0.033	0.029	0.032	0.027	0.031	0.035	0.026
10	0.034	0.030	0.033	0.027	0.032	0.036	0.027
11	0.018	0.021	0.026	0.021	0.023	0.026	0.020
12	0.046	0.040	0.039	0.032	0.038	0.043	0.032
13	0.030	0.025	0.027	0.023	0.027	0.030	0.023
14	0.011	0.009	0.015	0.012	0.009	0.011	0.008
15	0.031	0.028	0.031	0.025	0.030	0.034	0.026
16	0.000	0.000	0.000	0.000	0.000	0.000	0.000
17	0.000	0.000	0.000	0.000	0.000	0.000	0.000
18	0.000	0.000	0.000	0.000	0.000	0.000	0.000
19	0.000	0.000	0.000	0.000	0.000	0.000	0.000
20	0.000	0.000	0.000	0.000	0.000	0.000	0.000

Table C2. Alpha- and internal-Olefin Selectivity results for H_2/CO = 1.08

Run	R011	R011	R011	R011	R011	R011	R011
TOL [hr]	70.4	87.6	112.6	161.0	191.0	207.3	233.1
RR	0.0	0.0	0.0	0.9	0.8	0.8	0.9
Carbon No.	***n-Olefin Selectivity [% C-atom]***						
2	1.381	0.819	0.880	0.805	0.878	0.909	0.832
3	2.513	1.447	1.509	1.501	1.670	1.730	1.584
4	1.942	1.111	1.228	1.157	1.340	1.390	1.270
5	1.394	0.801	0.972	0.851	1.045	1.088	0.985
6	1.110	0.661	0.922	0.703	0.925	0.977	0.860
7	0.281	0.237	0.377	0.309	0.356	0.406	0.302
8	0.537	0.458	0.558	0.458	0.529	0.604	0.449
9	0.741	0.635	0.671	0.551	0.631	0.720	0.536
10	0.818	0.703	0.704	0.578	0.659	0.752	0.560
11	0.804	0.693	0.683	0.560	0.638	0.728	0.541
12	0.744	0.636	0.631	0.518	0.590	0.674	0.501
13	0.650	0.560	0.561	0.461	0.527	0.602	0.448
14	0.535	0.464	0.476	0.391	0.447	0.511	0.380
15	0.407	0.360	0.380	0.312	0.358	0.409	0.304
16	0.289	0.264	0.289	0.237	0.275	0.314	0.233
17	0.196	0.186	0.213	0.175	0.205	0.234	0.174
18	0.132	0.130	0.157	0.129	0.152	0.174	0.129
19	0.093	0.094	0.120	0.098	0.117	0.133	0.099
20	0.069	0.071	0.095	0.078	0.093	0.106	0.079
Carbon No.	***internal-Olefin Selectivity [% C-atom]***						
4	0.118	0.107	0.109	0.048	0.057	0.059	0.054
5	0.014	0.024	0.062	0.042	0.055	0.058	0.052
6	0.040	0.002	0.057	0.012	0.038	0.040	0.016
7	0.008	0.007	0.015	0.013	0.015	0.018	0.013
8	0.018	0.015	0.022	0.018	0.021	0.025	0.018
9	0.026	0.022	0.025	0.021	0.025	0.028	0.021
10	0.035	0.029	0.032	0.026	0.030	0.034	0.025
11	0.029	0.025	0.025	0.021	0.031	0.036	0.027
12	0.029	0.026	0.026	0.022	0.022	0.025	0.019
13	0.031	0.025	0.024	0.020	0.023	0.026	0.019
14	0.032	0.026	0.025	0.021	0.024	0.027	0.020
15	0.030	0.025	0.026	0.021	0.024	0.028	0.020
16	0.026	0.023	0.025	0.020	0.024	0.027	0.020
17	0.021	0.019	0.023	0.019	0.023	0.026	0.019
18	0.016	0.016	0.021	0.017	0.021	0.024	0.018
19	0.013	0.013	0.019	0.016	0.019	0.022	0.017
20	0.010	0.011	0.017	0.014	0.018	0.021	0.015

Table C3. Alcohol and oxygenates Selectivity results for H_2/CO = 1.08

Run	R011	R011	R011	R011	R011	R011	R011
TOL [hr]	70.4	87.6	112.6	161.0	191.0	207.3	233.1
RR	0.0	0.0	0.0	0.9	0.8	0.8	0.9
Carbon No.	***n-Alcohol Selectivity [% C-atom]***						
1	0.151	0.166	0.139	0.239	0.272	0.277	0.238
2	0.506	0.443	0.409	0.428	0.478	0.484	0.461
3	0.185	0.161	0.159	0.175	0.202	0.205	0.196
4	0.130	0.130	0.122	0.123	0.133	0.136	0.126
5	0.134	0.120	0.112	0.100	0.111	0.118	0.101
6	0.142	0.118	0.116	0.095	0.110	0.122	0.095
7	0.120	0.099	0.092	0.076	0.087	0.098	0.074
8	0.122	0.102	0.094	0.078	0.090	0.103	0.077
9	0.099	0.083	0.076	0.062	0.070	0.080	0.059
10	0.089	0.077	0.069	0.057	0.065	0.075	0.056
11	0.061	0.052	0.047	0.039	0.043	0.050	0.037
12	0.046	0.040	0.037	0.030	0.034	0.039	0.029
13	0.031	0.026	0.025	0.020	0.024	0.027	0.020
14	0.021	0.020	0.021	0.017	0.019	0.022	0.016
15	0.011	0.011	0.014	0.011	0.007	0.008	0.006
16	0.005	0.006	0.012	0.010	0.013	0.014	0.011
17	0.012	0.012	0.015	0.013	0.015	0.017	0.013
18	0.001	0.007	0.009	0.007	0.010	0.011	0.008
19	0.000	0.000	0.001	0.001	0.005	0.006	0.004
20	0.000	0.000	0.001	0.000	0.001	0.001	0.001
Carbon No.	***Other Oxygenates[1] [% C-atom]***						
2	0.368	0.338	0.346	0.304	0.316	0.317	0.297
3	0.241	0.199	0.173	0.222	0.252	0.255	0.176
4	0.050	0.047	0.047	0.044	0.047	0.047	0.044
5	0.024	0.021	0.023	0.021	0.022	0.022	0.020
6	0.010	0.009	0.014	0.012	0.013	0.014	0.011
7	0.007	0.007	0.006	0.005	0.010	0.011	0.008
8	0.000	0.000	0.000	0.000	0.000	0.000	0.000
9	0.000	0.000	0.000	0.000	0.000	0.000	0.000
10	0.000	0.000	0.000	0.000	0.000	0.000	0.000
11	0.000	0.000	0.000	0.000	0.000	0.000	0.000
12	0.000	0.000	0.000	0.000	0.000	0.000	0.000
13	0.000	0.000	0.000	0.000	0.000	0.000	0.000
14	0.000	0.000	0.000	0.000	0.000	0.000	0.000
15	0.000	0.000	0.000	0.000	0.000	0.000	0.000
16	0.000	0.000	0.000	0.000	0.000	0.000	0.000
17	0.000	0.000	0.000	0.000	0.000	0.000	0.000
18	0.000	0.000	0.000	0.000	0.000	0.000	0.000
19	0.000	0.000	0.000	0.000	0.000	0.000	0.000
20	0.000	0.000	0.000	0.000	0.000	0.000	0.000

[1] Sum of ketones, aldehydes and internal alcohols

Table C4. Normal-and iso-Paraffn Selectivity results for $H_2/CO = 1.32$

Run	R008	R008	R008	R008	R008	R008	R008	R008
TOL [hr]	45.5	70.2	88.6	136.6	143.3	165.2	188.9	206.9
RR	0.0	0.0	0.0	1.9	1.8	1.7	1.7	1.6
Carbon No.	***n-Paraffin Selectivity [% C-atom]***							
1	1.286	1.494	1.256	1.039	1.432	1.460	0.964	1.672
2	0.251	0.302	0.264	0.414	0.590	0.622	0.358	0.765
3	0.368	0.442	0.376	0.285	0.410	0.439	0.314	0.528
4	0.397	0.466	0.369	0.266	0.384	0.411	0.299	0.518
5	0.411	0.395	0.321	0.214	0.303	0.337	0.260	0.469
6	0.456	0.374	0.341	0.215	0.205	0.320	0.256	0.472
7	0.430	0.345	0.396	0.249	0.198	0.253	0.184	0.290
8	0.368	0.327	0.300	0.290	0.251	0.290	0.219	0.324
9	0.474	0.295	0.296	0.335	0.282	0.310	0.233	0.341
10	0.527	0.325	0.326	0.350	0.300	0.323	0.237	0.349
11	0.524	0.323	0.324	0.358	0.310	0.332	0.245	0.355
12	0.559	0.352	0.353	0.381	0.339	0.365	0.271	0.387
13	0.464	0.298	0.299	0.318	0.282	0.297	0.220	0.314
14	0.400	0.268	0.269	0.290	0.269	0.276	0.207	0.291
15	0.319	0.231	0.232	0.255	0.253	0.251	0.186	0.263
16	0.239	0.192	0.193	0.218	0.234	0.227	0.166	0.233
17	0.177	0.156	0.156	0.186	0.215	0.208	0.149	0.208
18	0.151	0.126	0.126	0.162	0.194	0.191	0.137	0.190
19	0.103	0.101	0.101	0.140	0.171	0.176	0.130	0.177
20	0.083	0.081	0.081	0.121	0.143	0.155	0.120	0.163
Carbon No.	***iso-Paraffin Selectivity [% C-atom]***							
4	0.000	0.000	0.000	0.000	0.000	0.000	0.000	0.000
5	0.004	0.003	0.003	0.000	0.000	0.000	0.000	0.010
6	0.018	0.007	0.007	0.037	0.017	0.028	0.018	0.112
7	0.105	0.043	0.069	0.044	0.048	0.076	0.050	0.095
8	0.030	0.021	0.021	0.020	0.025	0.030	0.017	0.024
9	0.050	0.036	0.036	0.036	0.033	0.038	0.029	0.055
10	0.048	0.033	0.033	0.045	0.036	0.039	0.030	0.031
11	0.029	0.021	0.021	0.026	0.027	0.029	0.021	0.030
12	0.067	0.044	0.044	0.045	0.043	0.046	0.035	0.050
13	0.034	0.027	0.027	0.024	0.022	0.029	0.017	0.025
14	0.026	0.015	0.015	0.024	0.025	0.026	0.020	0.028
15	0.038	0.028	0.028	0.027	0.032	0.036	0.027	0.034
16	0.000	0.000	0.000	0.000	0.000	0.000	0.000	0.000
17	0.000	0.000	0.000	0.000	0.000	0.000	0.000	0.000
18	0.000	0.000	0.000	0.000	0.000	0.000	0.000	0.000
19	0.000	0.000	0.000	0.000	0.000	0.000	0.000	0.000
20	0.000	0.000	0.000	0.000	0.000	0.000	0.000	0.000

Table C5. Alpha- and internal-Olefin Selectivity results for $H_2/CO = 1.32$

Run	R008	R008	R008	R008	R008	R008	R008	R008
TOL [hr]	45.5	70.2	88.6	136.6	143.3	165.2	188.9	206.9
RR	0.0	0.0	0.0	1.9	1.8	1.7	1.7	1.6
Carbon No.	***n-Olefin Selectivity [% C-atom]***							
2	0.947	1.174	1.027	0.522	0.700	0.700	0.599	0.727
3	1.733	2.117	1.826	1.378	1.932	1.984	1.360	2.260
4	1.496	1.805	1.473	1.034	1.456	1.494	1.049	1.779
5	1.231	1.460	1.175	0.789	1.115	1.176	0.854	1.536
6	1.333	1.283	1.178	0.724	0.407	1.075	0.817	1.515
7	1.229	1.142	1.309	0.776	0.701	1.006	0.633	1.340
8	1.108	1.027	0.874	0.904	0.832	0.955	0.717	1.054
9	1.278	0.857	0.859	0.950	0.904	0.989	0.739	1.051
10	1.313	0.885	0.887	0.946	0.890	0.964	0.703	1.006
11	1.222	0.841	0.844	0.882	0.821	0.870	0.644	0.910
12	1.069	0.748	0.750	0.782	0.723	0.756	0.559	0.791
13	0.861	0.627	0.629	0.657	0.615	0.635	0.469	0.658
14	0.649	0.494	0.495	0.519	0.499	0.504	0.369	0.517
15	0.456	0.364	0.365	0.386	0.386	0.382	0.277	0.387
16	0.303	0.257	0.257	0.275	0.286	0.278	0.199	0.278
17	0.200	0.178	0.179	0.193	0.206	0.200	0.142	0.197
18	0.132	0.124	0.125	0.137	0.148	0.143	0.103	0.141
19	0.093	0.089	0.090	0.100	0.107	0.105	0.077	0.104
20	0.067	0.066	0.066	0.075	0.078	0.078	0.059	0.079
Carbon No.	***internal-Olefin Selectivity [% C-atom]***							
4	0.041	0.113	0.039	0.062	0.127	0.152	0.076	0.179
5	0.149	0.082	0.167	0.078	0.122	0.145	0.066	0.101
6	0.052	0.006	0.006	0.036	0.392	0.070	0.031	0.092
7	0.145	0.041	0.112	0.042	0.045	0.077	0.042	0.100
8	0.043	0.028	0.028	0.050	0.060	0.069	0.046	0.074
9	0.065	0.041	0.041	0.062	0.062	0.071	0.052	0.079
10	0.079	0.049	0.049	0.073	0.073	0.083	0.059	0.089
11	0.065	0.041	0.041	0.075	0.080	0.088	0.065	0.092
12	0.059	0.043	0.043	0.055	0.055	0.061	0.045	0.065
13	0.065	0.044	0.044	0.056	0.060	0.067	0.053	0.070
14	0.055	0.041	0.041	0.052	0.058	0.062	0.047	0.066
15	0.045	0.038	0.038	0.049	0.057	0.059	0.045	0.063
16	0.035	0.034	0.034	0.044	0.054	0.055	0.041	0.057
17	0.025	0.028	0.028	0.039	0.049	0.049	0.036	0.051
18	0.000	0.023	0.023	0.034	0.043	0.044	0.032	0.045
19	0.014	0.018	0.018	0.029	0.037	0.039	0.029	0.039
20	0.011	0.015	0.015	0.025	0.030	0.033	0.026	0.035

Table C6. Alcohol and oxygenates Selectivity results for $H_2/CO = 1.32$

Run	R008	R008	R008	R008	R008	R008	R008	R008
TOL [hr]	45.5	70.2	88.6	136.6	143.3	165.2	188.9	206.9
RR	0.0	0.0	0.0	1.9	1.8	1.7	1.7	1.6
Carbon No.	***n-Alcohol Selectivity [% C-atom]***							
1	0.275	0.091	0.259	0.167	0.130	0.089	0.114	0.074
2	0.564	0.377	0.518	0.472	0.554	0.371	0.327	0.382
3	0.236	0.141	0.194	0.190	0.200	0.154	0.121	0.146
4	0.230	0.116	0.174	0.129	0.141	0.116	0.099	0.122
5	0.224	0.092	0.121	0.110	0.121	0.106	0.080	0.104
6	0.222	0.122	0.132	0.129	0.156	0.140	0.095	0.162
7	0.204	0.116	0.119	0.117	0.096	0.116	0.077	0.117
8	0.185	0.120	0.121	0.113	0.103	0.110	0.082	0.121
9	0.158	0.098	0.098	0.100	0.080	0.084	0.062	0.090
10	0.125	0.088	0.088	0.087	0.067	0.077	0.050	0.072
11	0.094	0.062	0.062	0.070	0.054	0.054	0.040	0.052
12	0.063	0.046	0.047	0.048	0.035	0.034	0.024	0.034
13	0.049	0.032	0.032	0.039	0.031	0.030	0.027	0.028
14	0.026	0.024	0.024	0.030	0.025	0.024	0.017	0.022
15	0.014	0.017	0.017	0.020	0.017	0.016	0.008	0.010
16	0.009	0.010	0.010	0.014	0.013	0.012	0.008	0.015
17	0.000	0.012	0.012	0.009	0.010	0.010	0.004	0.018
18	0.000	0.010	0.010	0.004	0.013	0.013	0.008	0.011
19	0.006	0.005	0.005	0.005	0.007	0.007	0.006	0.008
20	0.000	0.000	0.000	0.004	0.000	0.004	0.003	0.004
Carbon No.	***Other Oxygenates[1] [% C-atom]***							
2	0.000	0.000	0.000	0.000	0.000	0.000	0.000	0.000
3	0.145	0.168	0.156	0.066	0.127	0.098	0.098	0.134
4	0.016	0.009	0.013	0.012	0.015	0.009	0.009	0.005
5	0.000	0.000	0.000	0.000	0.000	0.000	0.000	0.000
6	0.047	0.006	0.018	0.012	0.016	0.014	0.011	0.020
7	0.007	0.005	0.005	0.023	0.006	0.007	0.005	0.008
8	0.000	0.000	0.000	0.000	0.000	0.000	0.000	0.000
9	0.000	0.000	0.000	0.000	0.000	0.000	0.000	0.000
10	0.000	0.000	0.000	0.000	0.000	0.000	0.000	0.000
11	0.000	0.000	0.000	0.000	0.000	0.000	0.000	0.000
12	0.000	0.000	0.000	0.000	0.000	0.000	0.000	0.000
13	0.000	0.000	0.000	0.000	0.000	0.000	0.000	0.000
14	0.000	0.000	0.000	0.000	0.000	0.000	0.000	0.000
15	0.000	0.000	0.000	0.000	0.000	0.000	0.000	0.000
16	0.000	0.000	0.000	0.000	0.000	0.000	0.000	0.000
17	0.000	0.000	0.000	0.000	0.000	0.000	0.000	0.000
18	0.000	0.000	0.000	0.000	0.000	0.000	0.000	0.000
19	0.000	0.000	0.000	0.000	0.000	0.000	0.000	0.000
20	0.000	0.000	0.000	0.000	0.000	0.000	0.000	0.000

[1] Sum of ketones, aldehydes and internal alcohols

Table C7. Normal-and iso-Paraffn Selectivity results for $H_2/CO = 1.36$

Run	R012	R012	R012	R012	R012
TOL [hr]	64.5	88.8	120.3	137.6	164.3
RR	0.0	0.0	0.0	0.9	0.8
Carbon No.	***n-Paraffin Selectivity [% C-atom]***				
1	0.813	0.961	1.045	0.715	0.661
2	0.161	0.197	0.214	0.203	0.192
3	0.247	0.330	0.359	0.218	0.200
4	0.248	0.330	0.359	0.202	0.192
5	0.214	0.270	0.295	0.149	0.158
6	0.198	0.249	0.272	0.124	0.145
7	0.198	0.231	0.254	0.110	0.137
8	0.133	0.173	0.116	0.120	0.139
9	0.173	0.171	0.171	0.130	0.175
10	0.194	0.192	0.204	0.144	0.197
11	0.223	0.204	0.215	0.151	0.206
12	0.234	0.231	0.239	0.169	0.230
13	0.217	0.215	0.218	0.154	0.209
14	0.210	0.207	0.208	0.145	0.198
15	0.194	0.191	0.190	0.130	0.178
16	0.167	0.166	0.167	0.112	0.153
17	0.136	0.138	0.142	0.094	0.129
18	0.107	0.112	0.119	0.079	0.108
19	0.085	0.090	0.100	0.066	0.091
20	0.070	0.075	0.086	0.058	0.079
Carbon No.	***iso-Paraffin Selectivity [% C-atom]***				
4	0.000	0.000	0.000	0.000	0.000
5	0.005	0.000	0.001	0.000	0.000
6	0.037	0.003	0.002	0.003	0.004
7	0.006	0.024	0.025	0.007	0.016
8	0.008	0.009	0.011	0.009	0.012
9	0.015	0.016	0.017	0.013	0.017
10	0.021	0.022	0.025	0.018	0.024
11	0.013	0.014	0.015	0.011	0.015
12	0.026	0.027	0.030	0.021	0.028
13	0.020	0.020	0.022	0.015	0.021
14	0.009	0.010	0.010	0.007	0.010
15	0.019	0.020	0.021	0.015	0.021
16	0.000	0.000	0.000	0.000	0.000
17	0.000	0.000	0.000	0.000	0.000
18	0.000	0.000	0.000	0.000	0.000
19	0.000	0.000	0.000	0.000	0.000
20	0.000	0.000	0.000	0.000	0.000

Table C8. Alpha- and internal-Olefin Selectivity results for $H_2/CO = 1.36$

Run	R012	R012	R012	R012	R012
TOL [hr]	64.5	88.8	120.3	137.6	164.3
RR	0.0	0.0	0.0	0.9	0.8
Carbon No.	***n-Olefin Selectivity [% C-atom]***				
2	0.627	0.778	0.845	0.495	0.443
3	1.120	1.455	1.582	1.010	0.917
4	0.887	1.146	1.247	0.740	0.684
5	0.681	0.871	0.950	0.508	0.514
6	0.619	0.763	0.833	0.387	0.440
7	0.589	0.679	0.743	0.325	0.393
8	0.394	0.508	0.295	0.334	0.391
9	0.463	0.463	0.434	0.346	0.455
10	0.484	0.466	0.497	0.352	0.480
11	0.462	0.464	0.496	0.347	0.474
12	0.425	0.431	0.460	0.322	0.439
13	0.370	0.380	0.406	0.283	0.386
14	0.305	0.315	0.339	0.235	0.320
15	0.235	0.244	0.265	0.181	0.247
16	0.172	0.180	0.197	0.132	0.181
17	0.120	0.127	0.140	0.093	0.127
18	0.083	0.088	0.098	0.065	0.088
19	0.059	0.063	0.071	0.046	0.063
20	0.044	0.047	0.054	0.035	0.048
Carbon No.	***internal-Olefin Selectivity [% C-atom]***				
4	0.022	0.042	0.046	0.035	0.036
5	0.053	0.054	0.059	0.031	0.037
6	0.015	0.041	0.020	0.017	0.021
7	0.004	0.034	0.006	0.010	0.014
8	0.011	0.011	0.012	0.011	0.015
9	0.017	0.017	0.019	0.015	0.020
10	0.025	0.025	0.026	0.019	0.027
11	0.020	0.020	0.021	0.015	0.021
12	0.022	0.022	0.022	0.016	0.022
13	0.022	0.022	0.023	0.017	0.023
14	0.023	0.022	0.023	0.016	0.022
15	0.022	0.022	0.023	0.016	0.022
16	0.020	0.020	0.021	0.015	0.020
17	0.017	0.017	0.019	0.013	0.017
18	0.014	0.014	0.016	0.011	0.015
19	0.011	0.012	0.013	0.009	0.013
20	0.009	0.010	0.012	0.008	0.011

Table C9. Alcohol and oxygenates Selectivity results for $H_2/CO = 1.36$

Run	R012	R012	R012	R012	R012
TOL [hr]	64.5	88.8	120.3	137.6	164.3
RR	0.0	0.0	0.0	0.9	0.8
Carbon No.	***n-Alcohol Selectivity [% C-atom]***				
1	0.283	0.288	0.326	0.168	0.203
2	0.136	0.312	0.360	0.265	0.351
3	0.121	0.133	0.158	0.110	0.142
4	0.095	0.104	0.112	0.089	0.120
5	0.086	0.082	0.093	0.066	0.095
6	0.082	0.080	0.086	0.061	0.083
7	0.094	0.073	0.077	0.054	0.073
8	0.074	0.071	0.078	0.054	0.074
9	0.059	0.061	0.065	0.045	0.062
10	0.055	0.058	0.062	0.043	0.059
11	0.040	0.040	0.043	0.030	0.041
12	0.032	0.033	0.035	0.024	0.033
13	0.023	0.029	0.031	0.021	0.029
14	0.018	0.017	0.020	0.014	0.019
15	0.009	0.017	0.012	0.012	0.017
16	0.006	0.011	0.013	0.008	0.012
17	0.010	0.011	0.013	0.008	0.011
18	0.007	0.007	0.009	0.006	0.008
19	0.003	0.004	0.006	0.004	0.005
20	0.000	0.000	0.000	0.000	0.000
Carbon No.	***Other Oxygenates[1] [% C-atom]***				
2	0.000	0.000	0.000	0.000	0.000
3	0.310	0.306	0.343	0.216	0.295
4	0.052	0.051	0.062	0.046	0.062
5	0.029	0.030	0.036	0.023	0.032
6	0.016	0.016	0.019	0.012	0.017
7	0.006	0.005	0.007	0.010	0.008
8	0.004	0.003	0.005	0.004	0.005
9	0.000	0.000	0.000	0.000	0.000
10	0.000	0.000	0.000	0.000	0.000
11	0.000	0.000	0.000	0.000	0.000
12	0.000	0.000	0.000	0.000	0.000
13	0.000	0.000	0.000	0.000	0.000
14	0.000	0.000	0.000	0.000	0.000
15	0.000	0.000	0.000	0.000	0.000
16	0.000	0.000	0.000	0.000	0.000
17	0.000	0.000	0.000	0.000	0.000
18	0.000	0.000	0.000	0.000	0.000
19	0.000	0.000	0.000	0.000	0.000
20	0.000	0.000	0.000	0.000	0.000

[1] Sum of ketones, aldehydes and internal alcohols

Table C10. Normal-and iso-Paraffn Selectivity results for $H_2/CO = 1.51$

Run	R007	R007	R007	R007	R007	R007	R007	R007	R007
TOL [hr]	122.0	136.5	239.0	253.8	280.9	329.8	351.6	422.5	450.3
RR	0.0	0.0	0.8	0.8	0.9	0.0	0.0	1.8	1.8
Carbon No.	***n-Paraffin Selectivity [% C-atom]***								
1	1.179	1.202	1.361	1.477	1.442	1.512	1.638	2.118	1.068
2	0.268	0.271	0.515	0.560	0.551	0.717	0.431	1.149	0.493
3	0.370	0.382	0.459	0.501	0.483	0.509	0.562	0.778	0.436
4	0.365	0.371	0.418	0.496	0.458	0.469	0.516	0.684	0.479
5	0.326	0.341	0.328	0.484	0.386	0.372	0.400	0.574	0.575
6	0.314	0.312	0.284	0.530	0.370	0.343	0.363	0.523	0.693
7	0.313	0.317	0.334	0.294	0.336	0.150	0.315	0.467	0.537
8	0.292	0.214	0.294	0.305	0.275	0.245	0.241	0.406	0.366
9	0.291	0.287	0.318	0.330	0.298	0.302	0.295	0.434	0.387
10	0.336	0.324	0.329	0.341	0.312	0.325	0.318	0.444	0.400
11	0.358	0.323	0.335	0.347	0.324	0.334	0.326	0.451	0.407
12	0.383	0.359	0.352	0.365	0.352	0.351	0.337	0.494	0.446
13	0.322	0.300	0.286	0.297	0.296	0.288	0.273	0.387	0.349
14	0.291	0.271	0.257	0.266	0.277	0.256	0.239	0.347	0.313
15	0.250	0.237	0.225	0.233	0.248	0.219	0.203	0.300	0.271
16	0.206	0.202	0.195	0.202	0.214	0.182	0.169	0.256	0.231
17	0.165	0.170	0.172	0.178	0.179	0.152	0.141	0.221	0.199
18	0.134	0.142	0.156	0.162	0.150	0.131	0.121	0.196	0.177
19	0.108	0.117	0.145	0.150	0.124	0.114	0.108	0.181	0.163
20	0.088	0.095	0.134	0.139	0.102	0.102	0.097	0.167	0.150
Carbon No.	***iso-Paraffin Selectivity [% C-atom]***								
4	0.000	0.000	0.000	0.000	0.000	0.000	0.000	0.000	0.000
5	0.000	0.000	0.003	0.000	0.000	0.012	0.004	0.000	0.000
6	0.006	0.006	0.038	0.138	0.026	0.017	0.019	0.039	0.035
7	0.038	0.078	0.073	0.081	0.064	0.050	0.055	0.115	0.153
8	0.026	0.022	0.021	0.021	0.028	0.026	0.026	0.054	0.037
9	0.029	0.032	0.040	0.041	0.036	0.038	0.038	0.046	0.042
10	0.031	0.040	0.032	0.033	0.031	0.039	0.040	0.034	0.031
11	0.022	0.024	0.026	0.027	0.025	0.028	0.031	0.031	0.028
12	0.039	0.042	0.045	0.047	0.044	0.042	0.041	0.060	0.054
13	0.021	0.023	0.022	0.023	0.023	0.019	0.022	0.027	0.025
14	0.017	0.015	0.023	0.024	0.025	0.023	0.022	0.034	0.030
15	0.026	0.024	0.026	0.027	0.028	0.025	0.020	0.034	0.031
16	0.000	0.000	0.000	0.000	0.000	0.000	0.000	0.000	0.000
17	0.000	0.000	0.000	0.000	0.000	0.000	0.000	0.000	0.000
18	0.000	0.000	0.000	0.000	0.000	0.000		0.000	0.000
19	0.000	0.000	0.000	0.000	0.000	0.000	0.000	0.000	0.000
20	0.000	0.000	0.000	0.000	0.000	0.000	0.000	0.000	0.000

Table C11. Alpha- and internal-Olefin Selectivity results for H_2/CO = 1.51

Run	R007	R007	R007	R007	R007	R007	R007	R007	R007
TOL [hr]	122.0	136.5	239.0	253.8	280.9	329.8	351.6	422.5	450.3
RR	0.0	0.0	0.8	0.8	0.9	0.0	0.0	1.8	1.8
Carbon No.	***n-Olefin Selectivity [% C-atom]***								
2	0.985	1.004	0.874	0.945	0.914	1.229	1.331	0.781	0.838
3	1.771	1.801	1.927	2.154	2.069	2.226	2.401	2.654	1.901
4	1.429	1.441	1.429	1.724	1.586	1.676	1.803	1.860	1.715
5	1.144	1.139	1.014	1.548	1.234	1.218	1.295	1.466	1.716
6	1.036	1.030	0.786	1.593	1.101	1.023	1.069	1.303	1.824
7	1.002	1.002	0.922	0.871	0.968	0.380	0.888	1.159	1.386
8	0.921	0.605	0.796	0.844	0.739	0.612	0.610	0.960	0.866
9	0.839	0.796	0.840	0.870	0.777	0.729	0.703	0.977	0.871
10	0.885	0.854	0.809	0.838	0.754	0.728	0.700	0.923	0.814
11	0.851	0.818	0.738	0.764	0.697	0.668	0.639	0.799	0.720
12	0.761	0.734	0.639	0.662	0.617	0.577	0.546	0.668	0.602
13	0.636	0.613	0.528	0.547	0.524	0.473	0.440	0.528	0.476
14	0.494	0.485	0.405	0.420	0.419	0.361	0.331	0.389	0.351
15	0.360	0.360	0.298	0.309	0.316	0.259	0.235	0.271	0.245
16	0.248	0.257	0.212	0.220	0.224	0.178	0.161	0.188	0.169
17	0.169	0.179	0.151	0.156	0.152	0.119	0.108	0.127	0.114
18	0.115	0.124	0.109	0.113	0.101	0.081	0.074	0.087	0.079
19	0.081	0.087	0.082	0.085	0.068	0.057	0.053	0.062	0.056
20	0.060	0.062	0.063	0.066	0.046	0.042	0.039	0.045	0.041
Carbon No.	***internal-Olefin Selectivity [% C-atom]***								
4	0.054	0.055	0.171	0.136	0.083	0.057	0.145	0.274	0.155
5	0.086	0.140	0.110	0.151	0.124	0.122	0.127	0.313	0.215
6	0.005	0.005	0.038	0.054	0.044	0.009	0.010	0.077	0.069
7	0.050	0.053	0.087	0.065	0.066	0.023	0.068	0.125	0.141
8	0.029	0.030	0.054	0.056	0.053	0.041	0.040	0.104	0.093
9	0.046	0.045	0.063	0.065	0.061	0.056	0.056	0.116	0.105
10	0.061	0.056	0.071	0.074	0.070	0.069	0.067	0.131	0.118
11	0.068	0.045	0.075	0.077	0.075	0.069	0.068	0.136	0.123
12	0.053	0.043	0.054	0.056	0.056	0.052	0.050	0.094	0.085
13	0.054	0.050	0.053	0.055	0.058	0.051	0.048	0.092	0.083
14	0.050	0.047	0.048	0.050	0.054	0.046	0.042	0.077	0.070
15	0.046	0.044	0.045	0.047	0.051	0.042	0.038	0.067	0.061
16	0.039	0.040	0.041	0.042	0.045	0.036	0.033	0.057	0.051
17	0.032	0.035	0.036	0.037	0.038	0.030	0.028	0.047	0.042
18	0.026	0.029	0.032	0.034	0.031	0.026	0.024	0.040	0.036
19	0.020	0.023	0.029	0.030	0.025	0.022	0.020	0.034	0.031
20	0.017	0.019	0.026	0.027	0.020	0.019	0.018	0.029	0.027

Table C12. Alcohol and oxygenates Selectivity results for H_2/CO = 1.51

Run	R007	R007	R007	R007	R007	R007	R007	R007	R007
TOL [hr]	122.0	136.5	239.0	253.8	280.9	329.8	351.6	422.5	450.3
RR	0.0	0.0	0.8	0.8	0.9	0.0	0.0	1.8	1.8
Carbon No.	***n-Alcohol Selectivity [% C-atom]***								
1	0.199	0.219	0.146	0.151	0.202	0.231	0.183	0.157	0.156
2	0.494	0.497	0.598	0.650	0.647	0.621	0.663	0.714	0.763
3	0.207	0.182	0.208	0.253	0.232	0.249	0.270	0.320	0.361
4	0.151	0.154	0.180	0.212	0.192	0.205	0.241	0.218	0.235
5	0.109	0.115	0.141	0.171	0.136	0.150	0.159	0.159	0.150
6	0.125	0.130	0.135	0.140	0.134	0.154	0.156	0.188	0.154
7	0.116	0.117	0.108	0.112	0.107	0.127	0.125	0.182	0.123
8	0.110	0.109	0.102	0.106	0.106	0.112	0.128	0.125	0.113
9	0.101	0.101	0.087	0.090	0.087	0.100	0.098	0.106	0.095
10	0.087	0.086	0.072	0.075	0.075	0.084	0.086	0.095	0.085
11	0.070	0.069	0.056	0.058	0.061	0.065	0.062	0.066	0.060
12	0.052	0.048	0.035	0.036	0.041	0.042	0.044	0.041	0.037
13	0.036	0.038	0.029	0.030	0.034	0.029	0.035	0.040	0.036
14	0.027	0.029	0.023	0.024	0.026	0.025	0.023	0.025	0.023
15	0.018	0.020	0.014	0.014	0.016	0.017	0.015	0.017	0.016
16	0.011	0.013	0.012	0.012	0.011	0.012	0.011	0.014	0.013
17	0.008	0.008	0.010	0.011	0.006	0.010	0.010	0.012	0.011
18	0.004	0.004	0.006	0.006	0.008	0.007	0.008	0.012	0.011
19	0.003	0.003	0.002	0.003	0.000	0.004	0.006	0.010	0.009
20	0.003	0.003	0.005	0.005	0.000	0.005	0.005	0.007	0.006
Carbon No.	***Other Oxygenates[1] [% C-atom]***								
2	0.000	0.000	0.000	0.000	0.000	0.000	0.000	0.000	0.000
3	0.192	0.169	0.190	0.187	0.156	0.166	0.185	0.164	0.196
4	0.013	0.010	0.016	0.017	0.020	0.017	0.017	0.017	0.016
5	0.000	0.000	0.000	0.000	0.000	0.000	0.000	0.000	0.000
6	0.005	0.005	0.019	0.018	0.011	0.018	0.008	0.017	0.023
7	0.006	0.007	0.008	0.008	0.010	0.009	0.009	0.015	0.013
8	0.000	0.000	0.000	0.000	0.000	0.000	0.000	0.000	0.000
9	0.000	0.000	0.000	0.000	0.000	0.000	0.000	0.000	0.000
10	0.000	0.000	0.000	0.000	0.000	0.000	0.000	0.000	0.000
11	0.000	0.000	0.000	0.000	0.000	0.000	0.000	0.000	0.000
12	0.000	0.000	0.000	0.000	0.000	0.000	0.000	0.000	0.000
13	0.000	0.000	0.000	0.000	0.000	0.000	0.000	0.000	0.000
14	0.000	0.000	0.000	0.000	0.000	0.000	0.000	0.000	0.000
15	0.000	0.000	0.000	0.000	0.000	0.000	0.000	0.000	0.000
16	0.000	0.000	0.000	0.000	0.000	0.000	0.000	0.000	0.000
17	0.000	0.000	0.000	0.000	0.000	0.000	0.000	0.000	0.000
18	0.000	0.000	0.000	0.000	0.000	0.000	0.000	0.000	0.000
19	0.000	0.000	0.000	0.000	0.000	0.000	0.000	0.000	0.000
20	0.000	0.000	0.000	0.000	0.000	0.000	0.000	0.000	0.000

[1] Sum of ketones, aldehydes and internal alcohols

Table C13. Normal-and iso-Paraffn Selectivity results for $H_2/CO = 2.01$

Run	R005	R005	R005	R005	R005	R005	R005
TOL [hr]	73.3	136.2	164.5	184.8	352.8	376.5	399.8
RR	0.0	0.8	0.9	0.8	1.8	0.0	0.0
Carbon No.	***n-Paraffin Selectivity [% C-atom]***						
1	2.754	1.813	1.710	1.695	2.503	1.721	1.808
2	0.364	0.536	0.527	0.518	1.137	0.509	0.558
3	0.422	0.478	0.461	0.458	0.863	0.572	0.625
4	0.455	0.553	0.467	0.489	0.888	0.607	0.656
5	0.429	0.578	0.475	0.529	0.930	0.619	0.679
6	0.457	0.623	0.281	0.565	0.945	0.703	0.802
7	0.478	0.475	0.427	0.442	0.779	0.333	0.474
8	0.518	0.544	0.510	0.520	0.683	0.424	0.555
9	0.558	0.593	0.557	0.560	0.710	0.483	0.572
10	0.606	0.625	0.593	0.580	0.743	0.504	0.583
11	0.616	0.652	0.628	0.557	0.779	0.512	0.606
12	0.680	0.703	0.687	0.617	0.873	0.589	0.650
13	0.547	0.591	0.605	0.531	0.753	0.509	0.553
14	0.507	0.532	0.560	0.484	0.703	0.474	0.510
15	0.455	0.455	0.488	0.422	0.622	0.418	0.446
16	0.374	0.375	0.401	0.356	0.528	0.350	0.369
17	0.334	0.306	0.319	0.294	0.440	0.285	0.297
18	0.274	0.252	0.252	0.243	0.370	0.232	0.239
19	0.221	0.211	0.202	0.200	0.319	0.195	0.198
20	0.169	0.172	0.162	0.162	0.278	0.164	0.164
Carbon No.	***iso-Paraffin Selectivity [% C-atom]***						
4	0.000	0.000	0.000	0.000	0.000	0.000	0.000
5	0.006	0.016	0.016	0.015	0.030	0.010	0.011
6	0.017	0.023	0.016	0.015	0.030	0.105	0.025
7	0.079	0.050	0.031	0.068	0.045	0.019	0.037
8	0.023	0.016	0.016	0.030	0.022	0.054	0.036
9	0.036	0.029	0.029	0.028	0.029	0.038	0.041
10	0.037	0.035	0.035	0.035	0.037	0.035	0.041
11	0.037	0.027	0.028	0.029	0.033	0.040	0.046
12	0.047	0.042	0.043	0.038	0.046	0.049	0.057
13	0.026	0.025	0.029	0.024	0.030	0.023	0.027
14	0.038	0.030	0.030	0.026	0.039	0.031	0.037
15	0.036	0.023	0.025	0.023	0.033	0.030	0.035
16	0.000	0.000	0.000	0.000	0.000	0.000	0.000
17	0.000	0.000	0.000	0.000	0.000	0.000	0.000
18	0.000	0.000	0.000	0.000	0.000	0.000	0.000
19	0.000	0.000	0.000	0.000	0.000	0.000	0.000
20	0.000	0.000	0.000	0.000	0.000	0.000	0.000

Table C14. Alpha- and internal-Olefin Selectivity results for $H_2/CO = 2.01$

Run	R005	R005	R005	R005	R005	R005	R005
TOL [hr]	73.3	136.2	164.5	184.8	352.8	376.5	399.8
RR	0.0	0.8	0.9	0.8	1.8	0.0	0.0
Carbon No.	***n-Olefin Selectivity [% C-atom]***						
2	1.031	0.629	0.690	0.624	0.405	1.147	1.215
3	1.915	1.785	1.817	1.713	2.040	2.211	2.374
4	1.668	1.686	1.526	1.546	1.734	1.928	2.044
5	1.451	1.692	1.434	1.566	1.819	1.837	1.930
6	1.417	1.740	1.231	1.576	1.947	1.933	1.737
7	1.404	1.250	1.155	1.273	1.812	0.898	1.313
8	1.381	1.408	1.371	1.394	1.499	0.952	1.282
9	1.382	1.433	1.408	1.398	1.346	1.033	1.203
10	1.355	1.352	1.346	1.337	1.194	0.955	1.070
11	1.205	1.206	1.231	1.163	1.016	0.853	0.938
12	1.029	1.007	1.064	0.987	0.822	0.704	0.783
13	0.832	0.794	0.869	0.796	0.631	0.556	0.627
14	0.632	0.573	0.651	0.591	0.455	0.406	0.467
15	0.462	0.393	0.456	0.414	0.304	0.272	0.326
16	0.323	0.257	0.298	0.274	0.200	0.174	0.210
17	0.221	0.167	0.187	0.178	0.125	0.107	0.132
18	0.150	0.109	0.117	0.115	0.078	0.064	0.080
19	0.102	0.074	0.075	0.076	0.051	0.040	0.051
20	0.070	0.051	0.051	0.051	0.034	0.026	0.033
Carbon No.	***internal-Olefin Selectivity [% C-atom]***						
4	0.079	0.103	0.080	0.084	0.311	0.092	0.105
5	0.066	0.132	0.071	0.077	0.259	0.084	0.107
6	0.087	0.100	0.036	0.086	0.233	0.134	0.161
7	0.067	0.068	0.054	0.062	0.144	0.063	0.079
8	0.077	0.078	0.066	0.063	0.131	0.135	0.070
9	0.079	0.097	0.053	0.081	0.153	0.083	0.097
10	0.148	0.118	0.100	0.094	0.177	0.103	0.118
11	0.171	0.128	0.109	0.065	0.188	0.072	0.126
12	0.128	0.094	0.082	0.073	0.122	0.081	0.094
13	0.132	0.095	0.085	0.074	0.121	0.081	0.093
14	0.117	0.083	0.078	0.066	0.101	0.069	0.081
15	0.107	0.074	0.070	0.060	0.086	0.060	0.070
16	0.003	0.062	0.059	0.051	0.069	0.047	0.057
17	0.074	0.050	0.047	0.042	0.054	0.036	0.043
18	0.059	0.040	0.036	0.034	0.042	0.027	0.033
19	0.045	0.032	0.028	0.027	0.033	0.020	0.025
20	0.033	0.026	0.022	0.021	0.026	0.016	0.019

Table C15. Alcohol and oxygenates Selectivity results for $H_2/CO = 2.01$

Run	R005	R005	R005	R005	R005	R005	R005
TOL [hr]	73.3	136.2	164.5	184.8	352.8	376.5	399.8
RR	0.0	0.8	0.9	0.8	1.8	0.0	0.0
Carbon No.	***n-Alcohol Selectivity [% C-atom]***						
1	0.395	0.302	0.343	0.327	0.298	0.363	0.469
2	0.589	0.649	0.611	0.586	0.801	0.742	0.791
3	0.196	0.185	0.164	0.163	0.270	0.299	0.322
4	0.163	0.140	0.122	0.126	0.182	0.213	0.234
5	0.138	0.118	0.112	0.107	0.134	0.162	0.180
6	0.168	0.135	0.129	0.126	0.142	0.172	0.197
7	0.146	0.120	0.116	0.112	0.117	0.175	0.160
8	0.145	0.127	0.126	0.127	0.122	0.143	0.168
9	0.136	0.115	0.114	0.108	0.107	0.119	0.140
10	0.125	0.101	0.107	0.096	0.096	0.106	0.127
11	0.093	0.076	0.080	0.074	0.074	0.079	0.098
12	0.070	0.055	0.061	0.055	0.052	0.053	0.069
13	0.059	0.037	0.050	0.045	0.042	0.039	0.051
14	0.042	0.031	0.034	0.031	0.033	0.030	0.041
15	0.030	0.020	0.020	0.020	0.022	0.019	0.027
16	0.020	0.014	0.014	0.015	0.017	0.014	0.019
17	0.013	0.010	0.009	0.010	0.012	0.009	0.013
18	0.009	0.006	0.005	0.007	0.010	0.006	0.009
19	0.004	0.003	0.002	0.003	0.016	0.004	0.006
20	0.003	0.003	0.002	0.002	0.004	0.004	0.004
Carbon No.	***Other Oxygenates[1] [% C-atom]***						
2	0.039	0.000	0.000	0.000	0.000	0.000	0.000
3	0.046	0.056	0.058	0.056	0.056	0.051	0.055
4	0.111	0.094	0.084	0.091	0.125	0.016	0.229
5	0.000	0.000	0.000	0.000	0.000	0.000	0.000
6	0.008	0.016	0.010	0.010	0.016	0.009	0.010
7	0.008	0.008	0.007	0.007	0.010	0.009	0.011
8	0.000	0.000	0.000	0.000	0.000	0.000	0.000
9	0.000	0.000	0.000	0.000	0.000	0.000	0.000
10	0.000	0.000	0.000	0.000	0.000	0.000	0.000
11	0.000	0.000	0.000	0.000	0.000	0.000	0.000
12	0.000	0.000	0.000	0.000	0.000	0.000	0.000
13	0.000	0.000	0.000	0.000	0.000	0.000	0.000
14	0.000	0.000	0.000	0.000	0.000	0.000	0.000
15	0.000	0.000	0.000	0.000	0.000	0.000	0.000
16	0.000	0.000	0.000	0.000	0.000	0.000	0.000
17	0.000	0.000	0.000	0.000	0.000	0.000	0.000
18	0.000	0.000	0.000	0.000	0.000	0.000	0.000
19	0.000	0.000	0.000	0.000	0.000	0.000	0.000
20	0.000	0.000	0.000	0.000	0.000	0.000	0.000

[1] Sum of ketones, aldehydes and internal alcohols

APPENDIX D

The data that was used for the olefin readsorption model is presented in this section.

Table D1. Data for % 1 Olefins in Linear Hydrocarbons that was used in the Olefin

			kd/kg 0.43				alpha 0.6993			MODEL			EXPERIMENTAL DATA			
													Ol-(1) in HCs (mol%)			
N	ka.mME/Vg	ka'.mME/Vg	k'd,Ol-(1) / kd,Ol-(1)	kd,Ol-(1)/ kd,P	k'd,EP /kd,P	kd',Ol-(1)/kd, Ol-(1)	V1/Vg	KN	c1,EP,N/c 1,Ol-(1),N	Ol-(1) in HCs (mol%)	A	pg,eff,N	NO RECYCLE, Set 1	NO RECYCLE, Set 2	WITH RECYCLE, Set 1	WITH RECYCLE, Set 2
2	10	14	0.87	20.00	1.82	1.00	1.80	0.36	3.131	24.21	0.29	0.88	79.80	79.80	70.87	69.76
3	0.989	0.664	0.90	20.00	2.03	1.12	2.02	1.59	0.227	81.50	0.73	0.76	81.50	81.50	82.23	82.11
4	1.0271	0.71	0.89	20.00	2.08	1.06	1.56	2.30	0.288	77.65	0.66	0.77	77.65	77.65	78.55	78.07
5	1.0159	0.709	0.90	20.00	2.00	1.03	1.56	3.39	0.310	76.33	0.65	0.78	76.33	76.32	77.28	76.44
6	1.0299	0.787	0.90	20.00	1.99	1.02	1.77	4.95	0.326	75.41	0.66	0.78	75.41	75.36	75.68	75.23
7	1.0308	0.884	0.91	20.00	1.95	1.01	2.03	7.23	0.340	74.62	0.68	0.77	74.62	74.50	74.62	74.18
8	1.1103	1.275	0.89	20.00	2.17	1.03	2.50	10.56	0.387	72.10	0.70	0.77	72.10	71.74	73.52	73.78
9	1.0603	1.147	0.91	19.99	1.94	1.00	2.40	15.41	0.390	71.93	0.70	0.76	71.93	71.69	71.99	71.99
10	1.0636	1.217	0.92	19.99	1.91	1.00	2.46	22.50	0.412	70.83	0.70	0.76	70.83	70.86	70.92	70.92
11	1.1155	1.409	0.91	19.99	2.08	1.01	2.51	32.85	0.441	69.41	0.70	0.77	69.41	69.77	69.71	69.71
12	1.0781	1.472	0.93	19.99	1.84	0.98	2.25	47.97	0.537	65.06	0.68	0.77	65.06	65.86	65.62	65.62
13	1.084	1.555	0.93	19.99	1.85	0.98	2.24	70.03	0.566	63.86	0.68	0.77	63.86	65.04	64.83	64.83
14	1.0807	1.711	0.94	19.99	1.84	0.97	2.08	102.25	0.660	60.25	0.66	0.77	60.25	62.02	61.86	61.86
15	1.0628	1.897	0.94	19.99	1.84	0.95	1.89	149.28	0.782	56.12	0.65	0.78	56.12	58.26	58.19	58.19
16	1.045	2.087	0.93	19.99	1.86	0.94	1.70	217.95	0.923	52.01	0.63	0.78	52.01	54.11	54.10	54.10
17	1.0508	2.201	0.94	19.99	1.84	0.93	1.51	318.21	1.085	47.97	0.60	0.79	47.97	49.64	49.61	49.61
18	1.0572	2.234	0.95	19.99	1.79	0.93	1.32	464.59	1.263	44.19	0.57	0.80	44.19	45.17	45.01	45.01
19	1.0516	2.232	0.95	19.99	1.76	0.93	1.16	678.31	1.430	41.15	0.54	0.80	41.15	41.36	41.07	41.07
20	1.0486	2.268	0.95	19.99	1.75	0.93	1.06	990.33	1.583	38.71	0.52	0.81	38.71	38.28	37.81	37.81